STUDY ON PERFORMANCE OF ENERGY STORAGE SYSTEM ON POWER GRID FOR FREQUENCY REGULATION

TANG ZHI XUAN

MASTER OF ENGINEERING SCIENCE

LEE KONG CHIAN FACULTY OF ENGINEERING AND SCIENCE
UNIVERSITI TUNKU ABDUL RAHMAN
DECEMBER 2017

STUDY ON PERFORMANCE OF ENERGY STORAGE SYSTEM ON POWER GRID FOR FREQUENCY REGULATION

By

TANG ZHI XUAN

A dissertation submitted to the Department of Electrical and Electronic Engineering,
Lee Kong Chian Faculty of Engineering and Science,
Universiti Tunku Abdul Rahman,
in partial fulfillment of the requirements for the degree of
Master of Engineering Science
December 2017

ABSTRACT

STUDY ON PERFORMANCE OF ENERGY STORAGE SYSTEM ON POWER GRID FOR FREQUENCY REGULATION

Tang Zhi Xuan

A stable grid frequency is maintained by balancing the load and generation of real power. In frequency regulation, being one of the main ancillary services managed by the Grid Service Operators (GSOs), power is traditionally supplied by spinning reserves to keep the frequency of a control area within the limits. Although these generators possess high grid inertia to act against frequency change, they are limited by their ramping duration and rate. These shortcomings will be further magnified with the higher penetration of intermittent renewable energy (RE) sources in near future, which decreases the grid inertia and results in a more frequent and higher magnitude of power mismatches, hence frequency events. To effectively carry out frequency regulation services, additional spinning reserves are required to be set aside, incurring a higher cost for power generation. Besides, varying power output renders a higher maintenance cost due to increased wear-and-tear on the plants. This research proposes a comprehensive work package of utilizing energy storage system (ESS) for grid frequency regulation. As such, two power networks are modelled, namely of the Peninsular Malaysia and IEEE 24-bus Reliability Test System (RTS). The work package mainly contains two items; first, a frequency response analysis in MATLAB/Simulink through the modelling

of power plants in the power system with transfer functions, their respective daily scheduling and load profiles and second, a load flow analysis in MATLAB/Matpower to study the grid voltage impacts of the operation of frequency regulation by ESS. Droop controllers with integral and derivative controls are proposed for the frequency regulation operation of ESS, while the state-of-charge (SOC) is conserved through a set of offset algorithm. The effects of undersizing ESS for frequency regulation under various scenarios and high photovoltaic (PV) penetration are studied, along with the identification of the optimal ESS placement on the power grid in terms of frequency response and minimal grid voltage impacts. The proposed controller is shown to be able to continuously regulate grid frequency effectively while maintaining the SOC within a healthy range throughout the simulation period. Besides, it demonstrates that the undersizing of ESS does not diminish the quality of frequency regulation service significantly due to the actions of the proposed offset algorithm. However, the undersizing of ESS introduces fluctuations to the SOC profiles, which is further magnified during high PV penetration. Although the actual impacts of the frequent ramping of ESS are beyond the scope of the research, it proves the technical feasibility of ESS undersizing for capital cost savings. Based on the power networks simulated in the dissertation, it is shown that the frequency regulation operation brings relatively little impact to the grid voltages.

ACKNOWLEDGEMENTS

I would like to express my deepest gratitude to my research supervisor, Prof. Ir. Dr. Lim Yun Seng for having enormous patience to spend his quality time and effort to teach and guide me throughout the course of this research. Not only has he inspired me in the field of engineering, but also shaped me in my professional, leadership, and character development.

Next, I would also like to thank my colleagues working in the same research cabin throughout my career here, for they have made my days more bearable, while constantly being informative and helpful for the research experience. My appreciation also goes to my co-supervisor, Dr. Stella Morris, for being supportive to address any inquiries and concerns that I have faced in the process.

Last but not least, I am grateful to my family, for making personal sacrifices to accommodate my decision to pick up a research experience, rather than a full-time job.

APPROVAL SHEET

This dissertation entitled "**STUDY ON PERFORMANCE OF ENERGY STORAGE SYSTEM ON POWER GRID FOR FREQUENCY REGULATION"** was prepared by TANG ZHI XUAN and submitted as partial fulfilment of the requirements for the degree of Master of Engineering Science at Universiti Tunku Abdul Rahman.

Approved by:

_____

(Prof. Ir. Dr. LIM YUN SENG) Date:
Professor/Supervisor
Department of Electrical and Electronics Engineering
Faculty of Engineering and Science
Universiti Tunku Abdul Rahman

_____

(Dr. STELLA MORRIS) Date:
Co-supervisor
Department of Electrical and Electronics Engineering
Faculty of Engineering and Science
Universiti Tunku Abdul Rahman

LEE KONG CHIAN FACULTY OF ENGINEERING AND SCIENCE

UNIVERSITI TUNKU ABDUL RAHMAN

Date: _____

SUBMISSION OF DISSERTATION

It is hereby certified that **TANG ZHI XUAN** (ID No: ***15UEM07431***) has completed this dissertation entitled "**Study On Performance Of Energy Storage System On Power Grid For Frequency Regulation**" under the supervision Prof. Ir. Dr. Lim Yun Seng (Supervisor) from the Department of Electrical and Electronic Engineering, Lee Kong Chian Faculty of Engineering and Science, and Dr. Stella Morris (Co-Supervisor) from the Department of Electrical and Electronic Engineering, Lee Kong Chian Faculty of Engineering and Science.

I understand that University will upload softcopy of dissertation in pdf format into UTAR Institutional Repository, which may be made accessible to UTAR community and public.

Yours truly,

_____

(*Tang Zhi Xuan*)

DECLARATION

I (TANG ZHI XUAN) hereby declare that the dissertation is based on my original work except for quotations and citations which have been duly acknowledged. I also declare that it has not been previously or concurrently submitted for any other degree at UTAR or other institutions.

Name : Tang Zhi Xuan

Date : December 2017

TABLE OF CONTENTS

LIST OF TABLES

LIST OF FIGURES

LIST OF ABBREVIATIONS/ NOTATION

AC	Alternating current
AGC	Automatic Generation Control
APS	Automatic programming system
BESS	Battery-based energy storage system
CAES	Compressed air energy storage
CAISO	California ISO
CC	Combined-Cycle
CCGT	Combined-Cycle Gas Turbine
CT	Combustion turbines
DC	Direct current
DMOL	Designed Minimum Operating Level
emf	Electromotive force
ENTSO-E	European Network of Transmission System Operators for Electricity
ESS	Energy storage system
EU	European Union
EV	Electric vehicle
FiT	Feed-in-Tariff
GPP	Gas power plant
GSO	Grid Service Operators
HELCO	Hawaii Electric Light Company
HPP	Hydro power plant

HVDC	High voltage direct current
IEA	International Energy Agency
ISO	Independent System Operator
ITE	Integrated test environment
LFC	Load-frequency control
LGU	Largest generating unit
MAS	Multi-Agent System
MGL	Minimum Generation Level
NEM	Net Energy Metering
NREL	National Renewable Energy Laboratory
OCGT	Open Cycle Gas Turbine
PID	Proportional-integral-derivative
PJM	Pennsylvania-New Jersey-Maryland Interconnection
PNNL	Pacific Northwest National Laboratory
PTM	Pusat Tenaga Malaysia
PV	Photovoltaic
R/X	Reactance to resistance
RC	Registered Capacity
RE	Renewable energy
ROI	Return of investment
RPM	Revolutions per minute
RTS	Reliability Test System
SAPP	South African Power Pool

SEB	Sarawak Energy Berhad
SEDA	Sustainable Energy Development Authority
SESB	Sabah Electric Sdn Bhd
SOC	State-of-charge
ST	Steam turbine
TC	Time constant
TNB	Tenaga Nasional Berhad
TPP	Thermal power plant
TSO	Transmission System Operators
UCTE	Union for the Coordination of the Transmission of Electricity
VFT	Variable frequency transformer
VSC	Voltage source converters
WPP	Wind power plant

CHAPTER 1

INTRODUCTION

1.1 Research Background

In large alternating current (AC) networks, three-phase synchronous generators are largely relied upon for power generation. Also known as alternators, these generators are used to convert mechanical power generated by steam or gas or hydraulic turbines to AC electric power. Essentially, a synchronous generator is formed by two main components: the stator and the rotor, as seen in Figure 1.1.

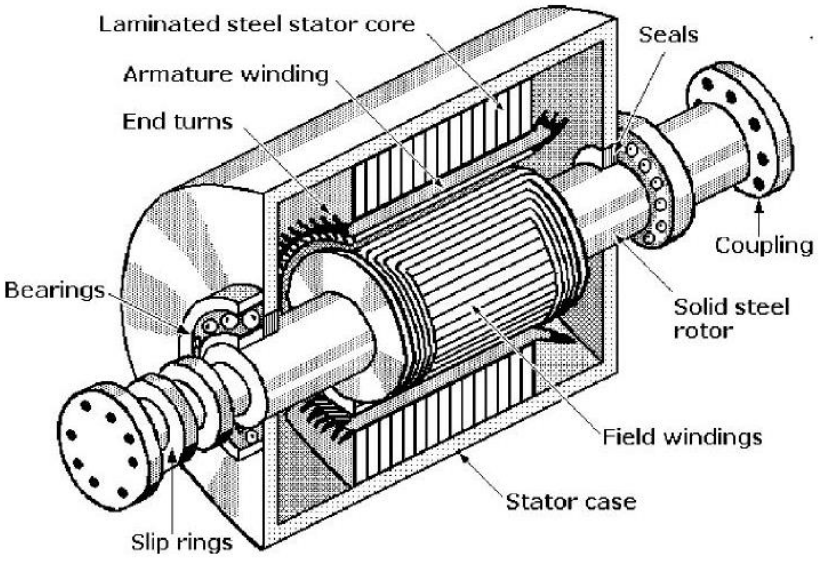

Figure 1.1: Main components of a synchronous generator (Sedky, 2009)

The stator, also known as the armature, is made of thin laminations of highly permeable steel, held together by a stator frame to provide mechanical support to the machine. Meanwhile, the inside surface of the stator are filled with slots to accommodate thick armature conductors, which are arranged symmetrically to form a balanced three-phase windings. A set of three conductors that constitutes the armature winding corresponds to three phases of power grid, as shown in Figure 1.2. To generate a uniform torque on the rotor, the phases are wound such that they are 120 degrees apart spatially on the stator.

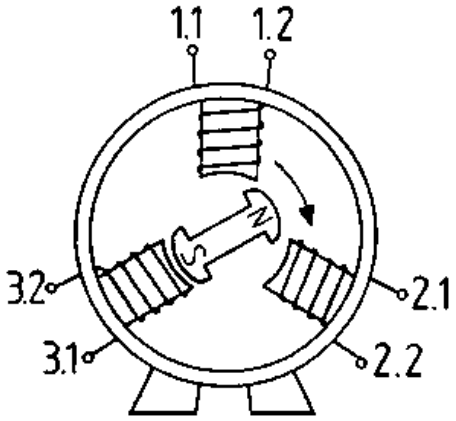

Figure 1.2: Three windings that constitute the armature winding in stator, corresponding to three phases of power grid (Department of Computer Science, University of Waikato)

On the other hand, the rotor contains the field winding, which is excited by direct current (DC) through the slip rings and brushes, shown in Figure 1.3. The DC supply typically comes from a DC generator known as the exciter that is usually mounted on the same shaft as the synchronous machine. In larger generators, AC exciters and solid state rectifiers are more commonly used instead.

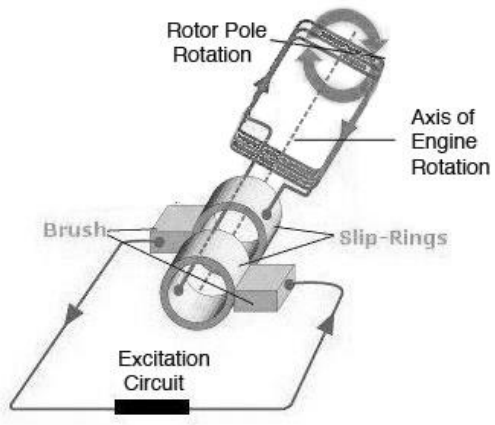

Figure 1.3: Components of a rotor (Holt, 2009)

Meanwhile, a detailed cross-section of a 500MW synchronous generator with a 2400kW DC exciter is shown in Figure 1.4. As such, the 25 kW pilot exciter controls the variable field of main exciter, which in turn supplies the electric current to the rotor through the slip rings and brush.

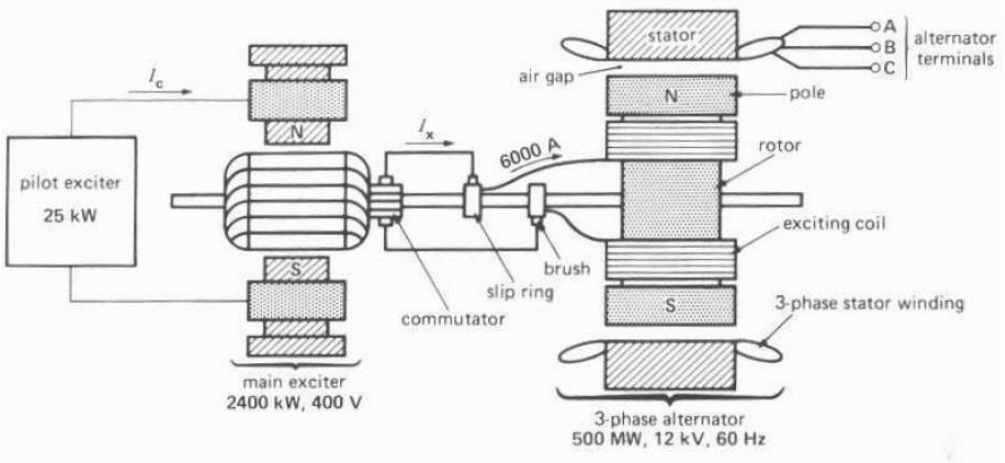

Figure 1.4: A detailed cross-section of a 500MW synchronous generator

(Sedky, 2009)

Based on Faraday's Law of Electromagnetic Induction, if there exists a conductor in a varying magnetic field or a conductor is moved in a magnetic field, an electromotive force (emf) is induced in the conductor. When a power source mechanically turns the rotor (acts as a magnet) at a constant speed, the magnetic field goes through the armature conductor that is electrically connected to the end-users (load); therefore current is induced into the stator and electrical power is generated.

The induced currents in the three conductors of the armature combine spatially to represent the magnetic field of a single rotating magnet. Similarly, the rotor represents a single dipole magnetic field. As these two fields spin, they move in synchronicity while maintaining a fixed position to each other. In simpler words, the term synchronous refers to the phenomenon whereby the rotor and the magnetic field rotate at the same speed.

The frequency of the induced voltage in the stator that corresponds to the utility frequency, f is directly proportional to the rotation rate of the rotor (in revolutions per minute, RPM), *N*. It is given in Eq. 1.1, where *P* is the number of magnetic rotor poles.

$$f = \frac{PN}{120} \tag{1.1}$$

Hence, the utility frequency is the nominal frequency at where the AC oscillates in the power transmission and distribution of an electric grid, from power plants to the end-users. While utility frequency is most commonly set at 50 Hz around the world, 60 Hz is also commonly seen in North Americas and some countries. Basically, the utility frequency is maintained by balancing the real power generation and load. The utility companies forecast the load demand for the next day on a daily basis; hence the number of generators and the power level they are running are planned ahead. Meanwhile, a certain amount of extra generating capacity of the generators connected to the network is to be reserved as for both the standby of the loss of generating unit and regulation provision, known as the spinning reserve. For instance in the case of Peninsular Malaysia, a total of 1,200MW of spinning reserve is allocated from 2015-2019; 1,000MW acts as a standby while 200MW is for regulation (Suruhanjaya Tenaga (Energy Commission), 2016).

The governor speed of generators is tied to the grid frequency, in which the governor operates under droop speed control. A droop speed control adjusts the governor speed based on the frequency deviation signals, by changing the position of control and intercept valves that dictates the power output. A figure of a mechanical speed governor is shown in Figure 1.5. In short, the governor adjusts its position output based on the rotor speed signal, ω_r. There are also variants of electronic governors and digital systems replacing the mechanical governors, with

similar overall functional requirements though with a faster response (Kundur, 1993).

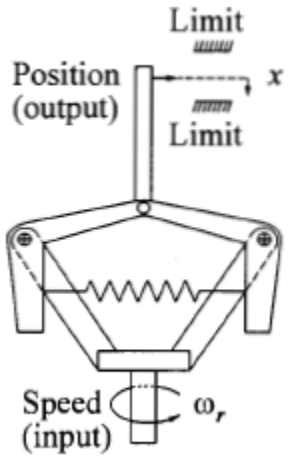

Figure 1.5: A mechanical speed governor (Kundur, 1993)

Magnitude of power mismatch aside, the frequency deviation is also mainly dependent on the grid inertia, which is provided by the rotating masses of generators. For instance, with large grid inertia in a power system in the event of a power mismatch, the rotor speed is not easily influenced as the rotor inertia keeps itself spinning at a constant speed, hence keeping a constant grid frequency.

However, with the increasing installations of intermittent power production sources like wind and photovoltaic (PV) systems in the power systems, the power mismatch between generation and load is anticipated to get worsened, driving the grid frequency to be out of the nominal range. A sample of 5-day averaged PV power profile measured within the university compound during the research work of this dissertation is shown in Figure 1.6, displaying high fluctuations of power

production. At the same time, replacing conventional power plants with intermittent power sources directly decrease the grid inertia, rendering power grid to be susceptible to the occurrence of frequency events.

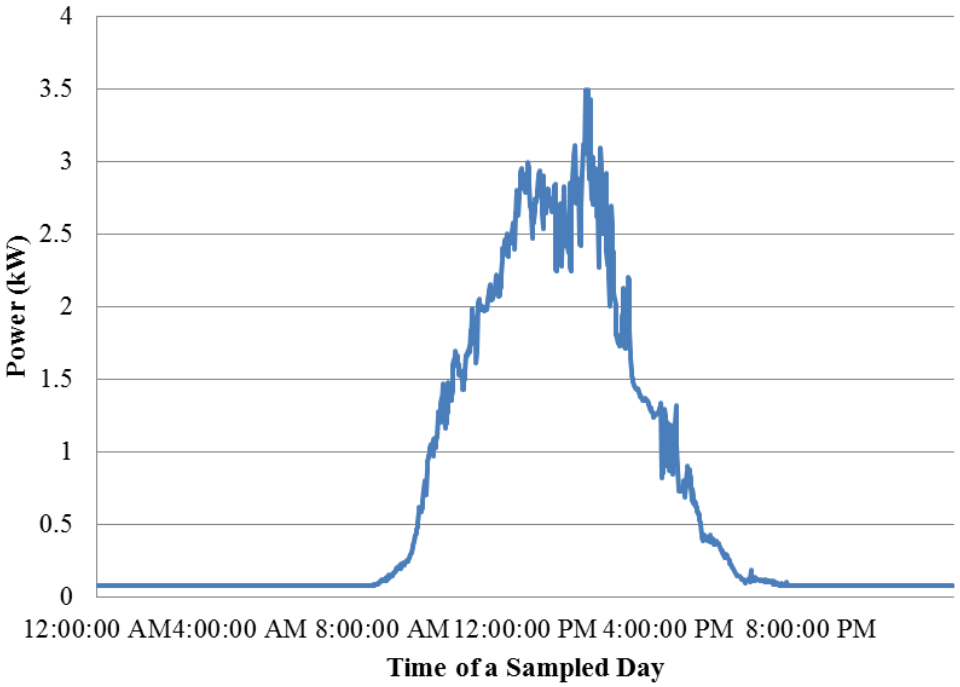

Figure 1.6: A 5-day averaged PV power profile

Based on Renewables 2016 Global Status Report compiled by the Renewable Energy Policy Network, PV and wind energy have average annual growth rates of 42% and 17% respectively from 2010 to 2015, contributing about 1.4% of global energy consumption in 2014 (REN21, 2016). In Malaysia in particular, although the total power generation from renewable energy (RE) is almost negligible in 2014, it is expected to increase to up to 3% in 2024 (Suruhanjaya Tenaga (Energy Commission), 2014).

It is crucial to maintain grid frequency within statutory limits to protect the operations and conditions of electrical equipment as they are designed to operate under certain system frequency; over- or under-frequency might contribute to overheating or spoiling the equipment. Besides, the impedance of a power system, specifically the reactance is dependent on frequency, thus a stable grid frequency is crucial to maintain the smooth operation of a power system.

Currently, the frequency regulation in the power system is performed by conventional power plants. However, the task requires frequent ramping up and down of power production, which increases the wear and tear of generators and decreases the efficiency. Besides, they have limited ramping rate and duration due to their mechanical components. It also requires a certain share of power plant capacity to be set aside as regulation capacity, hence they are run at a lower capacity, indirectly driving up the cost of electricity.

Energy storage system (ESS), on the other hand, possesses shorter response time than traditional generators, besides having higher ramp rates and high cycling ability. In fact, ESS has been recently utilised for small-scale regulation services in Europe and Americas. However, most researches (to be discussed in Chapter 2.6) mainly focus on the control performance without a long-term consideration of the state-of-charge (SOC) or capacity of the ESS, therefore neglecting its long-term sustainability in regulating frequency. Also, certain important aspects like

the placement of ESS for effective frequency regulation on the power grid and voltage issues have not been investigated by the current authors.

Hence, a comprehensive work package is developed and presented in the dissertation to address the important aspects of using ESS for frequency regulation on an interconnected power system. An offset control algorithm is developed in MATLAB/Simulink under this work package to study how ESS can regulate the frequency while conserving its energy under the constraints of the SOC. This model is able to determine the optimum capacity of ESS and is used to study the effects of ESS on the quality of frequency if the size of ESS is reduced under the penetration of RE sources on the networks. Then, a task is developed in MATLAB/Matpower to identify the best locations where ESS can be installed on a control area to carry out frequency regulation effectively without creating voltage regulation issues. Essentially, this work package is used to investigate the feasibility of using ESS as a means of frequency regulation in the power network under the increased penetration of PV.

1.2 Objectives

The objectives of this research work are as follows:

I. To propose a comprehensive work package for adopting ESSs to carry out frequency regulation continuously in an interconnected power system.

II. To evaluate the performance of the proposed framework in terms of the frequency regulation algorithm and the capacity conservation offset algorithm of ESS.

III. To identify the optimal ESS location for frequency regulation purpose in the transmission network in terms of frequency regulation quality and minimal voltage impact to the power grid.

IV. To evaluate the case studies of high PV penetration and the adoption of undersized ESSs for frequency regulation.

1.3 Research Methodology

This research aims to develop a comprehensive work package for adopting ESSs to carry out frequency regulation continuously in an interconnected power system. The study was carried out using simulation approach, where the flow chart of methodology is given in Figure 1.7. The research methodology is divided into 7 steps as follows:

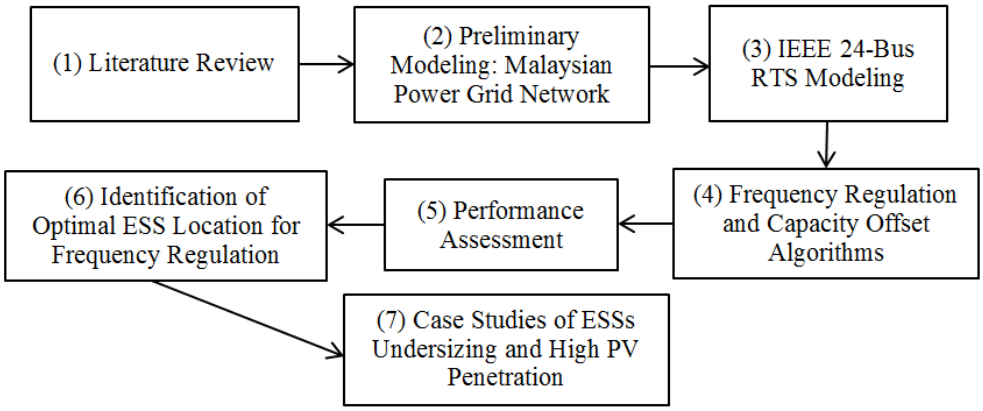

Figure 1.7: Flow chart of the methodology

Step 1: Literature Review

The mechanisms of traditionally frequency regulation and the pertinent current challenges are researched. Later, the proposed works and solutions of the academic and industrial authors are summarised and critically reviewed. A sensible approach to the solution of the problem is proposed based on the literature review.

Step 2: Preliminary Modelling: Malaysian Power Grid Network

A preliminary modelling to the problem is carried out in MATLAB/Simulink with the Malaysian power grid network. A simple single control area is modelled to prove the feasibility of the approach. In the meantime, the model shed lights on the shortcomings of the analysis due to the lack of grid network data. The results collected in the modelling serves to further improve on a more complicated modelling of the problem for a more in-depth study.

Step 3: IEEE 24-Bus Power System Modelling

A more complicated three control area of IEEE 24-Bus Reliability Test System (RTS) is modelled in MATLAB/Simulink. The RTS is modified so as to more closely resemble the current power system. The modelling is a step-up from Step 2 by including more advanced control features and detailed modelling of power system.

Step 4: Frequency Regulation and Capacity Offset Algorithms

The frequency regulation algorithm of ESSs is designed such that the frequency deviation can be minimised effectively. Besides, a capacity offset algorithm is designed such that the capacity of ESSs can be maintained in a healthy range for the continuous operation of frequency regulation.

Step 5: Performance Assessment

One week of load profile is simulated to evaluate the performance of the designed frequency regulation and capacity offset algorithms.

Step 6: Identification of Optimal ESS Location for Frequency Regulation

The optimal placement of ESS in network is identified by running repeated simulations while varying the positioning of ESS in the control areas. The time series of the power profile of each generating unit and the respective load profiles are obtained as input values for the subsequent modelling in Matpower, a load flow tool. The Matpower modelling of IEEE 24-Bus RTS is to identify the exact

busbar placement of ESS within the control areas for minimal impact on grid voltages.

Step 7: Case Studies of ESSs Undersizing and High PV Penetration

A case study of a high PV penetration in the power system is modelled to study its effects on the proposed methodology. Also, some case studies of undersizing ESSs for grid frequency regulation aided by the actions of capacity offset algorithm are simulated.

1.4 Research Outline

The structure of the dissertation is outlined in the following manner:

Chapter 2 summarizes the literature review on the conventional frequency regulation mechanisms, while also highlighting the respective shortcomings of the traditional generators and the potential challenges brought by intermittent RE sources. The research work carried out by other researchers is reviewed critically before the rationale for formulating the research objectives of the dissertation is stated.

Chapter 3 explains the methodology of the proposed work package, where two power networks are modelled, of the Peninsular Malaysia and IEEE 24-bus RTS.

The modelling of power plants with transfer functions in Simulink is described, along with their pertinent daily scheduling and load profiles in MATLAB/Simulink for frequency response analysis. The proposed frequency regulation control algorithm and capacity offset algorithm for ESS are illustrated as well. In addition, the use of an integrated automatic programming system (APS) test environment (ITE) through the cooperation with Newcastle University for the load flow studies in Matpower is elucidated. The case studies considered in the dissertation are also laid out.

Chapter 4 presents the simulation results of the Peninsular Malaysian and IEEE 24-bus RTS network separately. The effectiveness of the proposed algorithms for ESS under various scenarios and case studies is assessed. Other than that, the optimal placement of ESS in the power grid is identified while the effects of undersizing ESS are scrutinised.

Chapter 5 draws the conclusion of the dissertation by summarising the major findings and takeaways of the research work. Besides that, the potential future work is discussed for the reference of readers and other researchers.

1.5 Publications

Based on the research findings, a paper has been published in an international conference listed as follows:

Table 1.1: List of publication

No.	Title	Status	Journal/ Conference	Index/ Impact Factor
1	Frequency Regulation Mechanism of Energy Storage System for the Power Grid	Accepted	Conference: 4th IET International Conference on Clean Energy and Technology 2016	SCOPUS

Meanwhile, a journal paper is in the process of composition for submission as per the completion of this dissertation.

CHAPTER 2

LITERATURE REVIEW

2.1 Introduction

This chapter first summarises the general concepts of electricity markets and the description of the pertinent frequency regulation mechanisms. Next, the challenges of the conventional frequency regulation are presented, before delving into the works and solutions proposed by the academic and industrial authors. The rationales for the objectives of this research work are highlighted before the summary of this chapter.

2.2 Electricity Markets – Deregulated Market

The electricity market is mainly divided into two; first, it is the deregulated electricity wholesale market as it is seen in the Europe and United States (US), where electricity is traded as a commodity and second, it is a tightly regulated monopoly by an organisation where a single unified electricity tariff is adopted as it is with Malaysia. A regulated electricity structure is whereby one main company, known as the Utility, owns the entire infrastructure of transmission and

distribution, purchasing electricity from power generation companies before distributing it to the consumers. Meanwhile, in a deregulated market, multiple parties are involved; although the Utility still owns the infrastructure and distributing electricity to the consumers, it is not the sole buyer of electricity. Hence, there are multiple sellers in the market, encouraging competitive bidding and pricing in the electricity market.

A wide area synchronous electric grid is a regional electrical grid that is tied together, operating at a synchronised frequency. Some examples of the grid network are the Continental European Synchronous Area (formerly known as the Union for the Coordination of the Transmission of Electricity (UCTE) that covers multiple countries in Europe, NORDEL that covers the Nordic countries, and Eastern Interconnection that covers between eastern US and Canada. The interconnections between synchronous grids can be tied to each other via high voltage direct current (HVDC) power transmission lines and variable frequency transformers (VFTs). Most of the wide area synchronous electric grids are deregulated electricity markets. Besides the aforementioned grid networks, other examples are the Indian national grid and Southern African Power Pool (SAPP) (Indian Energy Exchange, 2017; Southern African Power Pool, 2016).

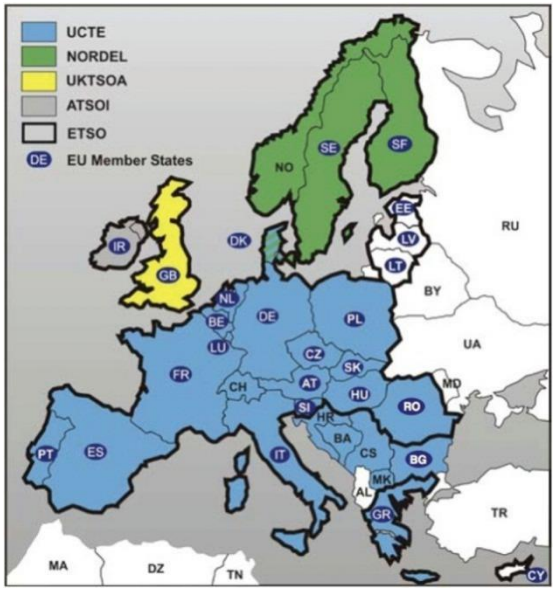

Figure 2.1: Wide area synchronous grids in Europe (Forschungsstelle für Energiewirtschaft e.V., 2017)

The wide area synchronous grids as seen in Europe and shown in Figure 2.1 forms the European Network of Transmission System Operators for Electricity, namely ENTSO-E, with the objectives of supporting the implementation of European Union (EU) energy policy. Therefore, the ENTSO-E regulates the electricity transmission and distribution frameworks of Europe, including frequency regulation. In fact, similar frequency regulation framework is applied all across the world; hence, only the ENTSO-E regulation is presented for the case of a deregulated electricity market. On the implementation of frequency regulation, there are more than 40 transmission system operators (TSOs) in ENTSO-E that are responsible for the task. As such, TSOs are the ones that are accountable for the purchasing of frequency regulation services in the deregulated market through biddings or auctions of power and energy.

There are basically two main commodities in the electricity supply: power and energy. Power is the net electrical transfer rate at any given time, measured in megawatts (MW) while energy is the electricity that flows through a point for a given time, measured in megawatt-hours (MWh). In this context, the bid amount is the power while the delivery duration gives the energy required out of the participating unit.

2.3 Conventional Frequency Regulation

In general, a stable utility frequency is achieved by maintaining the balance between real power generation and load. Should there be a shortage of power in the grid, power is temporarily drawn from the rotor to satisfy the load demand, decreasing the kinetic energy and the speed of the rotor, hence the utility frequency. The speed governor that detects such rotor speed change triggers the control valves to be opened to regulate the rotor to its nominal speed, hence the nominal frequency, f_0. The similar principle applies when there is an excess of power in the grid. The utility frequency deviation in the event of power mismatch is given by the Swing Equation, as shown in Eq. 2.1.

$$\frac{df}{dt} = f_0 \frac{P_m - P_e}{2H} \tag{2.1}$$

P_m and P_e are the mechanical and electrical power of the rotor respectively, where H is the inertia constant of machine. Hence, based on Eq. 2.1, the magnitude of frequency deviation is mainly dependent on two parameters; the mismatch between load and generation and the grid inertia.

On a side note, H is the normalisation of M, also known as the inertia constant of machine, given in Eq. 2.2, where ω is the angular speed of the rotor and S_{rated} is the three-phase rating of the machine in MVA.

$$H = \frac{M\omega}{2S_{rated}} \tag{2.2}$$

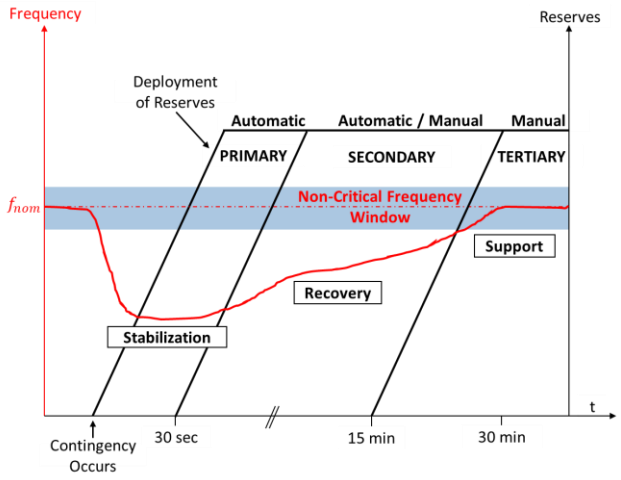

Figure 2.2: Three frequency regulation actions in the ENTSO-E

The frequency regulation in the ENTSO-E is carried out in three actions: primary, secondary, and tertiary, as seen in Figure 2.2 (UCTE, 2004). Each action of the frequency regulation has its respective tasks and desirable response times. In the case that a large frequency deviation occurs, the primary control is to take charge

within seconds to stabilise the frequency, before the secondary control sets in for frequency recovery. On the other hand, the tertiary control acts if the secondary control fails to restore the frequency.

2.3.1 Primary Frequency Control

On the primary frequency control, the activation is done automatically and locally by all participating units, with the main aim at reestablishing the balance between the supply and demand of power. The control is carried out automatically such that the governor of the generators is set to a droop control mode, in which the governor speed or the power output is linearly proportional with the frequency deviation (Kundur, 1993). The equation of droop rating, *R* is given in Eq. 2.3.

$$R = \frac{percentage\ of\ speed\ or\ frequency\ change}{percentage\ of\ power\ output\ change} x\ 100\% \tag{2.3}$$

Referring to Eq. 2.3 for instance, a 5% droop rating implies that a 5% frequency deviation results in 100% change in the power output. An illustration of a 5% droop rating assuming the generating unit is running at 50% power output initially is shown in Figure 2.3, in which the droop control renders the generating unit to ramp up the power to 100% power output (hence a 100% change) when it is subject to a 5% frequency deviation.

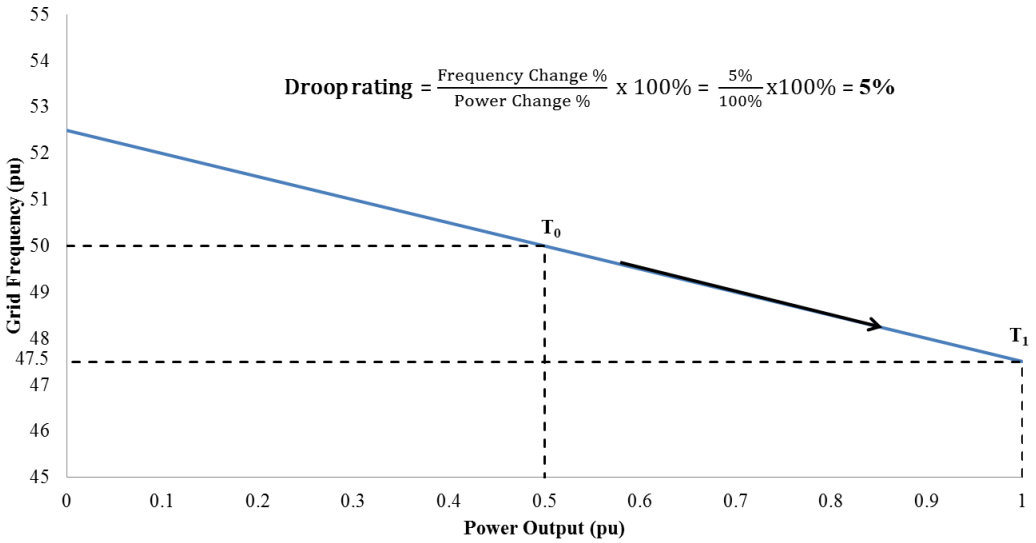

Figure 2.3: An illustration of the control mechanism of a 5% droop rating in primary frequency control

The maximum allowable "quasi steady-state" frequency deviation is ±0.2 Hz, while the primary frequency control is to set in within 15 seconds. The provisions for the primary control are to be fully activated after 30 seconds, which is known as the response time, while the minimum duration of delivering the power, namely delivery time, is 15 minutes, until the secondary or tertiary control is ready to take over.

2.3.2 Secondary Frequency Control

On the secondary frequency control, the participating unit is required to run at a power level that is between the maximum and minimum power output. This

criterion is to ensure that the participating unit has the ability to respond symmetrically. The term “symmetry” in frequency regulation context, implies that a participating unit is able to supply and absorb power, contributing to frequency regulation symmetrically in both the addition and subtraction of power. It is required to set in within 30 seconds the latest upon a frequency event, taking over from the primary frequency control (Schmutz, 2013).

2.3.3 Tertiary Frequency Control

Last but not least, tertiary frequency control is manually called upon if the grid frequency is not recovered back to its nominal value after 15 minutes. Tertiary reserves are expected to run continuously until the event is resolved by generation rescheduling.

2.3.4 Summary of Frequency Control Actions

The frequency regulation actions are summarised in Table 2.1. To qualify for the biddings, the prospective suppliers are to fulfil certain prequalification procedure conducted by the TSOs to demonstrate their ability to meet the technical requirements of frequency regulation as required, to ensure the reliability of service.

Table 2.1: Summary of frequency regulation actions

Frequency Regulation Actions	Primary	Secondary	Tertiary
Response Time	15 seconds Full activation: 30 seconds	30 seconds	15 minutes
Delivery Time	15 minutes	15 minutes	Until the situation is resolved
Power/Energy Provision Auction	Symmetrical	Symmetrical	Asymmetrical; successful power bidders are to bid for energy as well

2.4 Electricity Market – Regulated Market

Meanwhile in Malaysia, under the Malaysian National Grid framework, there are three grid service operators (GSOs) responsible to serve the three regions of Malaysia: Tenaga Nasional Berhad (TNB) in the Peninsular, Sabah Electric Sdn Bhd (SESB) in Sabah, and Sarawak Energy Berhad (SEB) in Sarawak. The Malaysian grid network is regulated in such a way that the GSOs are the sole buyers of the electricity generated by the power producers within their region of responsibility. In addition, the GSOs are also responsible for frequency regulation apart from the reliability of power supply.

However, unlike the earlier mentioned deregulated grid structure, each generating unit is to participate in all the actions of frequency regulation. In fact per Malaysian Grid Codes, “Each Generating Unit or Combined Cycle Gas Turbine

(CCGT) Module or Power Park Module must be capable of providing response" (Suruhanjaya Tenaga (Energy Commission), 2014).

A Power Park Module is comprised of a collection of non-synchronous generating units that are powered by an intermittent power source (in which the primary source of power is not controllable, wind and solar, for example) that is connected to the transmission system. In short, all the generating units that are connected to the grid network are to respond to the frequency deviation (Suruhanjaya Tenaga (Energy Commission), 2014). However, it is understood that the intermittent power sources are not able to respond to frequency deviation effectively.

The Malaysian grid frequency is to be maintained within the limits of 49.5 Hz to 50.5 Hz, except under exceptional circumstances. Some examples of the exceptional circumstances include the failure of operation of the generating unit and transmission system. The utility frequency regulation responses are divided into primary, secondary, and high-frequency response; the previous two deal with frequency decrease while the latter deals with frequency increase.

On the other hand, each generating unit connected to the Malaysian grid is to run above the Minimum Generation Level (MGL). The MGL is defined as a maximum of 65% of the Registered Capacity (RC) of a generating unit. Under normal circumstances, the generating unit will not be dispatched to run below the MGL; however, it must be capable of operating down to the Designed Minimum

Operating Level (DMOL). The DMOL is defined as a maximum of 55% of the RC. This is to cater for high-frequency events, where the generating unit has to be ramped down.

The response level of each generating unit during a frequency deviation depends on its loading levels and the magnitude of the deviation, unless it reaches its full capacity. A sample of minimum frequency response requirement profile for a certain frequency deviation is shown in Figure 2.4, in which the actual profile might differ for each generating unit. Any response level that is below this minimum requirement is considered unacceptable by the GSOs. From Figure 2.4, while it shows that a generating unit is not required to provide any response during a high-frequency event at DMOL, it is obliged to further ramp down the power output should the frequency is at or above 50.5 Hz.

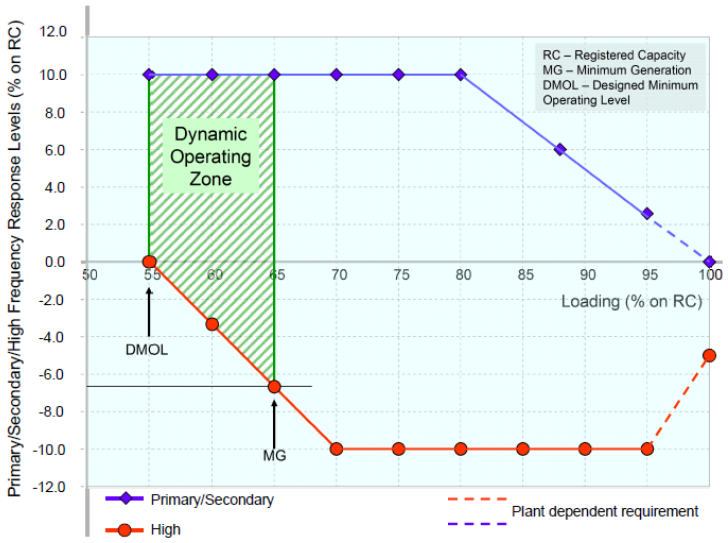

Figure 2.4: Minimum frequency response requirement profile for a certain frequency deviation of a generating unit (Suruhanjaya Tenaga (Energy Commission), 2014)

The response criteria for the three frequency control actions are shown in Table 2.2 below:

Table 2.2: Response criteria of three frequency control actions based on the Malaysian Grid Code

Control Actions for Frequency Regulation	Response Time (s)	Power Delivery Time
Primary Response	10	30 seconds
Secondary Response	30	30 minutes
High-Frequency Response	10	n/a

Unlike the primary and secondary response, high-frequency response does not require additional fuel to be carried out; since it deals with the ramping down of power, the response time of power plants is crucial. Compared with the ENTSO-E criteria, the delivery time of primary response does not overlap with that of the secondary response. Also, there is not a stipulation of the frequency response measures beyond the 30 minutes delivery time of secondary response. However, there is one additional regulation in the Malaysian Grid Code whereby the generating units are to be fully restored within 20 minutes to its full responsive capability after responding to a significant frequency disturbance.

To cater for regulation capacity, a certain percentage of power plant capacity has to be set aside as spinning reserves. Therefore, the cost of energy generation is indirectly increased as the power plants are running on part-loads, which is very likely to be channelled to the consumers (Koh et al., 2011).

2.5 Issues Related to the Conventional Mechanism of Frequency Regulation

2.5.1 Slow Response of Synchronous Generators towards Frequency Changes

As frequency regulation requires frequent ramping of generating units, their limited ramping capability due to their rotary turbo-machinery features may result in limited regulation ability. Based on a report from the Pacific Northwest National Laboratory (PNNL) (Makarov et al., 2008), the ramping capability of various types of the generating units managed by the California Independent System Operator (ISO) is shown in Table 2.3. While the regulation capacity can be increased by having more generating units, the frequency regulation quality is essentially limited by their ramp rate and ramp duration capability.

Table 2.3: Ramping capability and duration of various generating units

Unit Type	Averaging Ramping Capability, % per Minute	Average Duration Capability of Highest Ramp (minute)
Natural-Gas-Fired Steam Turbines (STs)	1.8	3.9
Combined-Cycle (CCs)	2	5.4
Combustion Turbines (CTs)	20.4	N/A
Hydro Aggregate	13.2	1.9
Hydro	44.5	0.9

In addition, varying the loads of fossil-based power plants induces thermal and pressure stresses within the system such as the boilers, steam lines, turbines, and auxiliary components (Lew et al., 2013). The effects are not only the resulting

wear-and-tear that may incur additional capital and maintenance costs due to the reduced life expectancies of components (Connolly et al., 2011; EPRI, 2001), a prolonged ramping also degrades the fuel conversion efficiency (Lefton and Besuner, 2001).

On the other hand, according to Wärtsilä, a Finnish manufacturer and service provider of power sources, the starting loading capability of gas turbines is different from their advertised ramp rate, in which the full ramp rates are only achieved when a particular unit reaches its self-sustaining speed (Wärtsilä). Traditionally, the ramp rates of CCGTs are limited to allow steam temperatures and pressures to rise within tolerable limits to control the thermal stress imparted on the steam generators and turbine. Recently, the achievements of improved boiler designs, along with the bypass system designs that allow ramping to be done independently of steam turbine, stretch the limits of CCGTs in terms of ramp rate. However, this is not achievable without incurring higher maintenance costs. As a side note, Wärtsilä claimed that its combustion engines are able to reach a ramp rate of 50% capacity per minute.

Meanwhile, in a report of Cost and Performance Data for Power Generation Technologies prepared to the National Renewable Energy Laboratory (NREL), the ramp rate values presented by them to evaluate the cost and performance date for power generation technologies are shown in Table 2.4 (Black & Veatch, 2012).

Table 2.4: Ramp rates of various generating unit types

Unit Type	Ramp Rate, % per Minute
Nuclear	5
Gas Turbine	8.33
CCs	5
Pulverised Coal-Fired	2

2.5.2 Reduction in the Inertia of Power System Caused by the Increased PV Systems and Wind Turbines

The limitations of the traditional generating units are not helped by the increased penetration of PV systems and wind turbines in the near future. Such phenomenon reduces the number of synchronous generators on power systems. As a result, the moment of inertia in the power system is reduced, hence making the system frequency to be very susceptible to the power mismatches (Knap et al., 2014). With the current low response of the generators to the frequency changes, the existing mechanism of controlling the frequency may not be effective.

According to the estimated RE share on the global electricity production in 2015 (REN21, 2016), wind and PV are estimated to contribute 3.7% and 1.2% respectively of the total generation. While the projection for the future wind and PV contribution is inconsistent based on the assumptions made in forecasting models (U.S. Energy Information Administration, 2016), the historical trends as shown in Figures 2.5 and 2.6 suggest that the pickup is exponential.

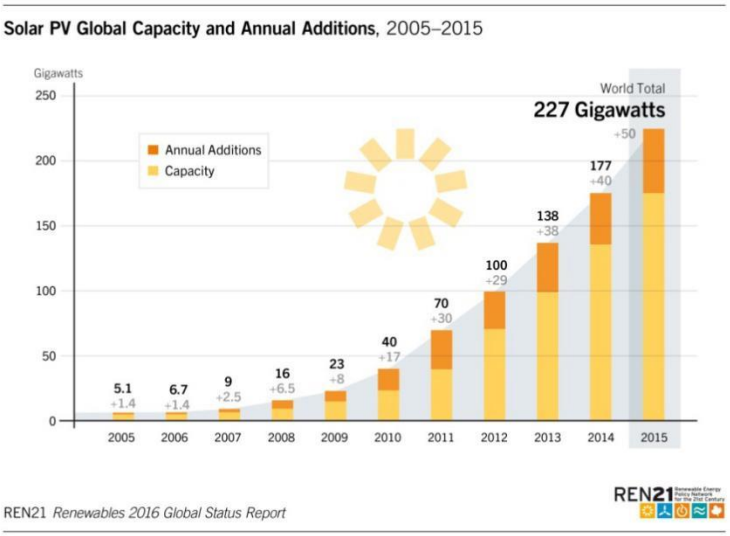

Figure 2.5: Solar PV global capacity and annual additions, 2005-2015

(REN21, 2016)

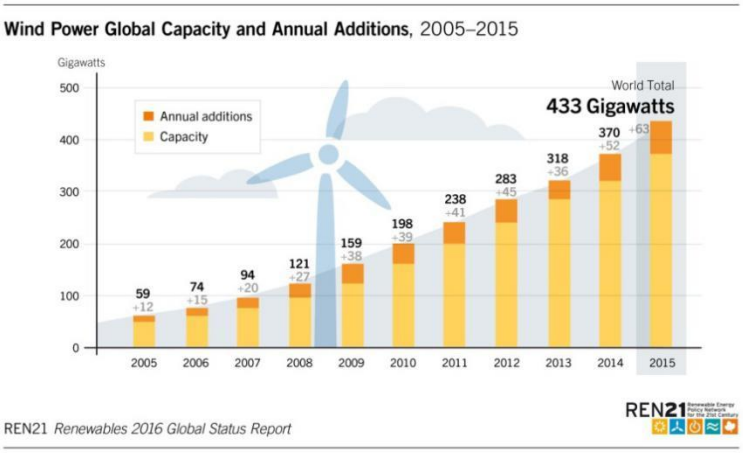

Figure 2.6: Wind power global capacity and annual additions, 2005-2015

(REN21, 2016)

In Malaysia, the power generation derived from RE is almost negligible in 2014, but it is planned for the share to reach at least 3% by 2024 (Suruhanjaya Tenaga (Energy Commission), 2014). To achieve the goal, the Sustainable Energy Development Authority (SEDA) Malaysia first incurred a 1% surcharge on electricity bills to pool funds for the Feed-in-Tariff (FiT) of RE in 2011. The FiT was meant to provide incentives for the industrial, commercial, and residential consumers to install RE resources for electricity production to the common grid. The figure was later revised to 1.6% in 2014 before being phased out in 2016, in favour of a lower-rate net energy metering (NEM) after the Malaysian RE industry, in particular the PV industry was established.

In a longer horizon, the solar energy is projected to contribute at least 6,500 MW by 2030, by the Pusat Tenaga Malaysia (PTM) and the International Energy Agency (IEA) (Augustin et al., 2012). Meanwhile, wind energy is less favourable in Malaysia due to the geographical location and climate in the equatorial region (Wong J., 2015).

2.6 Proposed Solutions for Supplementing the Existing Mechanism for Frequency Regulation

2.6.1 ESSs

There are various types of ESSs that are employed for industrial use, summarized in Table 2.5. ESSs are mainly utilised to capture the energy production preferably when extra energy is generated in the system, such that the energy can be supplied during occasions that it is needed and the energy production from other sources is scarce.

Table 2.5: Types of ESSs with the pertinent examples

Types of ESSs	Examples
Mechanical	Compressed Air Energy Storage
	Flywheel Energy Storage
	Pumped-Storage
	Gravitational Potential Energy
Electrical/Electromagnetic	Capacitor
	Super Capacitor
	Superconducting Magnetic Energy Storage
Electrochemical	Battery
Thermal	Molten Salt Storage
	Solar Pond
	Liquid Nitrogen Engine
	Phase Change Material
	Thermal Energy Storage
	Steam Accumulator
Chemical	Biofuels
	Hydrogen Storage
	Hydrated Salts

The most common usage of ESSs is for electricity production, especially when they are coupled with RE sources. As RE sources are known for their

intermittency in power production, ESSs allow the energy produced throughout the day to be stored and released at strategic times, hence rendering RE sources relevant for some beneficial industrial applications. Besides providing heating and cooling in general, ESSs are also recently used to provide ancillary services in the power grid, including voltage regulation, operating reserve, peak shaving, and demand side management (Wong J. , 2015).

In fact, utilising ESS for frequency regulation services is an emerging idea since ESS has been commercialised for such purpose in Europe and Americas because of their fast response time and high cycling operation (Gyuk and Eckroad, 2003; Laszarewicz and Arseneaux, 2006). A summary of the advantages and disadvantages of the more common energy storage technologies is shown in Table 2.6 (Gustavsson, 2016).

Table 2.6: The advantages and disadvantages of some energy storage technologies

Energy Storage Technologies	Advantages	Disadvantages
Lead acid batteries	- Low cost - Mature technology - Able to provide high current	- Short lifespan, further shortened by deep discharge
Lithium ion batteries	- High energy density - Low weight	- High cost
Redox flow batteries	- Long cycle life - Short charging time	- Low efficiency (60-70%) - Low energy density - A more complicated design involving pumps, sensors, and control units
Flywheel	- High efficiency - Long cycle life	- High self-discharge rate - Sophisticated technology
Super capacitor	- Long cycle and shelf life	- High self-discharge rate - Low energy density
Pumped-storage	- Long lifetime - Mature technology	- Relatively slow response - Inflexible in terms of geographical restrictions - Huge capital expenditure - Low energy capacity

Based on the references (Black & Veatch, 2012; First Hydro Company, 2009), the ramp rates of ESSs are presented in Table 2.7, showing higher ramp rates than the conventional power plants.

Table 2.7: Ramp rates of ESSs

ESSs	Ramp Rate, % per Minute
Pumped-Storage Hydro	50
Battery-based Energy Storage System (BESS) (Sodium Sulfide)	20%/sec
Compressed Air Energy Storage (CAES)	10 (Black & Veatch, 2012)
	15-40 (First Hydro Company, 2009)
Flywheel	100

In fact, in one of the case studies presented (First Hydro Company, 2009), although the pumped hydro energy possesses the ability to achieve a ramp rate of 3% of capacity per second, a waiting period of several minutes is incurred for a change of its operating mode due to the massive hydrodynamic and mechanical inertia in the turbine. To counter the lag time, faster-responding sodium sulfide battery is picked as the backup resource.

On the other hand, in another report prepared by PNNL (Kintner-Meyer et al., 2012), it was discussed that the high ramp rates and cycling abilities of battery presents the opportunity for grid balancing to be done more effectively. In particular, the vanadium redox flow batteries have a response time of milliseconds, with the ability to sustain more than 200,000 cycles.

Some of the actual deployed physical projects for frequency regulation are a 1MW and 250kWh of lithium ion BESS at Hawaii (Hawai'i Natural Energy Institute, 2014), a 4MW and 8MWh lithium ion BESS at Jeju Island (Castillo et

al., 2014), and a 1MW and 580kWh of lithium ion BESS at Zurich (Koller et al., 2014).

In Hawaii, where the power grid is maintained by Hawaii Electric Light Company (HELCO), the wind and distributed PV contribute to approximately 15% and 3% of the total generation respectively. The phenomenon has limited further installation of intermittent RE sources as they have frequently resulted in grid-wide power imbalances. Therefore, HNEI developed a 1MW and 250kWh ESS made of lithium ion batteries on the grid system to perform frequency regulation and wind power smoothing. To test out the control algorithm before being deployed to the actual system, computer simulations were carried out to study hypothetical disturbance scenarios such as sudden loss of power generation and step load and wind power production change (Hawai'i Natural Energy Institute, 2014) .

In the algorithms developed, when the battery is close to its full capacity, its charge power limit is reduced; likewise, when the battery is close to being fully discharged, its discharge power limit is reduced. Besides that, the charging and discharging power limits are also adjusted based on the battery temperature. In the results, only graphical presentations were shown on the effectiveness of frequency control response, without quantifying the improvements. Besides that, the SOC profiles were not presented during the course of investigation; neither the effects of limiting the power control limits to the frequency profile were discussed.

In one of the substations in Jeju Island (Castillo et al., 2014), a 4MW and 8MWh ESS was connected for frequency regulation and shown to be operating continuously for three days. While a discharge limit is set for the steady-state operation, the ESS is automatically instructed to charge or discharge according to its SOC. However, the ESS is set to operate as required at all times, thus exposing the risk of overdischarging or overcharging the ESS. As such, the authors have not discussed about the risks of rendering the ESS inoperable due to overdischarging or overcharging. As the authors largely concentrated on the communication between hardware, the simulation only presented SOC and frequency profiles of three days, which may not be sufficient to justify the viability of regulating the network frequency using ESS.

2.6.2 Existing Methods of SOC Conservation for ESS

On the other hand, in the case of Zurich (Koller et al., 2014), the 1MW and 580kWh BESS was responsible for 1MW of frequency regulation power. The authors introduced a moving average approach to control the SOC of BESS by decreasing the overall power and energy required by BESS. Meanwhile, the value of power offset is capped and the offset rate is limited so as not to interfere with the frequency control performance. In short, in a moving average approach, the BESS power control is almost offset at all times. A simulation was run based on one year of actual frequency measurements. It was shown that the SOC was

within operating limits (0% $\leqslant$ SOC $\leqslant$ 100%) throughout the course of simulation, although the frequency profile was not presented. Since frequency regulation service of a predetermined power or energy magnitude is auctioned in a deregulated grid network, it is not required to model the other generating units of power systems but the BESS itself, hence the BESS operates independently. For real-time measurements, a few hours of frequency and SOC profiles were presented.

Meanwhile, the regulatory and market conditions molded the task of frequency regulation to be “net-zero” (or “zero-mean”) on the timescale of 10 to 15 minutes, in which the net energy supplied for frequency regulation is zero by balancing the occasions of over-generation and under-generation (Rojas and Lazarewicz, 2004).

For instance, ISOs such as Pennsylvania-New Jersey-Maryland Interconnection (PJM) and California ISO (CAISO) decompose the power required for frequency regulation known as Automatic Generation Control (AGC) signal into a few power commands to be allocated to various generating units (Campbell and Bradley, 2014). An illustration of the power command amplitude being decomposed into 5 power commands for 5 generating units is shown in Figure 2.7. As such, the power commands represent a sine curve to achieve a “net-zero” frequency regulation.

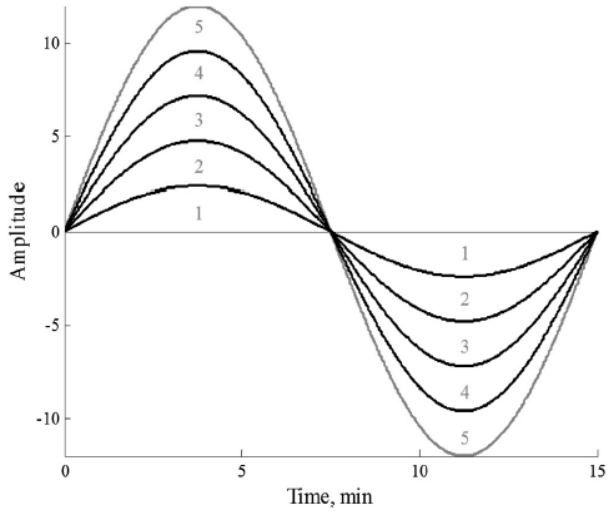

Figure 2.7: An illustration of the decomposed AGC signal of 5 power commands for 5 generating units (Campbell and Bradley, 2014)

However, frequency regulation services especially secondary control are not strictly zero-mean as system losses are unavoidable (Megel et al., 2013) Also, another statistical analysis shows that while frequency deviation profiles are close to a normal distribution, it presents a net outflow of energy in the long term (Borsche et al., 2013).

Nonetheless, Megel, et al. (2013) proposes to only manage fast and zero-mean frequency deviations with BESS while passing the rest of the tasks to other response resources. As such, another concept of offset algorithm based on SOC thresholds is recommended in an ENTSO-E grid. In simpler terms, the BESS power is only offset when its SOC goes out of a predefined range. This approach focuses on keeping the SOC in between the defined lower and upper thresholds to minimise the degradation of BESS. Meanwhile, the ramp rate of offset is set such

that it is slow enough for the power plants to follow so as not to negatively impact the quality of frequency regulation services. However, the paper mainly focuses on the return of investment (ROI) of the proposed primary frequency control while the overall frequency and SOC profile are not evaluated, therefore neglecting the impact of passing the non-zero-mean frequency deviations to the power plants.

In terms of SOC conservation, some authors proposed to rely on a mixture of methods while proposing BESS for primary frequency control (Oudalov et al., 2007). First, the paper proposes adjustable SOC limits while also incorporating the selling of energy to the market when the BESS is close to its full capacity. It is mentioned that the main intention of selling is to maintain the operability of BESS rather to make a profit. However, such approach only works in a deregulated electricity market. It is not necessary that there are buyers when electricity is needed to be sold off. Besides that, the authors included deadband charging when the frequency is within a non-critical range that does not require BESS action. This discharges to resistors as an emergency measure and introduces two groups of BESS units where they are only responsible for power injection and absorption respectively. While the paper aims to optimise the sizing and operation of BESS, it might have incurred additional costs and wastage by utilising dump loads and redundancy in BESS units as the results were not compared with other methods. Also, the authors presented that the frequency profile in UCTE is relatively stable on the simulated network, with a few frequency excursions being outside the

tolerance of ±0.1 Hz per month. While one month of healthy SOC profile was presented, the challenges brought by RE sources on the proposed BESS operability remains to be investigated.

2.6.3 Other Pertinent Solutions

Other forms of energy storage being used for frequency regulation purpose include flywheels (Rojas and Lazarewicz, 2004), vanadium redox flow battery (Lucas and Chondrogiannis, 2016; Shankar et al., 2016; Johnston et al., 2015), pumped storage (Perez-Diaz et al., 2014), electric vehicles (EVs) (Zhong et al., 2014), fuel cell and aqua electrolyser (Mallesham et al., 2011), and capacitors (Das et al., 2011), ranging from interconnected power systems, microgrids, and isolated networks.

Other than that, a small-scale laboratory test-bench is set up to investigate the frequency and voltage support of BESS in a microgrid, especially during islanding and grid synchronisation mode (Serban and Marinescu, 2014). Fuzzy logic-based droop control for both frequency and voltage regulation in an AC microgrid with PV source and wind turbines on the grid are also simulated by some others (Ahmadi et al., 2015). The works of other authors are summarised in Table 2.8.

Table 2.8: Summary of works of other authors

Authors	Network Type	Regulation Action/ ESS	SOC Conservation/ SOC Profile	Main/Other Features
(Li et al., 2014)	Two-area power system	Primary/ BESS	Three variable droop control strategies/ 1 day of SOC profile presented	- Voltage profiles are presented - No frequency profile presented
(Delille et al., 2012)	Island (French Island of Guadelou-pe)	Primary/ Ultra-capacitor	Deadband charging/ No SOC profile presented	- Wind and solar penetration - Mainly to mitigate the impact of non-inertia type generation - 50 s of frequency profile presented
(Rojas and Lazarewicz, 2004)	PJM at USA	Primary and secondary/ Flywheel	Not discussed/ Ran out of capacity after 30 minutes of continuous action	- Reacted well to fast transients and deep discharges - No frequency profile presented
(Lucas and Chondrogia nnis, 2016)	Microgrid	Primary/ Vanadium redox flow BESS	Not considered	- Performs load shaving as well - 30 s of frequency profile presented
(Shankar et al., 2016)	Two-area power system	Primary/ Redox flow BESS	Not considered	- Economic load dispatch and small signal stability analysis are included - Multiple types of generations units are modelled - 100 s of frequency profile presented

Table 2.8 continued: Summary of works of other authors

Authors	Network Type	Regulation Action/ ESS	SOC Conservation/ SOC Profile	Main/Other Features
(Johnston et al., 2015)	UK wind power plants (WPPs)	Primary/ Vanadium redox flow BESS	Not discussed/ 24 h of SOC profile presented	- Mainly on the economic optimisation of ESS in WPPs - No frequency profile presented
(Perez-Diaz et al., 2014)	Isolated power system	Primary and secondary/ Hydraulic short-circuit pumped-storage power plant	Capacity is mostly not an issue	- 20 minutes of frequency profile presented
(Zhong et al., 2014)	Two-area power system	Primary and Secondary/ Electric vehicles (EVs) and BESS	Based on the assumptions by author, the regulation capacity is almost available at all times and the scenario of unavailability is not addressed.	- Mainly on the coordination of EV charging facilities and energy storage devices in frequency regulation - 180 s of frequency profile presented
(Mallesham et al., 2011)	Microgrid	Primary/ Aqua electrolyzer, fuel cell, battery, and flywheel	Not considered	- Mainly to fine-tune the controller of various generating units - 300 s of frequency profile presented

Essentially, ESS acts as a source of synthetic inertia through its fast response to support the grid frequency. Besides ESS, other means of providing inertial

response have also been proposed, including utilising wind power plants and power electronics (Christensen and Tarnowski, 2011; Miller and Marken, 2010) and voltage source converters (VSC) -HVDC (Zhu et al., 2013) to provide inertial response on behalf of synchronous generators. Meanwhile, an unconventional method of multi-stage load shedding in the event of under frequency, as an effort of demand side management in a microgrid island is also investigated (Gu et al., 2013). However, the aforementioned methods are not practical to be adopted in conventional interconnected power systems.

2.6.4 The Rationale for Formulating the Research Objectives in this Dissertation

Based on the literature review, many research works may not focus on several important aspects of using ESS for achieving satisfactory frequency control on the networks. The first aspect is that the current works mainly focus on the control performance of ESS without much consideration of the long-term sustainability of the SOC of the ESS for frequency regulation. Secondly, most of the researchers have not thoroughly assessed the placement of the ESS across the power systems for achieving maximum quality of frequency. In addition, the voltage regulation imposed by the connection of ESS across the power systems should be studied to avoid any voltage violation. Also, additional research efforts should be carried out to investigate the quality of frequency as a result of the cooperative actions by the

ESS and the governors with respect to the amount of RE on the power systems. All the shortcomings as found in the literature review form the bases for formulating the research objectives in this dissertation to further validate the viability of using the ESS for frequency control under the increased penetration of RE in the future.

2.7 Summary

With the increased penetration of RE sources to the power grid in near future, it presents a challenge for the conventional grid frequency regulation, mainly due to three reasons: the limited ramp rate and duration of conventional power plants, the inconsistent power production of these RE sources, and the decrease of grid inertia for frequency support. Among the methods to support the grid frequency stability, fast-responding ESS acting as synthetic grid inertia emerges as the most potential solution.

However, most of the existing studies have not focused on the important criterion of utilising ESSs for a sustainable and an effective frequency control, namely the long-term sustainability of SOC of an ESS, the placement of ESS on the power grid for maximum quality of frequency with minimum voltage impact, and the inclusive modelling that includes the regulation actions of ESSs and governors with RE penetration. Therefore, a more comprehensive study of frequency

regulation by ESS is needed for the continuous effective service without causing disturbances to the general grid.

CHAPTER 3

METHODOLOGY

3.1 Introduction

This chapter describes the methodology of the dissertation, namely the concepts and the description of the simulation modelling of two grid networks; the Peninsular Malaysia and IEEE 24-bus RTS network. The first modelling of the Peninsular Malaysia grid network is carried out in MATLAB/Simulink; while presenting positive results in Chapter 4. Meanwhile, the second modelling of IEEE 24-bus RTS network is implemented in both MATLAB/Simulink and Matpower. The chapter ends with the description of the proposed comprehensive framework of utilising ESS for frequency regulation and summarising the earlier sections of the chapter.

3.2 Power System Model of Peninsular Malaysia

To study the feasibility of utilising ESS for frequency regulation purposes, the first chosen power network of the study is Peninsular Malaysia. Based on the available references at the time of the study, the power network dated at the end

of 2013 is modelled. As of 31st December 2013, the fuel mix in Malaysia is made up of coal, gas, and hydro, in which the detailed breakdown is shown in Table 3.1 (Suruhanjaya Tenaga (Energy Commission), 2014).

Based on the references dated at a later period of 2016 (Suruhanjaya Tenaga (Energy Commission), 2016), the fuel mix dated at the end of 2014 was given. As shown in Table 3.1, the capacity of each fuel mix for the two years has not differed by much.

Table 3.1: Breakdown of Malaysian fuel mix in 2013 and 2014

Type	Fuel	Capacity (MW) in 2013	Capacity (MW) in 2014
Conventional Thermal	Coal	7,056	8,066
Conventional Thermal	Gas	564	564
CCGT	Gas	9,200	8,030
Open Cycle Gas Turbine (OCGT)	Gas	2,340	1,900
Hydroelectric	Hydro	1,899	2,150

Based on Table 3.1, the fuel mix is summarised to three types of power plants, namely thermal power plants (TPPs), gas power plants (GPPs), and hydro power plants (HPPs). The classification is required as each type of power plants possesses its individual characteristics of response based on the components that it contains, which will be described in the later section. Hence, Table 3.1 is modified as shown in Table 3.2 for the simulation modelling.

Table 3.2: Capacity breakdown of power plant types in the simulation model

Power Plant Type	Capacity (MW) in 2013
TPPs	7,620
GPPs	11,540
HPPs	1,900

3.3 Modelling of Peninsular Malaysia's Power System in MATLAB/Simulink

Essentially, the power system of Peninsular Malaysia is modelled in MATLAB/Simulink as a single control-area with transfer functions in block diagrams as shown in Figure 3.1. MATLAB/Simulink is used for simulation as it offers a diagram representation of the control system to be modelled, while presenting the flow and linkages of parameters in a user-friendly way. Besides, it also allows repeated simulations to be run easily, especially when it deals with different value inputs of parameters without changing the building blocks. Meanwhile, the individual components in Figure 3.1 are described in the following sections.

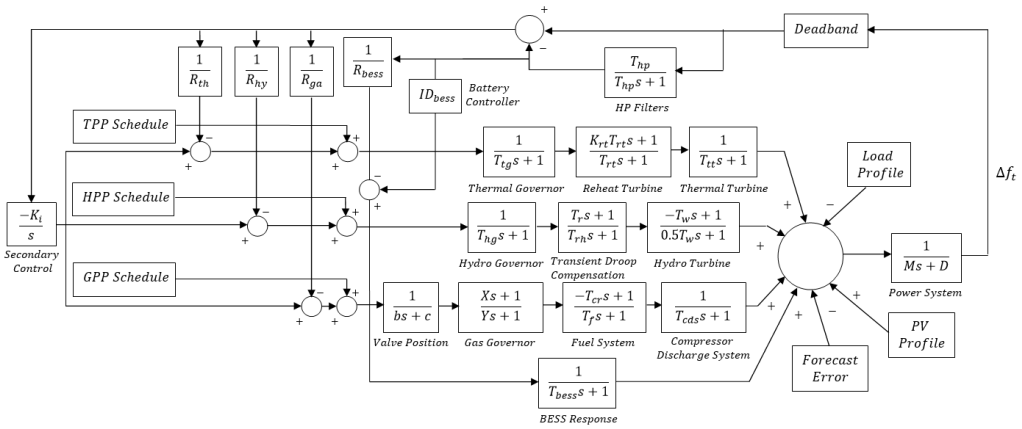

Figure 3.1: Modelling of power system of Peninsular Malaysia with transfer functions in MATLAB/Simulink

3.3.1 Block Diagrams in Matlab/Simulink

Generally, the block diagrams model in Figure 3.1 is an evaluation of power balance between the load and power supply in Peninsular Malaysia. As such, the power mismatch is converted to frequency deviation signals, which are split into two: high-frequency and low-frequency signals. The previous high-frequency signals are proposed to be picked up by fast-responding ESS, while the latter low-frequency signals are picked up by conventional power plants. At the same time, all the power plants in Peninsular Malaysia are lumped into a single generating unit based on the type of power plant, which are TPPs, HPPs, and GPPs. Also, each lumped power plant is to follow a daily scheduling of power generation, other than carrying out frequency regulation based on the frequency deviation signals.

3.3.1.1 Transfer Function of Power System for Power Mismatch

In the analysis of frequency regulation known as load-frequency control (LFC), the collective performance of the generating units within the power system is the focus. Therefore, the inter-machine oscillations and the performance and conditions of the transmission system are not considered (Kundur, 1993). As such, by assuming a coherent response from all the generating units towards load changes, essentially the response is represented by an equivalent generator. The inertia constant, *M* of the equivalent generator is the sum of all inertia constants of the generating units. Meanwhile, the effects of the system loads on the frequency deviation are represented by the load-damping constant, *D*. In short, the conversion of power mismatch to frequency deviation is shown in Figure 3.2.

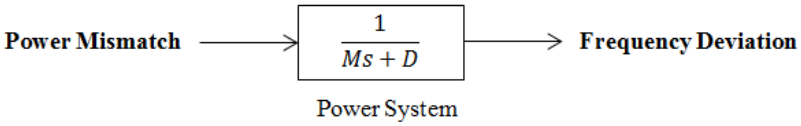

Figure 3.2: Transfer function of power system

3.3.1.2 Transfer Functions of TPP

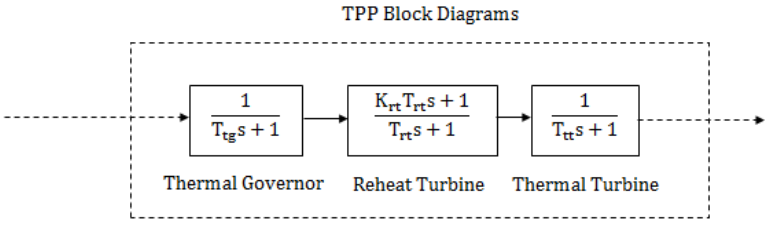

Figure 3.3: Transfer functions of TPP

In the modelling of TPP as shown in Figure 3.3, as the reheating of steam is included, the main components modelled are the governor, the reheat turbine and the thermal turbine. The thermal governor is modelled with a first-order transfer function. Meanwhile, there are two factors that mainly contribute to the dynamic response of reheat-type steam turbine; the steam transportation from the inlet valve to the first stage of turbine and the storage action in the reheater that causes the steam output at low-pressure stage to lag the high-pressure stage (Sivanagaraju, 2009). Therefore, the thermal and reheat turbine are modelled with a first-order transfer function and a lag compensator respectively.

3.3.1.3 Transfer Functions of GPP

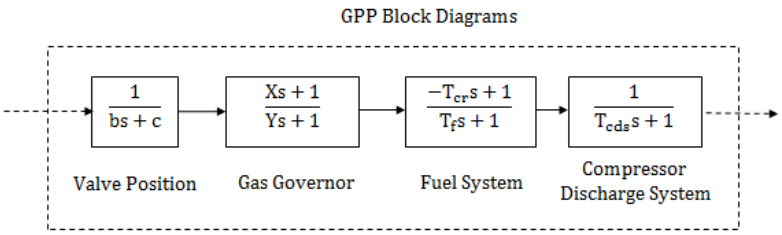

Figure 3.4: Transfer functions of GPP

In the modelling of GPP as shown in Figure 3.4, the components modelled are the valve position, gas governor, fuel system and compressor discharge system. The valve position and compressor discharge system are modelled by first-order transfer function while the gas governor and fuel system are modelled with a lag compensator. For information, the fuel system in GPP exhibits an initial negative power response to the power signal.

3.3.1.4 Transfer Functions of HPP

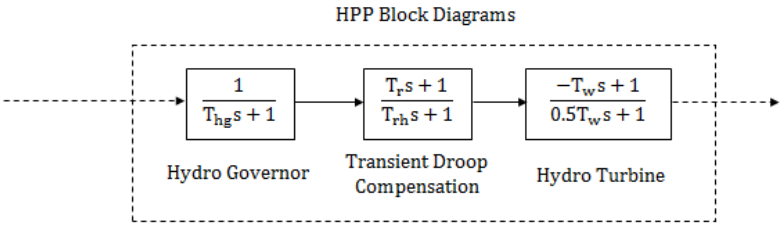

Figure 3.5: Transfer functions of HPP

In the modelling of HPP as shown in Figure 3.5, the components modelled are the hydro governor, transient droop compensation and hydro turbine. The hydro governor is modelled with a first-order transfer function while the latter two are modelled with a lag compensator. As a hydro turbine exhibits a peculiar response of having an initial opposite power change to the power signals, a transient droop compensation with long resettling time is required for a stable control performance. In fact, the long resettling time is achieved by slowing down the gate movement until the water flow catches up with the power signals.

3.3.1.5 Droop and Secondary Control

In conventional power plants, primary droop control is implemented to share the load between the power plants so as to ensure the power plants not to counteract

each other when making adjustments in the ramping up or down of power. In the model, a standard 5% of droop rating is assumed on all generating units.

Meanwhile for secondary control, an integral control is implemented to evaluate the total amount of power to be ramped up or down, taking over the frequency regulation action from primary droop control.

An illustration of the primary and secondary control mechanisms is shown in Figure 3.6.

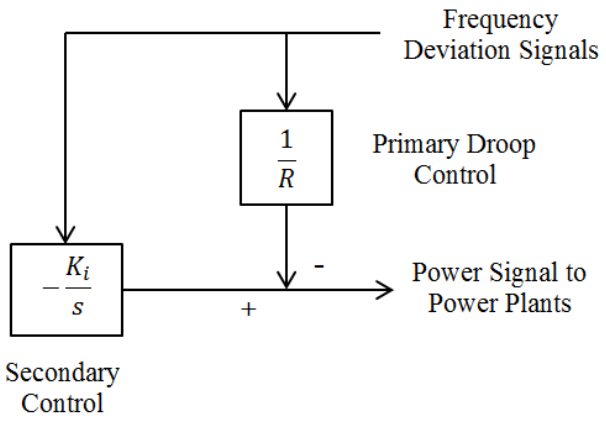

Figure 3.6: Modelling of primary and secondary controls by power plants

3.3.2 Load Profile and Power Plant Scheduling

The actual load profile of Peninsular Malaysia used for simulation is obtained from the website of the Energy Commission of Malaysia. A daily sample of

recorded power generation parameters is given in Appendix A. As a single control area is assumed for the grid network, a lumped load that represents the total load of Peninsular Malaysia is modelled.

Besides, since the power generation data points are provided at the interval of 30-minute, the obtained time series load profile is not fine enough for frequency regulation simulation. Therefore, two improvisations are employed; first is to interpolate the in-between data points and second is to add a random number generator of up to ±1% of peak load at every 10 seconds that represents the random load deviations.

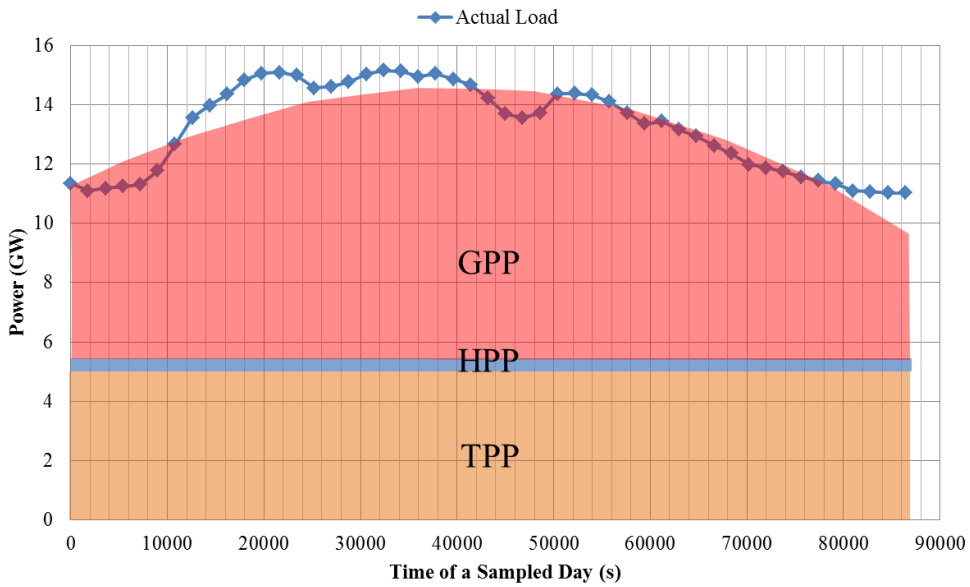

Figure 3.7: Daily load scheduling of power plants and load profile in Peninsular Malaysia

For the daily load scheduling of each power plant type and simplification of simulation, HPP and TPP are scheduled to provide a constant power while GPP is

proposed to track a second-degree function of the load profile as shown in Figure 3.7. In fact, in conventional power generation, GPPs possess the shortest response time as they are the main contributors for frequency regulation services. The mismatch between the scheduled power generation and total load in the power system is represented as frequency deviation signals (as described in Section 3.3.1.1), which are picked up both the power plants and ESS modelled in the power system.

3.3.3 Transfer Function of ESS

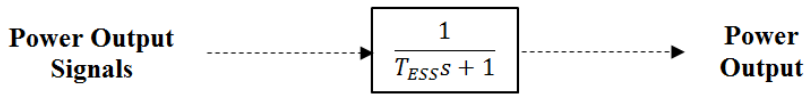

Figure 3.8: Transfer function of ESS

ESS is modelled with a first-order transfer function as its response is fast without the involvement of mechanical parts as it is with the power plants.

3.3.3.1 ESS Controller

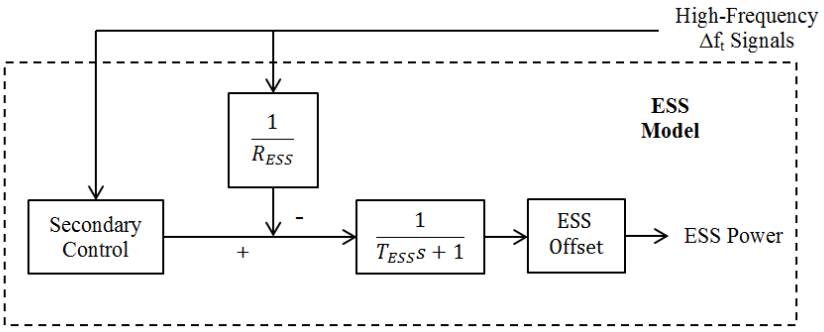

Figure 3.9: Modelling of ESS controller

A primary droop control is proposed for the use of all ESS units designated for frequency regulation. Meanwhile, the secondary control is a combination of integral and derivative control; the former to sum up the power mismatches through time while the latter acts as a predictive control and virtual inertia to handle high-frequency frequency deviation signals. The power output reference signals are passed to the ESS transfer function model for power generation or absorption. An offset control is implemented should the SOC be out of a defined healthy operation range, which is described in the following section.

On a side note, the modelling of ESS in the simulation represents a lumped generating unit of multiple ESS units rather than a single unit. However, in the case of a centralized ESS within a control area, the primary droop and secondary control can be replaced by a proportional-integral-derivative (PID) controller instead.

3.3.3.2 SOC of the Batteries

The below formulae is used to estimate the SOC of ESS, where η_d and η_c are the discharging and charging efficiencies, equally set at 90% and E is the nominal energy capacity of the ESS.

$$SOC(k+1) = SOC(k) - \frac{\int_k^{k+1} \eta P(t)dt}{E}, \tag{3.1}$$

$$\eta = \frac{1}{\eta_d} if\ P(t) > 0, \quad \eta = \eta_c \quad otherwise \tag{3.2}$$

Due to the efficiencies of ESS, it absorbs less while injecting more power than an ideal operation in which a net outflow of energy is anticipated on most of the operation days. Therefore, an offset control is required to ensure the continuous operation of ESS.

3.3.3.3 Offset Algorithm

In the study, the ESS power response is proposed to be offset when the SOC of ESS is out of the specified SOC thresholds, SOC_T, with a fixed rate of power offset, P'_o. When the SOC recovers within the threshold after an offset is applied, the offset is ramped back to zero (an opposite offset) with the same rate. The value of P'_o is set such that the offset ramp rate is slow enough for the power

plants in the power grid to follow, hence it does not contribute negatively to the frequency regulation. The algorithm of the proposed offset is shown in the equations below:

$$P_o(t) = P_{OU}(t) + P_{OUR}(t) + P_{OL}(t) + P_{OLR}(t) \tag{3.3}$$

$$P_{OU}(t) = \int_k^{k+1} P'_o\, dt \qquad if\ SOC \geq SOC_{TU} \tag{3.4}$$

$$P_{OUR}(t) = -\int_k^{k+1} P'_o dt \qquad if\ P_{OH}(t) > 0\ and\ SOC < SOC_{TU} \tag{3.5}$$

$$P_{OL}(t) = -\int_k^{k+1} P'_o\, dt \qquad if\ SOC \leq SOC_{TL} \tag{3.6}$$

$$P_{OLR}(t) = \int_k^{k+1} P'_o dt \qquad f\ P_{OH}(t) < 0\ and\ SOC > SOC_{TL} \tag{3.7}$$

$P_O(t)$ is the offset power, $P_{OU}(t)$ is the offset power when SOC exceeds SOC_{TU}, the upper threshold of SOC, $P_{OUR}(t)$ is the opposite offset power when the SOC recovers from SOC_{TU}. Similarly, $P_{OL}(t)$ is the offset power when SOC goes below SOC_{TL}, the lower threshold of SOC, $P_{OLR}(t)$ is the opposite offset power when the SOC recovers from SOC_{TL}.

Since the cycle length of batteries decrease exponentially with its depth of discharge (Martin II, 2016), a SOC_{TL} of 65% is set to prevent deep discharge of batteries to maintain its lifespan in the simulation. Meanwhile, a SOC_{TU} of 80% is imposed to ensure that the batteries can cater for potential power absorption during frequency regulation.

3.3.4 Penetration of PV Systems

While it is planned for RE to reach at least 3% of the total power generation mix by 2020 (Suruhanjaya Tenaga (Energy Commission), 2016), a case study of 10% PV penetration of the maximum load demand is presented in the study.

To generate the PV profile utilised in the simulation, 4 strings of 8 Panasonic PV panels each with an output 230W were connected to two Zigor PV inverters, installed at the open-space car park in the campus, titled at 5°. The PV power output is recorded every 1 minute and the 5-day averaged profile is scaled up to 10% penetration to represent one daily PV profile in Peninsular Malaysia.

3.3.5 Loss of Largest Generating Unit (LGU)

Based on the reserve classification in Peninsular Malaysia in 2014, 700MW of spinning reserve is allocated to cater for the loss of LGU in the network (Suruhanjaya Tenaga (Energy Commission), 2014)**.** This figure is later revised to be 1000MW in 2016 (Suruhanjaya Tenaga (Energy Commission), 2016). While the item is not within the main proposal objective of the dissertation as it requires a large capacity of ESS, it is presented as a side case study.

3.4 IEEE 24-Bus RTS

The IEEE 24-Bus RTS is initially proposed as a reference test system that contains the basic data required in power system reliability evaluation, approved by the IEEE Power System Engineering Committee (Reliability Test System Task Force, 1979). Due to the lack of grid network data of Peninsular Malaysia, the RTS is chosen to be modelled as a step-up for a more detailed analysis as it contains load and generation system and transmission network data that are required for the study.

Meanwhile, the RTS is also a larger transmission network than the previous model of Peninsular Malaysia, therefore it is able to be divided into a few control areas to simulate the interactions between and the combined actions of them. While there are larger test systems available for simulation, the RTS is picked as it fulfils the main criterion of being a reasonable size to be modelled, such that further analysis is achievable within the time frame of the study.

3.4.1 MATLAB/Simulink

The IEEE 24-bus RTS is modelled in MATLAB/Simulink with transfer functions in block diagrams. As such, the RTS is divided into three interconnected control

areas as shown in Figure 3.10, in which the generation in each area is sufficient to meet its load.

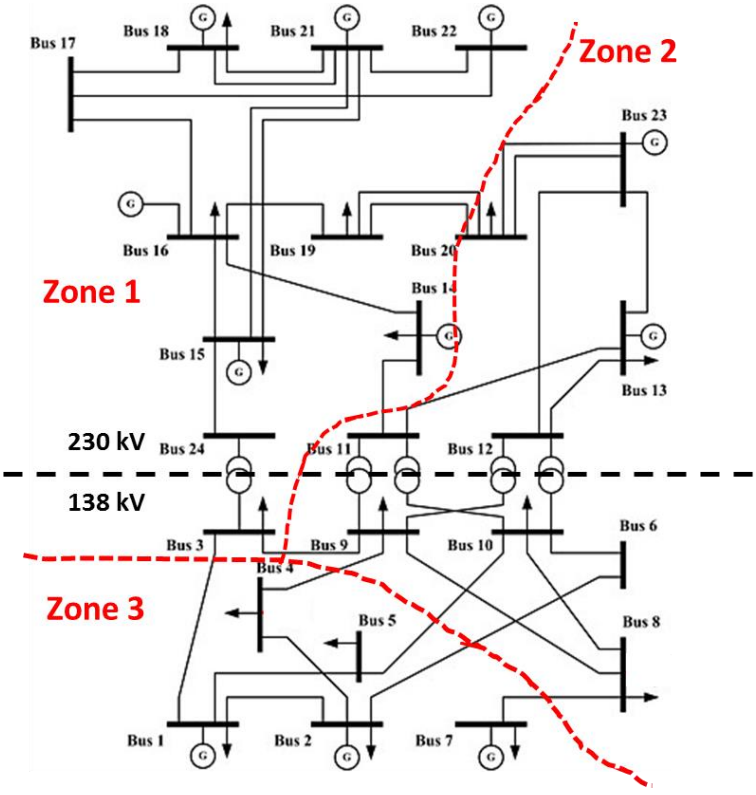

Figure 3.10: IEEE 24-bus RTS with three interconnected control areas

Since RTS is of an old test system, its composition is modified to represent a more realistic mix of power plants in the power system. Hence, certain thermal power plants are substituted by fast-responding GPPs. Essentially, the RTS is improvised to contain three types of power plants; HPPs, TPPs and GPPs. Besides, each control area is allocated with GPPs for grid regulation purposes. The description for the substitution is given in Table 3.3.

Table 3.3: Substitution of power plants on IEEE 24-bus RTS

Bus Number	Original	Substituted by
Bus 1 and Bus 2	2 x 20MW GPPs respectively	2 x 20MW TPPs respectively
Bus 7	3 x 100MW TPPs	3 x 100MW GPPs
Bus 13	3 x 197MW TPPs	3 x 197MW GPPs
Bus 15	5 x 12MW and 155MW TPPs	5 x 12MW and 155MW GPPs
Bus 18	400MW Nuclear Power Plant	400 MW TPP
Bus 21	400MW Nuclear Power Plant	400 MW GPP

3.4.1.1 Block Diagrams of Power System

As the RTS is divided into three control areas in MATLAB/Simulink model, the general layout of the block diagrams are given in Figure 3.11.

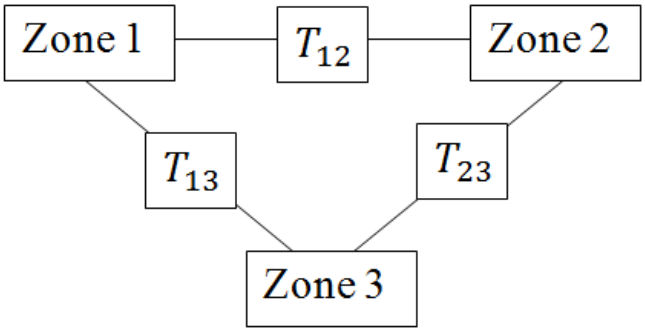

Figure 3.11: Modelling of the interconnection between control areas in MATLAB/Simulink

Each zone is interconnected to the adjacent zones through tie lines, where the power flow from one zone to another zone (say Zone 1 to Zone 2, P_{12}) is given by

Eq. 3.8, where E and δ stand for the voltage of the equivalent voltage source of the control area and phase difference respectively, while X_T represents the impedance of the tie line. The electrical equivalent of the power flow that illustrates the formulation of Eq. 3.8 is shown in Figure 3.12.

$$P_{12} = \frac{E_1 E_2}{X_T} \sin(\delta_1 - \delta_2) \tag{3.8}$$

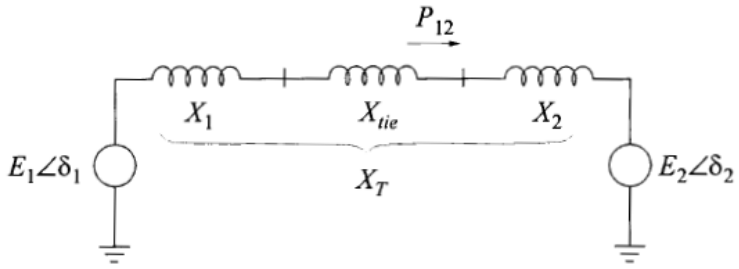

Figure 3.12: Electrical equivalent of power transfer between two control areas (Kundur, 1993)

Eq. 3.8 can be later represented by the synchronizing torque coefficient, *T*, given in Eq. 3.9, which is utilised as a simulation parameter in the model.

$$T_{12} = \frac{E_1 E_2}{X_T} \cos(\delta_1 - \delta_2) \tag{3.9}$$

In each of the control area, power plants on each bus of the similar type are lumped into a single unit to simplify the simulation. The modeling of a sample control area (Zone 1) is shown in Figure 3.13. The revisions made as compared to the earlier model to represent multiple control areas are such that a bias factor, *B* and interconnection power transfer are included. A bias factor essentially controls

the magnitude of contribution of one particular control area to frequency regulation of the interconnected power system.

The recommended bias factor for a control area is given in Eq. 3.10 (Kundur, 1993), where R_{eq} and D are the equivalent droop rating and load-damping constant of the particular control area. Meanwhile, R_{eq} is given in Eq. 3.11, a summation of all the droop ratings of the generating units within the control area.

$$B = \frac{1}{R_{eq}} + D \tag{3.10}$$

$$R_{eq} = \frac{1}{\frac{1}{R_1} + \frac{1}{R_2} + \cdots + \frac{1}{R_n}} \tag{3.11}$$

As for the interconnection power transfer, it is modelled such that if power is supplied from other control areas, the power reference signal for frequency regulation is decreased by the same magnitude, and vice versa.

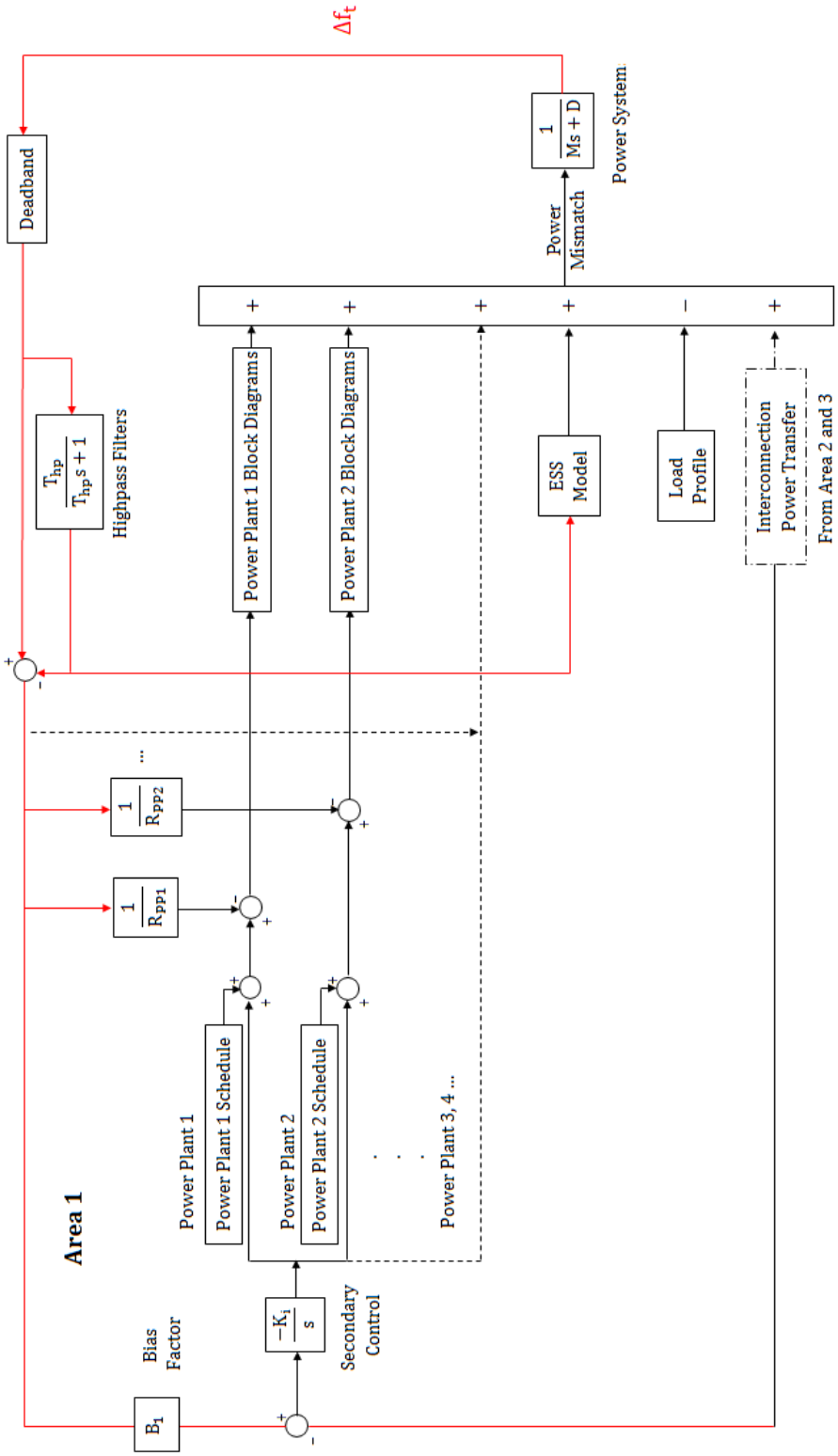

Figure 3.13: Block diagram of the power system model of Area 1 of the RTS

(red lines represent frequency deviation and black lines represent power)

The transfer functions of the TPPs, GPPs and HPPs are as described in Sections 3.2.1.2, 3.2.1.3 and 3.2.1.4, where each power plant is assumed to have a 5% droop rating. As compared to the previous model, multiple units of the similar power plant type are modelled if they are on different busbars in the control area to better represent the combined actions of multiple generating units in frequency regulation. In addition, two enhancements to the modelling of power plants are made. First, the maximum and minimum outputs of each busbar are capped to avoid under and over supplying of power based on the defined capacity. Next, a ramp rate is applied to model the ramping ability of each type of power plant, where the figures are given in Table 3.4.

Table 3.4: Ramp rates of various power plant types modelled in MATLAB/Simulink

Power Plant Types	Ramp Rate (% of Power Capacity/min)
TPPs	2
GPPs	10
HPPs	50

3.4.1.2 Load Profile and Power Plant Scheduling

Week 51 of the RTS load profile is chosen for simulation as it displays the biggest magnitude of load profile change during the year. Since the load profile is given at per-hour data point, the values are interpolated while a random number generator of a Gaussian distribution with 3 standard deviations of 1% of peak load per second is added to model the load fluctuations.

Meanwhile, the scheduling of power plant is similar to Section 3.2.2., where GPPs are set to track a second-degree function of the load profile. While only one equivalent GPP is modelled previously, there are multiple GPPs in certain control area where the tracking of load profile is shared based on their respective rated power capacities. The maximum load in Week 51 and the generation capacity on each control area is shown in Table 3.5.

Table 3.5: Maximum load in Week 51 and the respective generation capacity in the control areas in RTS

Control Area	Maximum Load (MW)	Generation Capacity (MW)
Zone 1	1305	1470
Zone 2	1070	1251
Zone 3	475	684

3.4.1.3 Modelling of ESS

The structure of the ESS model is similar to Section to 3.2.3. However, there are some enhancements made on the offset algorithm. First, the magnitude of offset is capped at a ceiling limit for the stability of the algorithm. Second, the rate of offset, P'_o differs for each control area such that the value is lower than the total ramp rate of all the generating units in the particular control area.

An illustration to describe the proposed offset algorithm in a control area is shown in Figure 3.14. Initially, the ESS is injecting power to the grid network for frequency regulation where the SOC is decreasing. At the time of T1, the SOC

breaches the defined lower threshold at 65%, hence a constant rate of offset that is slow enough for the power plants to pick up is applied. Therefore, the ESS power is offset downwards to conserve its capacity, injecting less power and absorbing more power than it was intended. Meanwhile, the shaded region in the figure shows the energy that has to be picked up by the power plants. When the SOC recovers back to the threshold value at the time of T2, the offset is ramped back to zero. The same condition applies when SOC exceeds the upper threshold. The only difference in the illustration of the operating concept of the proposed offset algorithm from the Peninsular Malaysia network is such that the offset power is capped at a certain value in RTS.

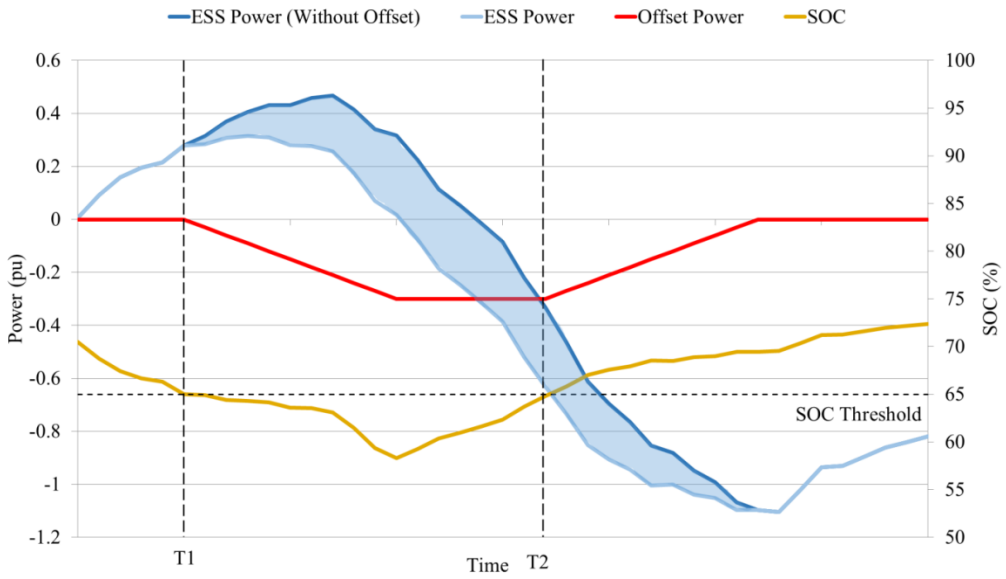

Figure 3.14: Illustration of the operation of the proposed offset algorithm

3.4.1.4 Identification of Optimal Control Area Placement of ESS

The ESS is placed alternatively on the control area to identify the optimal placement of ESS for maximum frequency regulation quality.

3.4.2 Scenarios of Study

Two scenarios of simulation are considered; the penetration of solar PV in the RTS and the undersizing of ESS for frequency regulation.

3.4.2.1 Penetration of PV Systems

Utilising similar PV profile obtained previously, PV sources are positioned on the RTS network as shown in Figure 3.15. The PV Placement on Bus 19 in Area 1 is intended to act as a solar farm while the spreading out of PV on several buses in Area 2 and Area 3 mimics residential PV. In the simulation, 25% of PV penetration in each control area is modelled.

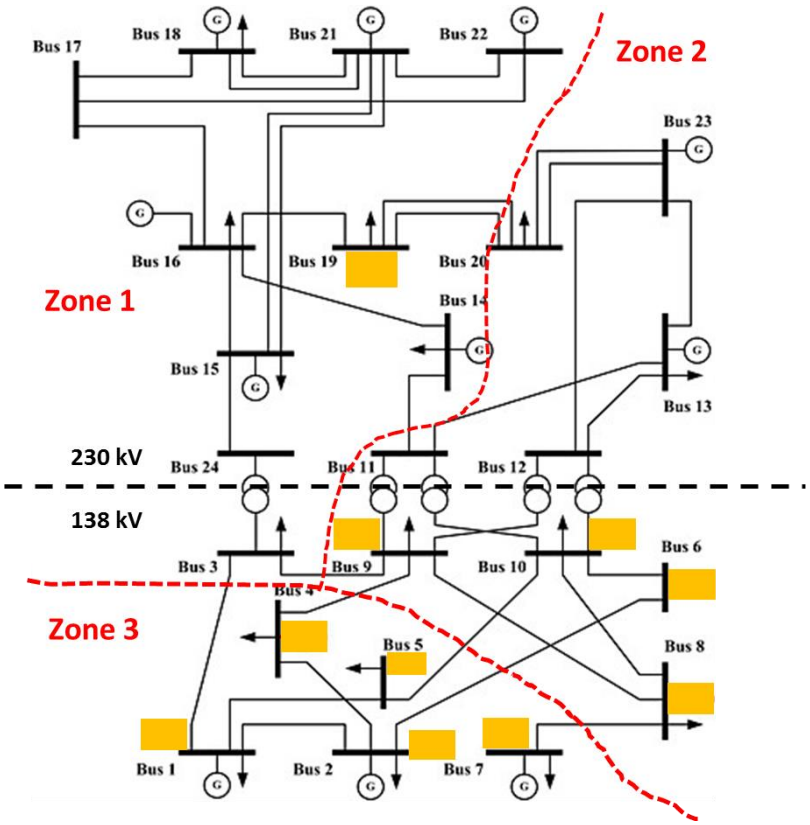

Figure 3.15: Positioning of PV (Represented by Yellow Blocks) in the RTS

3.4.2.2 Undersizing of ESS

Repeated simulations with the similar conditions are run by decreasing the capacity of ESS, at 80%, 60%, 40% and 20% respectively to study its effects on the frequency regulation quality, while exploring the possibility of utilising a smaller capacity of ESS for potential capital cost savings.

3.4.3 Summary of Improvements and Changes from Previous Model

The summary of the improvements and changes of RTS model from the previous Peninsular Malaysia model is shown in Table 3.6.

Table 3.6: Improvements and changes of RTS model from the previous Peninsular Malaysia model

Items	Peninsular Malaysia Model	RTS Model
Number of Control Area	1	3
Power Generation	- No interconnection power transfer - Single unit of each type of power plants	- Interconnection power transfer - Multiple units of each type of power plants - Ramp rates of power plants are modelled
Fluctuation of Load Profile	A random number generator of up to ±1% of peak load per 10 seconds.	A random number generator of a Gaussian distribution with 3 standard deviations of 1% of peak load per second.
Offset Algorithm of ESS	Magnitude of offset is not capped	- Magnitude of offset is capped for the stability of algorithm. - Rate of offset differs for each control area
Percentage of PV Penetration	10%	25%

3.4.4 Parameters of the Simulation Models

The constants used in both the simulation models that are of similar values are shown in Table 3.7.

Table 3.7: Similar parametrical values in both simulation models

Components	Parameters	Value
TPP	Speed Governor Time Constant (TC), T_{tg} (s)	0.08
	Coefficient of Reheat Steam Turbine, K_{rt}	0.3
	Reheat TC, T_{rt} (s)	10
	Turbine TC, T_{tt} (s)	0.3
HPP	Main Servo TC, T_{hg} (s)	0.2
	Speed Governor Rest Time, T_r (s)	5
	Transient Droop TC, T_{rh} (s)	28.75
	Water TC, T_w (s)	1
GPP	b	0.05
	c	0.1
	Speed Governor Lead TC, X (s)	0.6
	Speed Governor Lag TC, Y (s)	1
	Combustion Reaction Time Delay, T_{cr} (s)	0.01
	Fuel TC, T_f (s)	0.23
	Compressor Discharge Volume TC, T_{cds} (s)	0.2
Power System	High-Pass Filter TC, T_{hp} (s)	10
	Frequency Deadband (Hz)	±0.01

Meanwhile, the constants used that are of different values are shown in Table 3.8.

Table 3.8: Other differing parametrical values in both simulation models

Components	Parameters	Peninsular Malaysia	RTS		
			Z1	Z2	Z3
Power System	Grid Inertia Constant, M (GW/Hz/s)	3.5	0.261	0.214	0.095
	Load Damping Constant, D (GW/Hz)	0.36	0.039	0.032	0.014
	Secondary Control Integral Gain, K_i (GW/Hz/s)	2	0.131	0.107	0.048
	Bias Factor, B	-	0.627	0.533	0.288
	Synchronizing Torque Coefficient, T	-	Z12	Z23	Z13
			4	1.5	1
ESS	ESS TC, T_{ess} (s)	0.5	1		
	Controller Integral Gain, I_{ess} (GW/Hz/s)	30	2.5		
	Controller Derivative Gain, D_{ess} (GWs/Hz)	30	2.5		
	SOC Threshold, SOC_T	65%/80%	65%/85%		
	Droop, R_{ess} (Hz/GW)	0.2	0.1		
	Rate of Power Offset, P'_o (GW/hr)	0.04	0.003	0.001	0.0006

3.5 Matpower

Matpower is a package of MATLAB input file-based power flow and optimal power flow solver (Zimmerman et al., 2011). The components of the network are buses, branches and generators to be defined for the solution. Some major parameters defined in the components are as follows:

Table 3.9: Major components and the respective parameters in Matpower

Components	Parameters
Bus	Bus type (PV/PQ/Swing), real and reactive power demand, shunt conductance and susceptance, voltage magnitude and angle, base voltage, maximum and minimum voltage magnitude, etc.
Branch/ Transformer	"From" and "To" bus number, line resistance, reactance and susceptance, MVA ratings, transformer turn ratio (a value of '1' implies a 'branch'), etc.
Generator	Real and reactive power output, maximum and minimum real and reactive power output, voltage magnitude setpoint, total MVA base of machine, etc.

3.5.1 Modelling of Power System and ESS

The input parameters for Matpower are provided in the reference (Reliability Test System Task Force, 1979). The bus with the largest generating capacity, Bus 23 is identified as the swing bus. Meanwhile, the buses that contain generators are modelled as PV buses and ESS is modelled as a generator on a PQ bus as it does not possess any voltage regulation ability in the simulation.

3.5.2 Identification of Optimal Busbar Placement of ESS

To ensure the frequency regulation operation of ESS does not cause any voltage issues, Matpower is used to identify its optimal busbar placement within the previously identified control areas with minimal impact on the grid voltages. While the frequency regulation model in MATLAB/Simulink is evaluated

continuously throughout a defined simulation time, Matpower evaluates the power flow solution based on the input parameters of a given time step.

Therefore, due to the time constraints and the large amount of data to be processed if power flow is to run continuously for the 1-week input data, certain time steps of daily results are simulated instead. As such, the load and generation profiles at the time step where the maximum and minimum power mismatch occur during a day are simulated, with the assumption that those time steps will deal the greatest impact on the grid voltage. Hence, MATLAB/Simulink is programmed to output the respective load and generation value of all supplying units in the RTS at the identified time steps to be fed into the Matpower load flow model, which outputs the resulting voltage profiles across the network.

In the simulation, the scenarios investigated for various busbar locations in the RTS network are as follows:

(a) A PV busbar (Bus 14) in Control Area 1

(b) A PQ busbar (Bus 19) in Control Area 1

(c) A PV busbar (Bus 13) in Control Area 2

(d) A PQ busbar (Bus 20) in Control Area 2

(e) A PV busbar (Bus 2) in Control Area 3

(f) A PQ busbar (Bus 5) in Control Area 3

(g) A PV busbar (Bus 14, 13 and 2) in every control area

(h) A PQ busbar (Bus 19, 20 and 5) in every control area

(i) All buses

3.5.3 Integrated Test Environment (ITE) in Cooperation with Newcastle University

As running repeated simulations with different parameter values in Matpower are time-consuming, it is achieved with a developed ITE through the cooperation with Newcastle University. Simply put, the ITE enables the interaction between a Java-based Multi-Agent System (MAS) and Matpower input files, as shown in Figure 3.16.

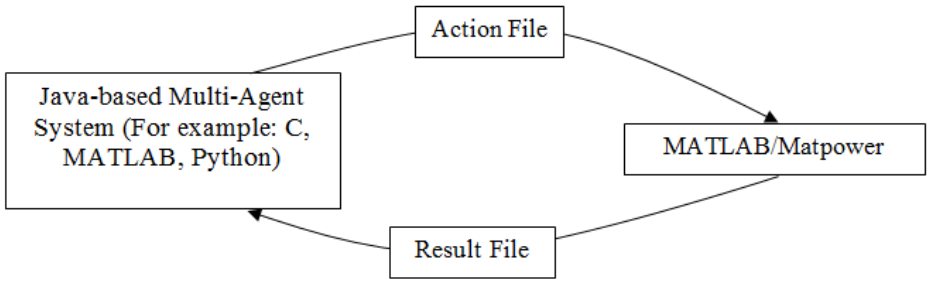

Figure 3.16: An overview diagram of ITE

Based on Figure 3.16, the ITE allows both the simulation on Java-based MAS and Matpower to run simultaneously. First, the MAS initiates the power flow simulation in Matpower, where the results of each time step of the simulation are passed back to the MAS. Should the logic of the programme be developed, the

MAS dictates that certain control activity is required on the power system (i.e. changing the transformer tap position, shutting down a generating unit, etc.), the control commands are sent to Matpower before the next time step of simulation resumes (Yi et al., 2016). Some of the example platforms of MAS are C, MATLAB, Python, etc., therefore enabling the interaction between Matpower and various programming languages while enhancing the maneuverability of power flow simulation in Matpower.

Meanwhile for the simulation in this study, the ITE is utilised for the interaction between MATLAB and Matpower to carry out repeated simulations of Matpower based on the earlier identified input profiles. While the ITE demonstrates the prospects of offering variable control actions to the simulation, it is not applied in the dissertation. However, the potential future work is discussed at Chapter 5.

3.6 A Comprehensive Work Package for ESS as Frequency Regulation Provision

The main motivation of the dissertation is to propose a comprehensive work package of using ESS for frequency regulation, where a summary flow chart of the earlier described methodology is shown in Figure 3.17.

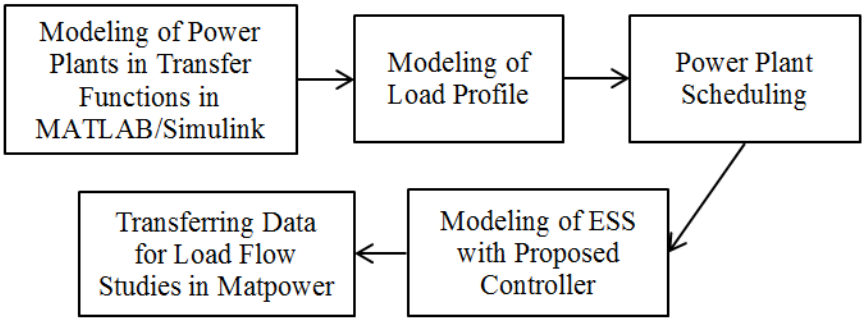

Figure 3.17: The proposed comprehensive work package of utilising ESS for frequency regulation

Firstly, the power plants in the defined grid network are modelled in MATLAB/Simulink with transfer functions, along with the load profile. This is followed by the scheduling of power plants and the modelling of ESS and its respective frequency regulation controller. In the paper, a droop controller for primary control and an integral and derivative controller for secondary control are proposed for ESS. Also, a set of offset algorithm is proposed to conserve the SOC of ESS for its continuous operation. The simulation model in MATLAB/Simulink studies the frequency regulation quality based on the proposed solution and identifies the ESS placement in the control areas. Next, the power network data at certain time steps is transferred to Matpower for load flow studies to generate the overall network voltage profile.

The work package also allows the incorporation of various types of ESSs and generating units by modelling its respective transfer functions and power generation profiles. The penetration of RE sources is easily able to be included in

the simulation model. Essentially, the proposed work package provides a flexible framework to analyze grid frequency regulation problems with various possibilities of scenarios and solutions are able to be tested for the use of academic and commercial researchers.

3.7 Summary

The chapter describes the modelling of two simulation models, namely the Peninsular Malaysia grid network and the IEEE 24-bus RTS to utilize ESS for frequency regulation. The IEEE 24-bus RTS model represents a step-up from the previous model, extending the scope of the study mainly by including the simulation of interconnection power transfer and power flow studies. The latter is achieved through the cooperation with Newcastle University that developed the ITE, which allows more possibilities to the study. Last but not least, a comprehensive work package of frequency regulation by ESS, which is the main objective of the dissertation, is summarised.

CHAPTER 4

RESULTS AND DISCUSSION

4.1 Introduction

This chapter presents the simulation results of the two modelled grid networks, namely the Peninsular Malaysia and IEEE 24-bus RTS. For the Peninsular Malaysia grid network, the presented results include the frequency deviations and SOC profiles of ESS, the actions of offset algorithm and the power profiles of all generating units in the network. Meanwhile for the IEEE 24-bus RTS network, the frequency deviation histograms, the SOC profiles and the network voltage profiles are included. The sizing of ESS required is also identified, along with the optimum ESS placement in the control areas and the busbars for maximum frequency quality and minimum impact on grid voltages.

4.2 Peninsular Malaysia Network

The simulation results of the Peninsular Malaysia network are presented in the following sections.

4.2.1 Frequency Deviations and Power Profiles

This section presents the frequency deviation profile of the power system with and without ESS. The pertinent generation and load profiles are presented along to manifest the ineffectiveness of power plants to track the daily fluctuating load profiles, in contrast with the fast-response of ESS. As such, Figure 4.1 shows the frequency deviation profiles of a sampled day, where the frequency deviation is minimised significantly by the actions of ESS. The frequency deadband is set at ±0.01 Hz in the simulation; based on the Malaysian Grid Code, it should be set not more than ±0.025 Hz. Essentially, a narrower frequency deadband results in more frequent regulations, hence producing better frequency quality at the expense of more power injection or absorption.

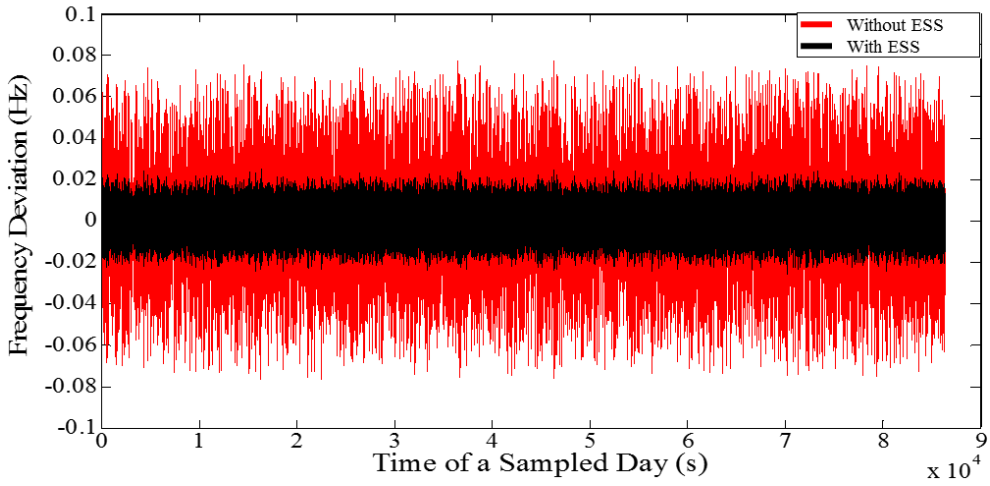

Figure 4.1: Frequency deviation profile of a sampled day with and without ESS

On the other hand, Figure 4.2 shows the power profiles of various generating units on the equivalent sampled day for the case of without ESS. The three shaded regions represent the energy supplied by each type of power plants, where their combined actions are represented by the black line.

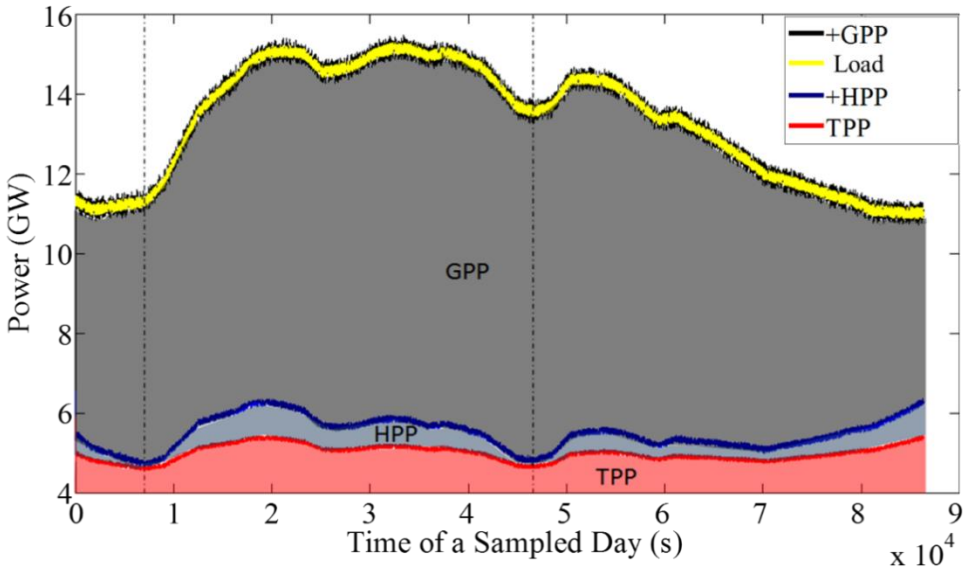

Figure 4.2: Power profiles of different generating units of a sampled day without ESS

As seen from Figure 4.2, the power plants are not able to track the daily load fluctuations represented by the yellow band effectively due to their slow response time, hence resulting in a larger frequency deviation as shown in Figure 4.1. Although the TPP and HPP are scheduled to provide a constant power acting as base loads, they are still performing a certain degree of frequency regulation based on the signals fed into them. As described in Section 3.3.1.4, hydro turbine possesses an initial opposite power change with respect to the power signals. This phenomenon is seen at two instances in Figure 4.2; when large power ramping is

required due to the increase in load, HPP ramped itself down instead initially before ramping the power production back up.

Meanwhile, the power profiles of different generating units on the equivalent sampled day for the case of with ESS is shown in Figure 4.3. It is shown that the ESS is performing majority of the frequency regulation instead with the frequent ramping up and down of power due to its response being faster than that of the power plants.

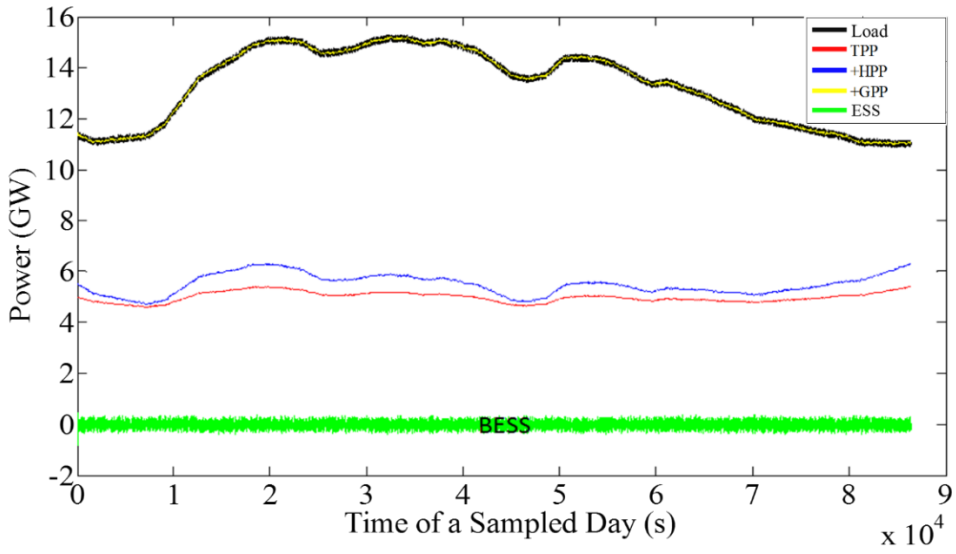

Figure 4.3: Power profiles of different generating units of a sampled day with ESS

4.2.2 SOC Profiles and the Actions of Offset

The SOC profiles of the ESS and the actions of the offset algorithm on the equivalent sampled day are shown in Figure 4.4. The SOC is kept at a healthy operating range by the actions of the offsets, defined at 65% and 80%; when the SOC exceeds SOC_{TU} at the beginning of the day, an up-ramp is applied on the power offset such that the ESS supplies more or absorbs less power during the frequency regulation, whereby the offset is made up by the power plants. Once the SOC is recovered within the defined healthy range, a down-ramp is applied to zero out the offset. Likewise, when the SOC decreases beyond SOC_{TL} later of the day as seen in Figure 4.4, a negative-ramp is applied such that the ESS supplies less or absorbs more power. It is important to point out that ESS is not a power source therefore it requires constant charging from the power plants from time-to-time to maintain its capacity. Without the offset algorithm, its SOC collapses in the middle of the day as seen in Figure 4.5 due to the fact that frequency regulation is not zero-mean and the non-ideal efficiencies of ESS.

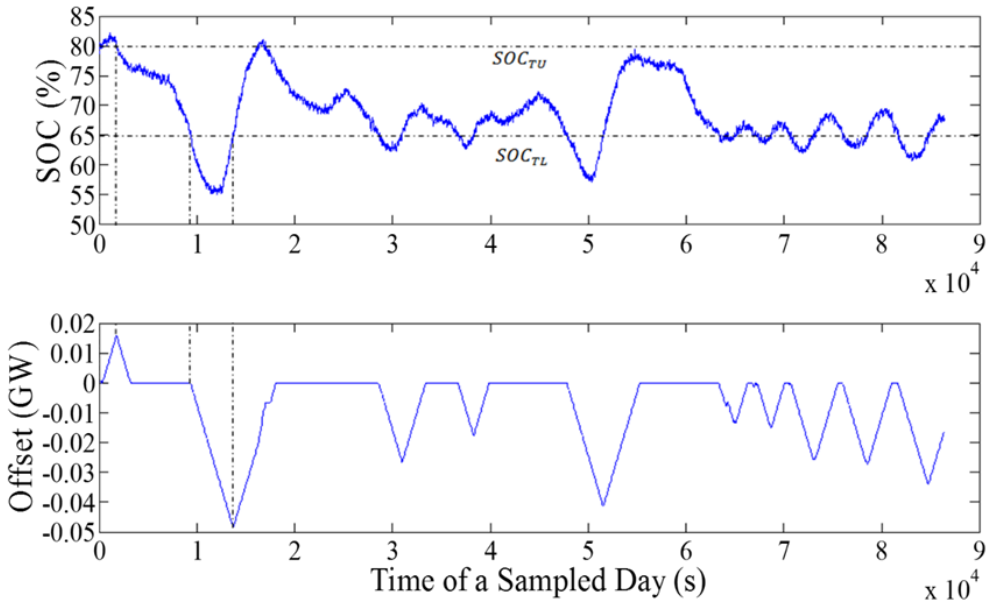

Figure 4.4: SOC and power offset signals of ESS on the sampled day

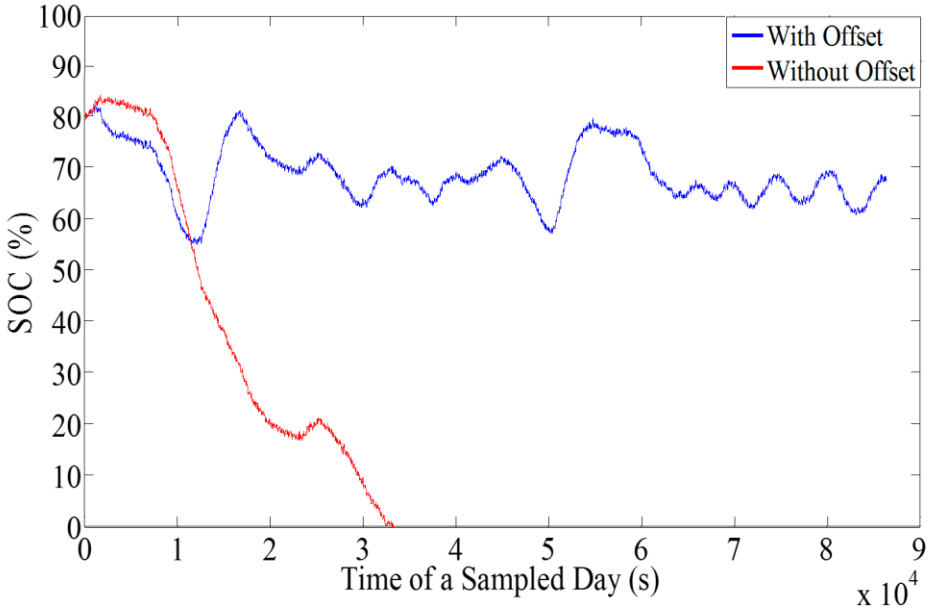

Figure 4.5: SOC profiles of ESS with and without offset algorithm on the sampled day

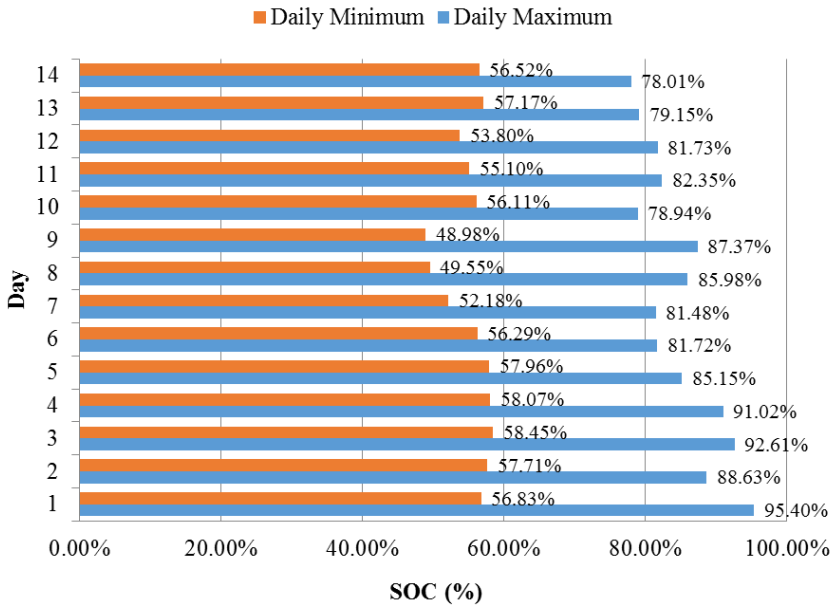

Figure 4.6: Daily maximum and minimum SOC of ESS for two-week of continuous frequency regulation

The effectiveness and feasibility of the offset algorithm is verified by running the simulation based on continuous first two weeks of Peninsular Malaysian load profiles in February 2016. The pertinent daily maximum and minimum SOC of ESS are shown in Figure 4.6, which is within the operable range of ESS. Meanwhile, the performance of the ESS is quantified using the standard deviation and range of the two-week frequency deviation profile, as shown in Table 4.1.

Table 4.1. Standard deviation and range of two-week frequency deviation profile

Scenario	Frequency Deviation (Hz)		
	Standard Deviation	Maximum	Minimum
No ESS	0.0148	0.0742	-0.0735
With ESS	0.0102	0.0227	-0.0218

4.2.3 10% PV Penetration

The effectiveness of ESS for frequency regulation under 10% PV penetration is highlighted in Figure 4.7, while the improvement is tabulated in Table 4.2.

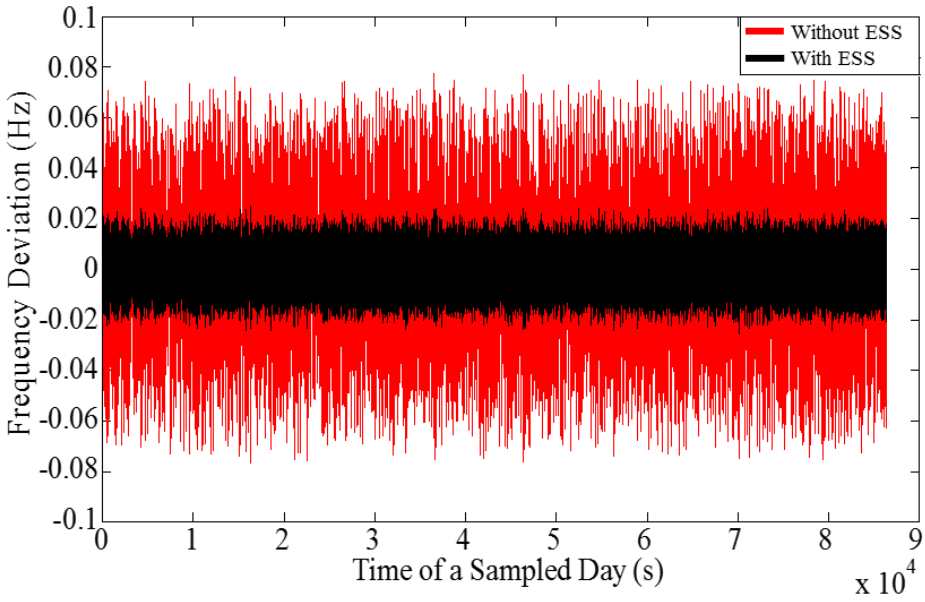

Figure 4.7: Frequency deviation profiles of a sampled day with and without ESS under 10% PV penetration

Table 4.2. Standard deviation and range of frequency deviation under 10% PV penetration

Scenario	Frequency Deviation (Hz)		
	Standard Deviation	Maximum	Minimum
No ESS	0.0161	0.0779	-0.0768
With ESS	0.0109	0.0252	-0.0257

On the other hand, Figure 4.8 shows PV being included as the power producer in the Peninsular Malaysia grid network. The power plants are shown to adjust their power production to balance out the power mismatch with the load.

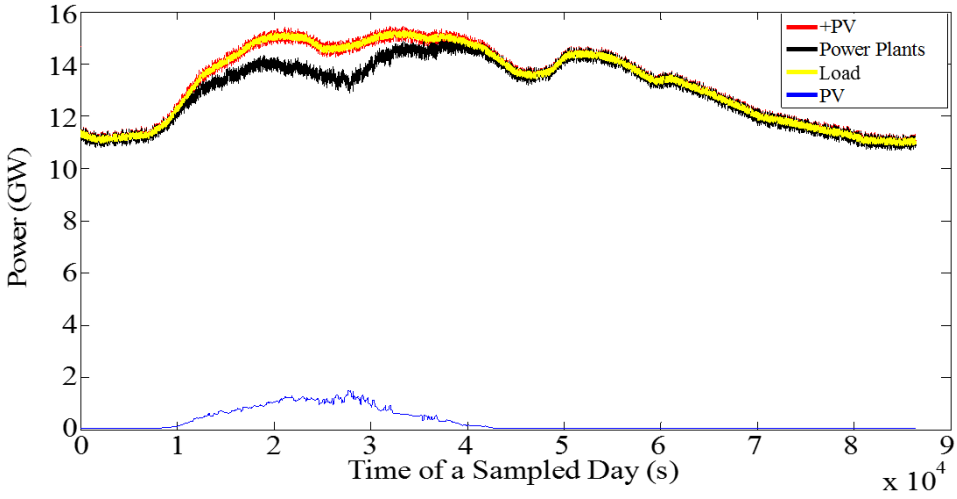

Figure 4.8: Power profiles of different generating units without ESS under 10% PV penetration

Meanwhile, Figure 4.9 shows the power profiles of all the generating units in the network along with the inclusion of PV. As such, the power plants are shown to be ramping with a lower rate as compared to Figure 4.8, where the results tabulated in Table 4.3 shows a reduction of close to a factor of 16. In fact, the power profile of power plants is smoothened out by the fast-response ESS, therefore indirectly decreases the occasions and the degree of wear-and-tear of the mechanical components in the power plants.

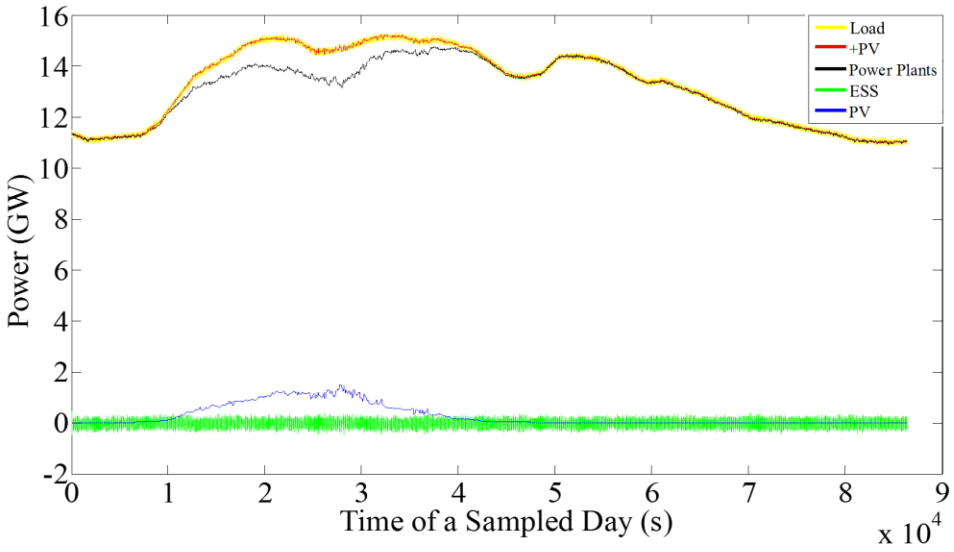

Figure 4.9: Power profiles of different generating units with ESS under 10% PV penetration

Table 4.3. Average ramp rate of power plants with and without ESS under 10% PV penetration

	No ESS	With ESS
Average Ramp Rate (MW/s)	25.166	1.591

4.2.4 ESS to Cater for the Loss of LGU

An incident of the loss of LGU in the middle of the day in the Peninsular Malaysia network is simulated and the results are shown in Figure 4.10 and 4.11. The frequency deviation is shown to be successfully maintained within ±0.05 Hz and the SOC operation range is secured, however the ESS power required for such operation indicates an additional equivalent capacity. While admittedly such

ESS capacity is to incur a huge capital cost to the Utility, the case study nonetheless demonstrates the ability of ESS for such application.

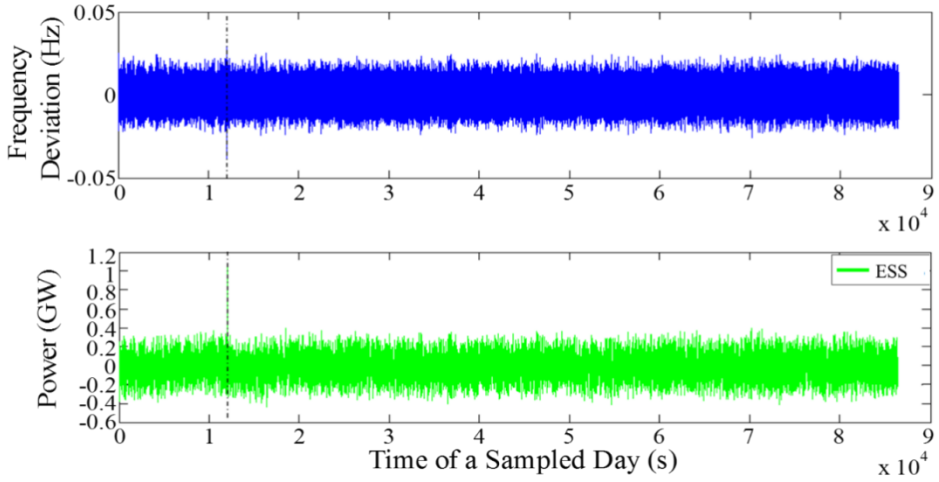

Figure 4.10: Frequency deviation profile and power profile of ESS in the event of the loss of LGU

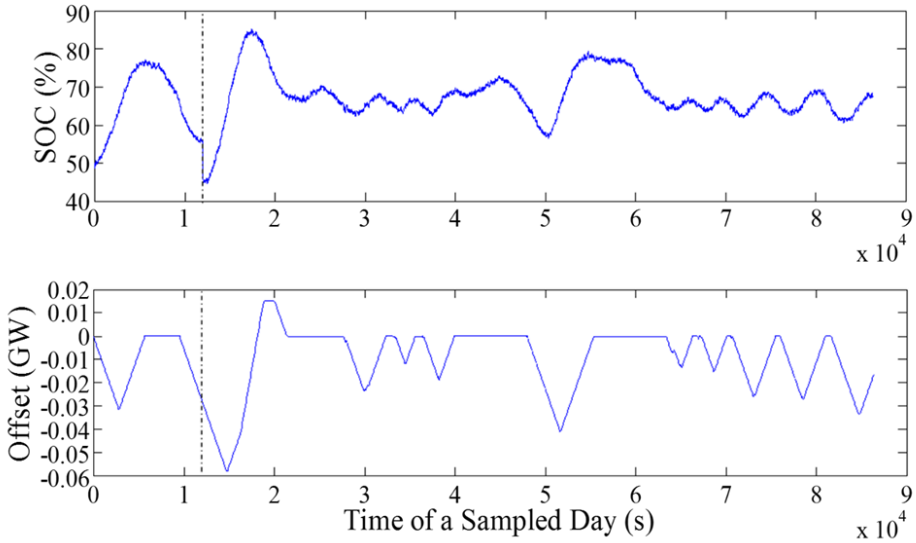

Figure 4.11: SOC and power offset signals of ESS in the event of the loss of LGU

4.3 IEEE 24-bus RTS

The simulation results of the IEEE 24-bus RTS are presented in the following sections.

4.3.1 Frequency Deviation Histograms and Identification of Optimal Control Areas Placement of ESS for Maximum Frequency Quality

This section presents the 1-week frequency deviation histograms of the RTS with ESS being placed at various control areas to identify the optimal placement for maximum frequency quality. Figure 4.12 shows the frequency deviation profiles without ESS in the network, where the frequency deviation runs up to ± 0.1 Hz. Meanwhile, Figure 4.13, Figure 4.14 and Figure 4.15 show the histograms of frequency deviation when ESS is placed in the individual control area 1, 2 and 3 respectively. It is noticed that the frequency quality of the particular control area is improved but not of other control areas. This phenomenon is quantified and shown in bold in Table 4.1. The simulation implies that the reliance on the power transfer from other control areas is not effective in terms of frequency regulation.

On other hand, Figure 4.16 shows the profiles where ESS is placed at every control area where the frequency deviations in all zones are minimised significantly. Hence, it is deduced that the provision for frequency regulation

should be available in each control area. The numerical results on the range and the standard deviations of the histograms are shown in Table 4.4 and having ESSs in every control area displays the smallest range and standard deviation in all control areas.

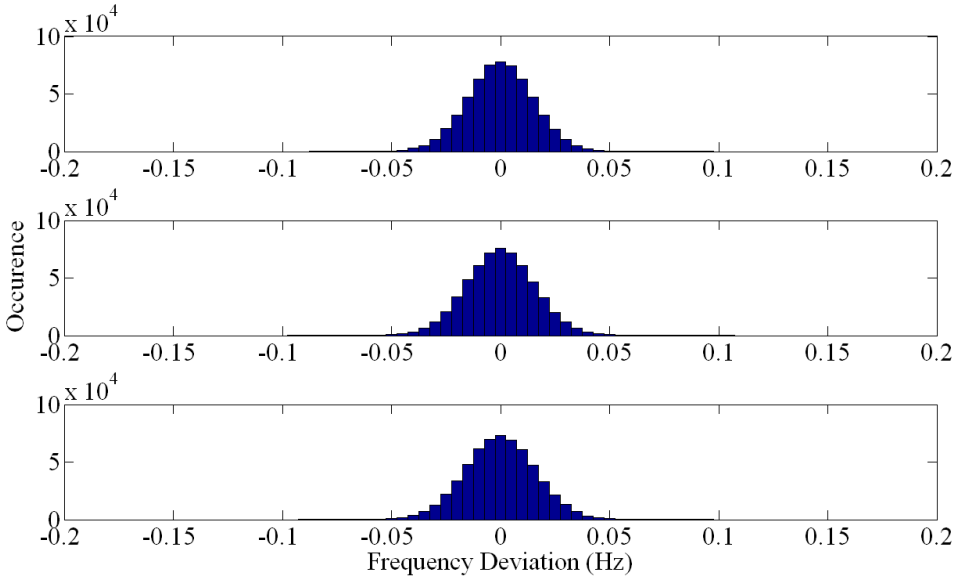

Figure 4.12: Histogram of 1-week frequency deviation for 3 control areas in RTS without ESS

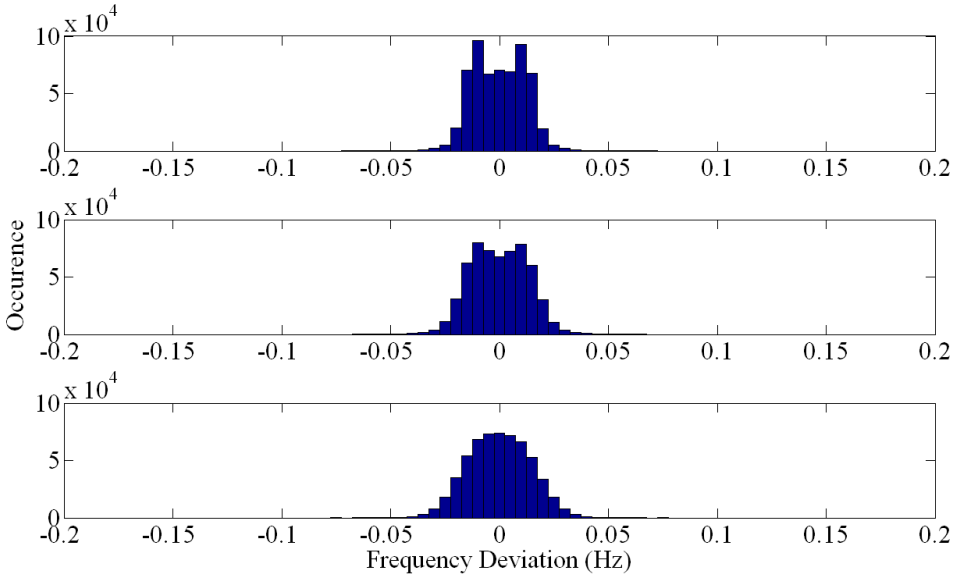

Figure 4.13: Histogram of 1-week frequency deviation for 3 control areas in RTS with ESS in Area 1

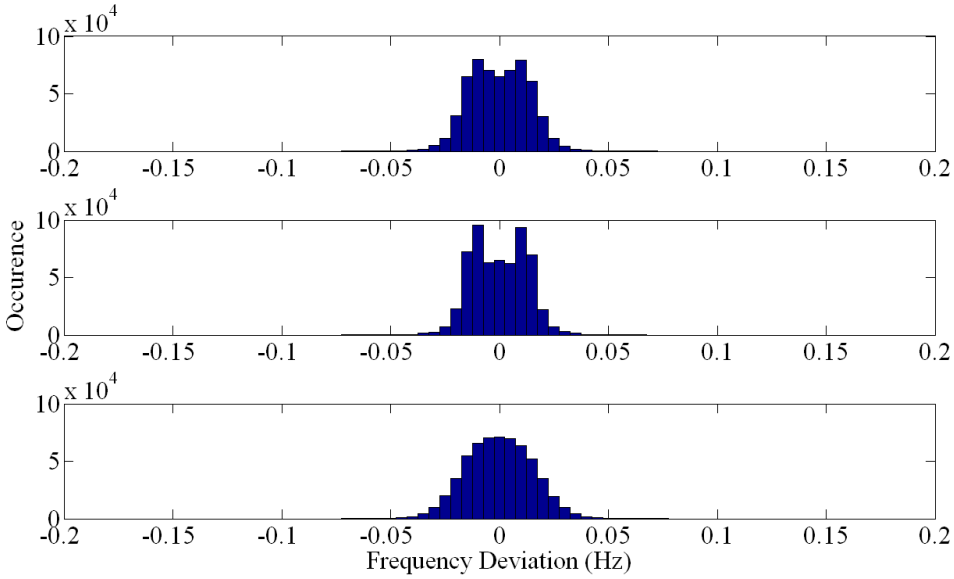

Figure 4.14: Histogram of 1-week frequency deviation for 3 control areas in RTS with ESS in Area 2

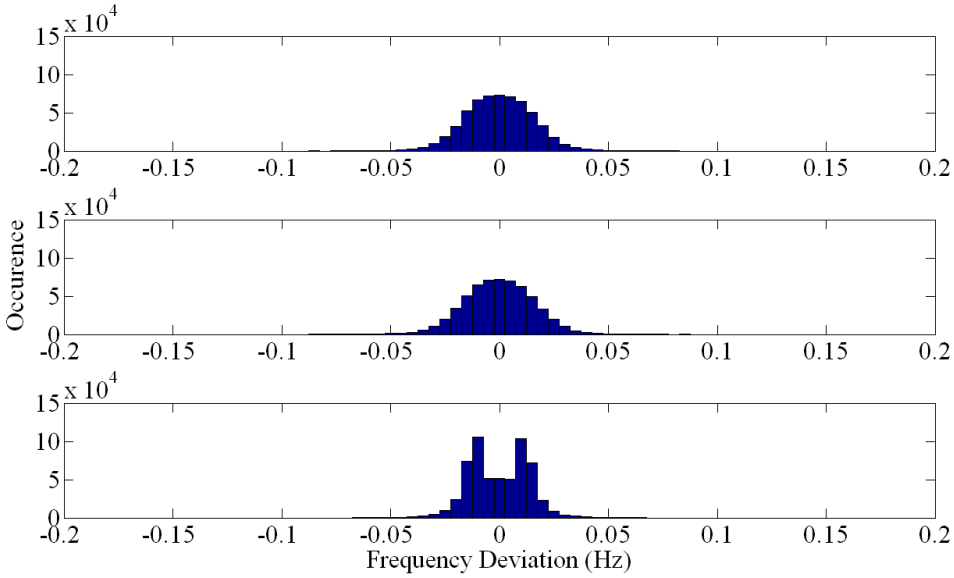

Figure 4.15: Histogram of 1-week frequency deviation for 3 control areas in RTS with ESS in Area 3

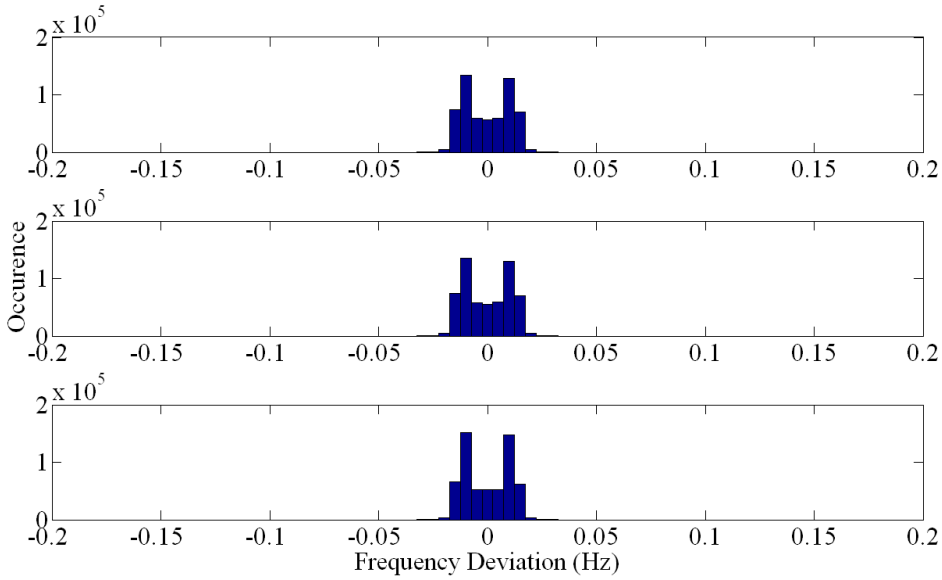

Figure 4.16: Histogram of 1-week frequency deviation for 3 control areas in RTS with ESS in all control areas

Table 4.4: Standard deviation and range of histogram of 1-week frequency deviation profile for various ESS locations

ESS Location	Frequency Deviation (Hz)			
	Control Zone	Standard Deviation	Maximum	Minimum
No ESS	Z1	0.0153	0.0961	-0.0839
	Z2	0.0158	0.1042	-0.0938
	Z3	0.0162	0.0927	-0.0881
Zone 1 (Z1)	Z1	**0.0121**	0.0698	-0.0694
	Z2	0.0131	0.0666	-0.0668
	Z3	0.0143	0.0742	-0.0745
Zone 2 (Z2)	Z1	0.0134	0.0706	-0.0686
	Z2	**0.0126**	0.0668	-0.0704
	Z3	0.0150	0.0763	-0.0723
Zone 3 (Z3)	Z1	0.0155	0.0805	-0.0866
	Z2	0.0159	0.0857	-0.0838
	Z3	**0.0136**	0.0625	-0.0653
All Three Zones	Z1	0.0105	0.0311	-0.0293
	Z2	0.0106	0.0310	-0.0293
	Z3	0.0105	0.0298	-0.0290

4.3.2 ESS Sizing

The maximum and minimum daily power and energy capacity required for ESSs placed at various locations for frequency regulation are summarised in Table 4.5. While it is shown that having one single ESS is not able to regulate frequency effectively regardless of the control area that it is placed in, the identified power and energy capacities are nonetheless determined to be about 50MW and 15MWh respectively. On the other hand, since having an ESS in every control area provides the best frequency quality, the total power and energy capacity required for the RTS are identified to be about 50MW and 50MWh respectively. Having to

set the operating range of ESS at 65% to 85%, the usable capacity is only 20%. To identify the exact ESS capacity sizing, the identified required energy capacity is multiplied by 5 to give a 250MWh. In short, the ESS sizing proposed in the dissertation is derived from historical load profiles based on the modelled control algorithm.

Table 4.5: Maximum and minimum daily power and energy capacity required for ESS based on 1-week simulation for various ESS locations

ESS Location	Max. ESS Power (MW)	Min. ESS Power (MW)	Max. ESS Capacity (MWh)	Min. ESS Capacity (MWh)
Zone 1	44.39	-40.45	12.12	-14.48
Zone 2	42.16	-44.2	11.39	-15.06
Zone 3	47.75	-48.56	11.30	-13.94
Each Zone	50.72	-48.29	37.01	-51.48

4.3.3 Network Voltage Profiles

The network voltage profiles are simulated at the time steps when daily maximum and minimum power mismatch occur during the course of frequency regulation. To identify the busbar location of ESS that contributes the least impact to the grid voltage, ESS has been placed at various locations as described in Section 3.4.2. For the last scenario where a unit of ESS is placed on all buses, the sized ESS power and capacity for a control area is divided equally among all buses. For instance, as there are 10 buses in Control Area 1, each ESS is rated at 5MW and 25MWh.

Figure 4.17 and Figure 4.18 show the network voltage profiles at the identified time steps of one sampled day, where the results of ESS being placed at various control areas and busbar types are presented. As the power injection and absorption of ESSs required during frequency regulation is small to result in voltage violations in the transmission network, the voltage profiles of having one ESS in the RTS and of spreading the ESSs on every single bus do not make a significant difference. This is also contributed by the fact that the line reactance to resistance ratio (R/X ratio) is low in the transmission network; hence the transmission loss and the voltage drop are low. In the meantime, the voltage magnitude on certain buses remained unchanged in all scenarios as they contain generators with voltage regulation ability and modelled as PV buses. The complete 1-week result is shown in Appendix B.

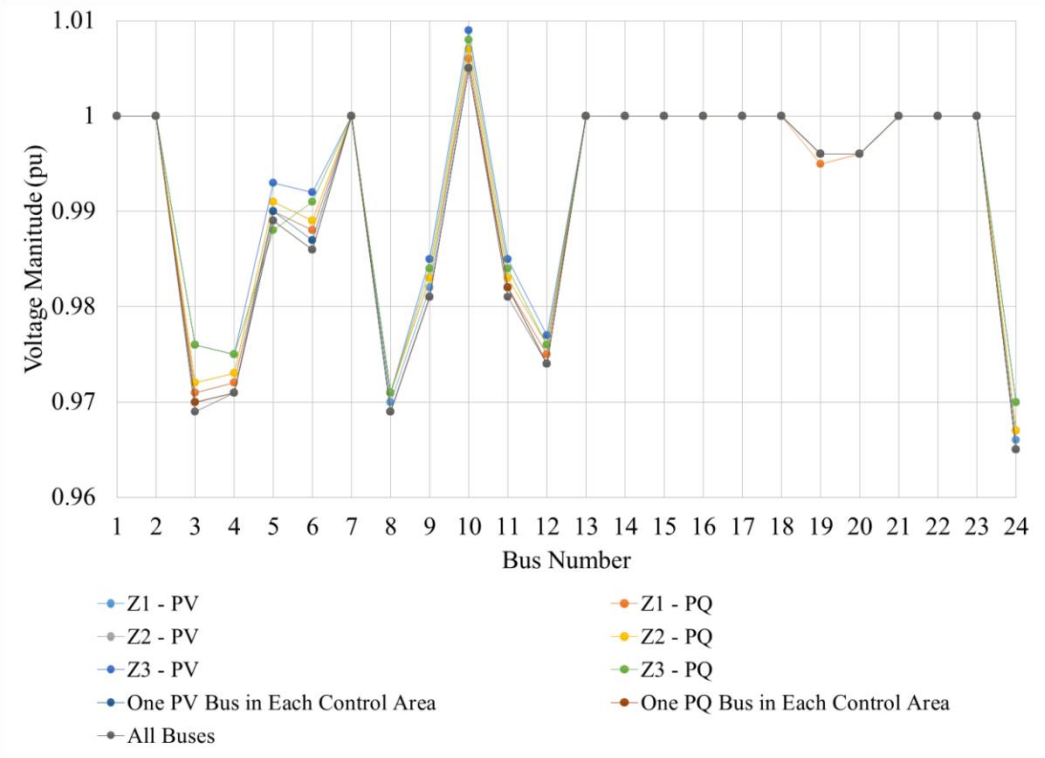

Figure 4.17: Network voltage profiles of various ESS placement combinations at maximum power mismatch of a sampled day

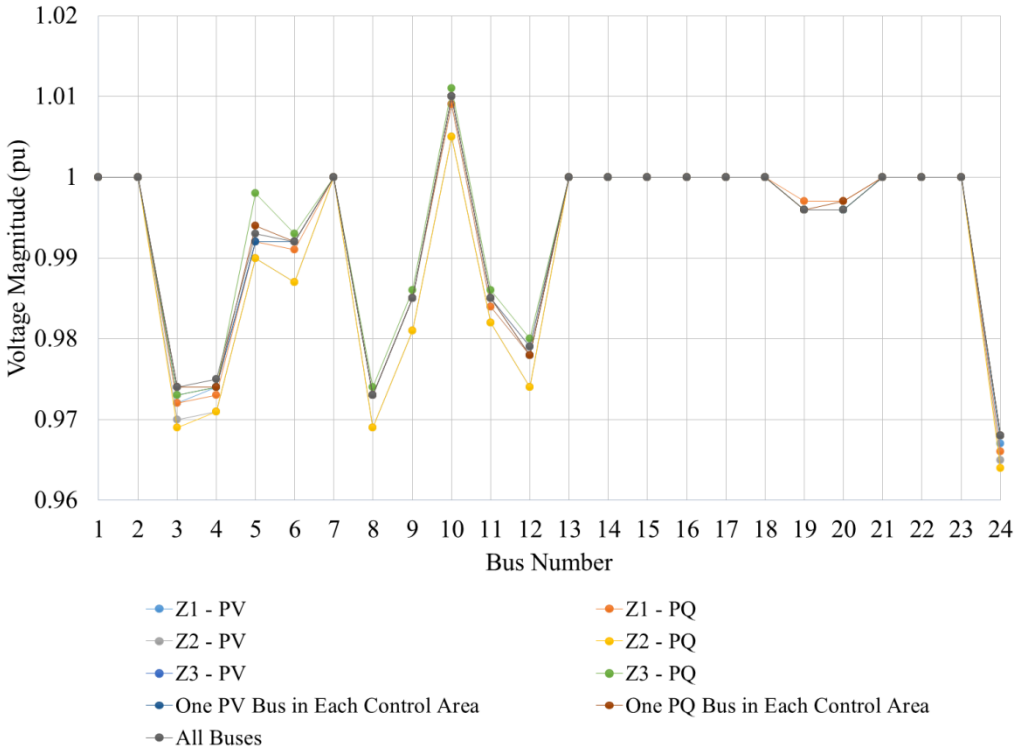

Figure 4.18: Network voltage profiles of various ESS placement combinations at minimum power mismatch of a sampled day

4.3.4 Results of Undersized ESS

As the capacity sizing of ESS is identified to be 250MWh (about 83MWh per control area), the simulation is repeated with 80%, 60%, 40%, 20% sizing of ESSs in every control area. The histograms of the pertinent 1-week frequency deviation profiles are shown in the following figures, demonstrating consistent frequency quality for all of them. Meanwhile, the results are tabulated in Table 4.6. The main reason of obtaining similar frequency quality for an undersized ESS is that the actions of the proposed offset algorithm allows ESSs to keep track with

the load changes rather than supplying the exact power required for frequency regulation when the ESSs are out of the defined healthy operating range. For instance, at a time when a certain regulation power is required but the ESSs are running out of capacity, the offset renders the ESSs to supply the determined power initially. The supplied power is later slowly ramped down to conserve the ESS capacity, where the balance is picked up by the power plants. Therefore, rather than supplying the exact amount of power required for frequency regulation, ESSs are tracking the change of the power required, such that certain portion of the power is eventually passed and to be supplied by the power plants.

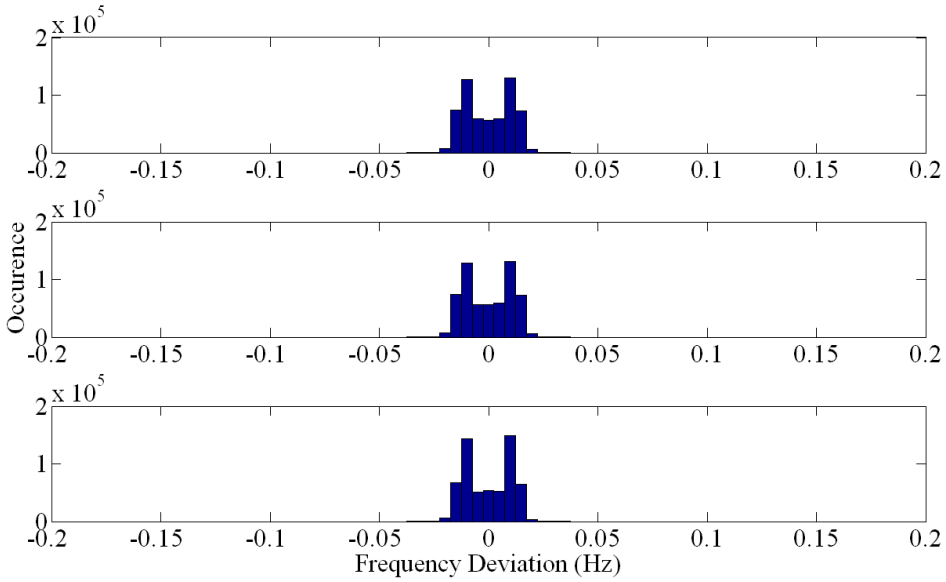

Figure 4.19: Histogram of 1-week frequency deviation for 3 control areas in RTS with an 80%-sized ESS in all control areas

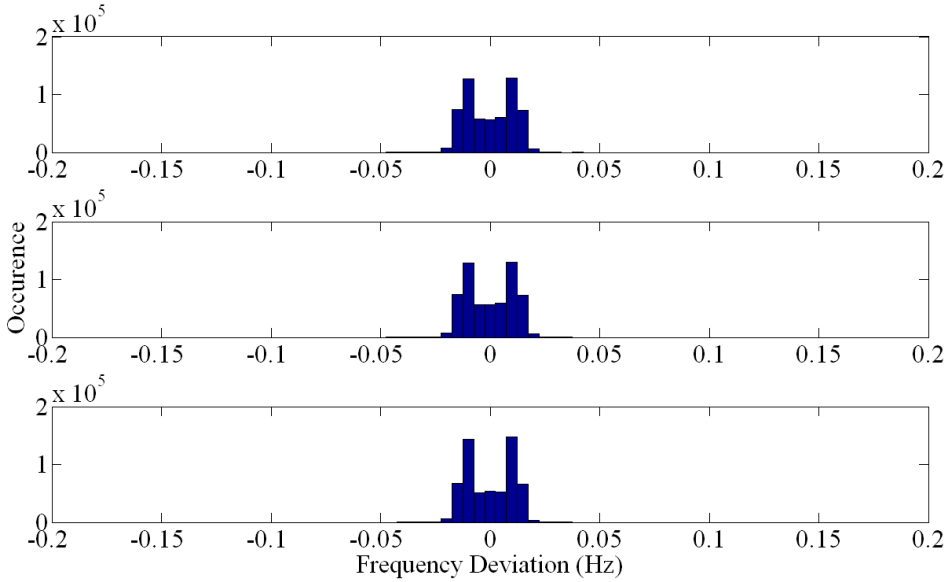

Figure 4.20: Histogram of 1-week frequency deviation for 3 control areas in RTS with a 60%-sized ESS in all control areas

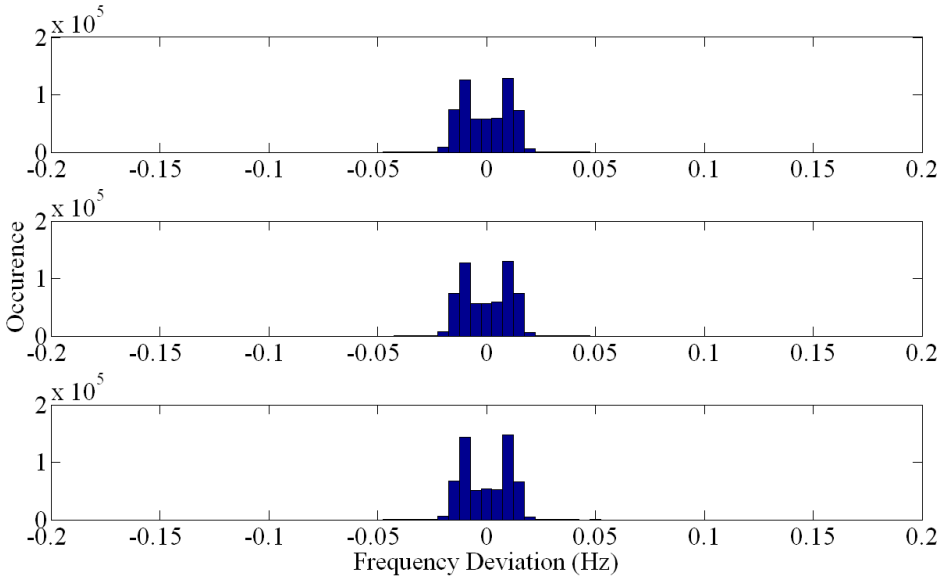

Figure 4.21: Histogram of 1-week frequency deviation for 3 control areas in RTS with a 40%-sized ESS in all control areas

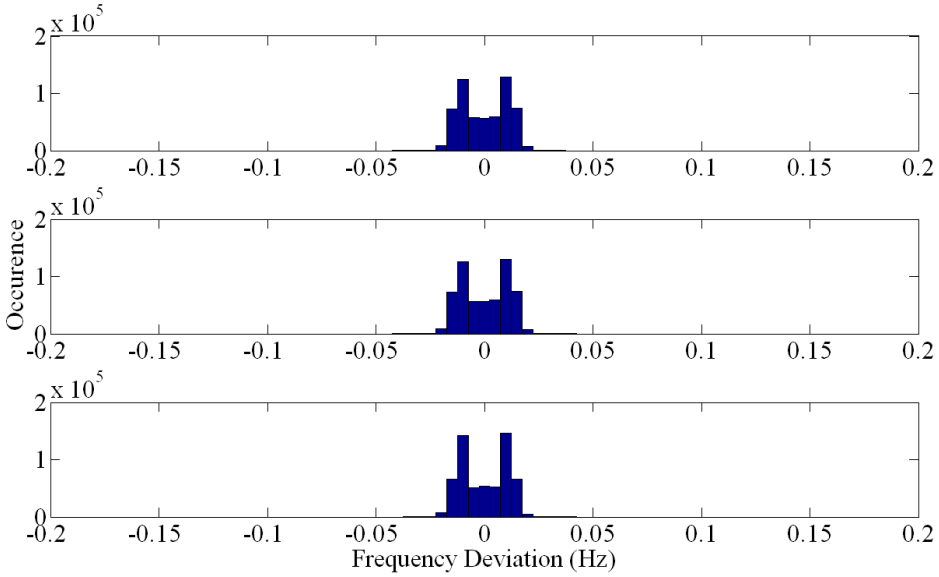

Figure 4.22: Histogram of 1-week frequency deviation for 3 control areas in RTS with a 20% sized ESS in all control areas

Table 4.6: Standard deviation and range of histogram of 1-week frequency deviation profile for various ESS sizing

ESS	Frequency Deviation (Hz)			
	Control Area	Standard Deviation	Maximum	Minimum
No ESS	Z1	0.0153	0.0961	-0.0839
	Z2	0.0158	0.1042	-0.0938
	Z3	0.0162	0.0927	-0.0881
100%-Sized	Z1	0.0106	0.0346	-0.0345
	Z2	0.0106	0.0317	-0.0356
	Z3	0.0106	0.0346	-0.0345
80%-Sized	Z1	0.0107	0.033	-0.037
	Z2	0.0107	0.0334	-0.0358
	Z3	0.0106	0.0334	-0.0367
60%-Sized	Z1	0.0107	0.0398	-0.0445
	Z2	0.0107	0.0328	-0.0465
	Z3	0.0107	0.0353	-0.039
40%-Sized	Z1	0.0107	0.0433	-0.0431
	Z2	0.0108	0.0431	-0.0393
	Z3	0.0107	0.0484	-0.0429
20%-Sized	Z1	0.0108	0.0374	-0.0397
	Z2	0.0108	0.0378	-0.0395
	Z3	0.0107	0.0393	-0.0371

However, if the ESSs are undersized by a large factor, the frequency and the magnitude of ramping increase due to the actions of the offset. In this context, Fig 4.23 shows the full-sized ESSs with smooth SOC profiles while Fig 4.24 shows 20%-sized ESSs with turbulent and fluctuating profiles. Nevertheless, it is beyond the scope of the dissertation to investigate the prolonged chemical and physical effects of such operation to the batteries but it demonstrates the possibility of undersizing ESSs with the combined actions of offset algorithm.

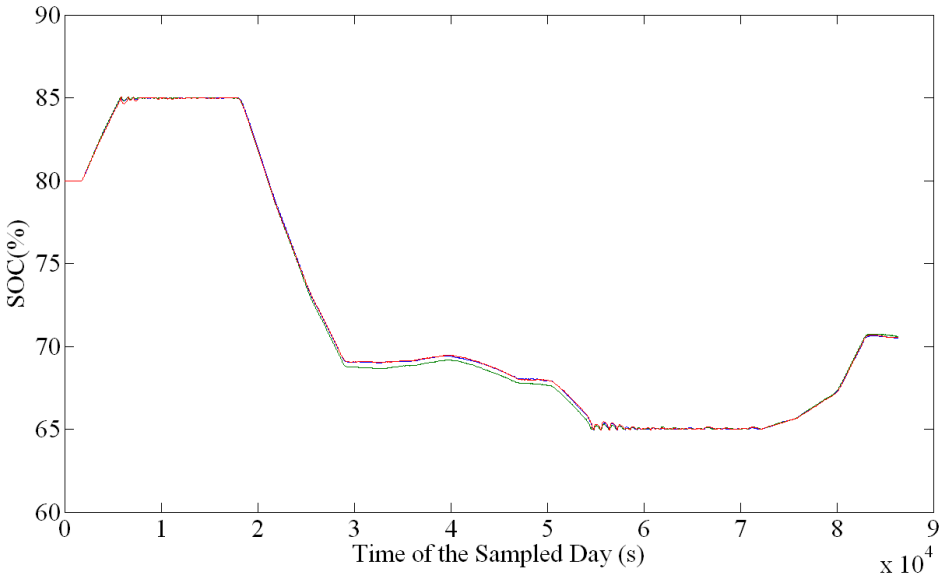

Figure 4.23: SOC profiles of a sampled day of a 100%-sized ESS in all control areas

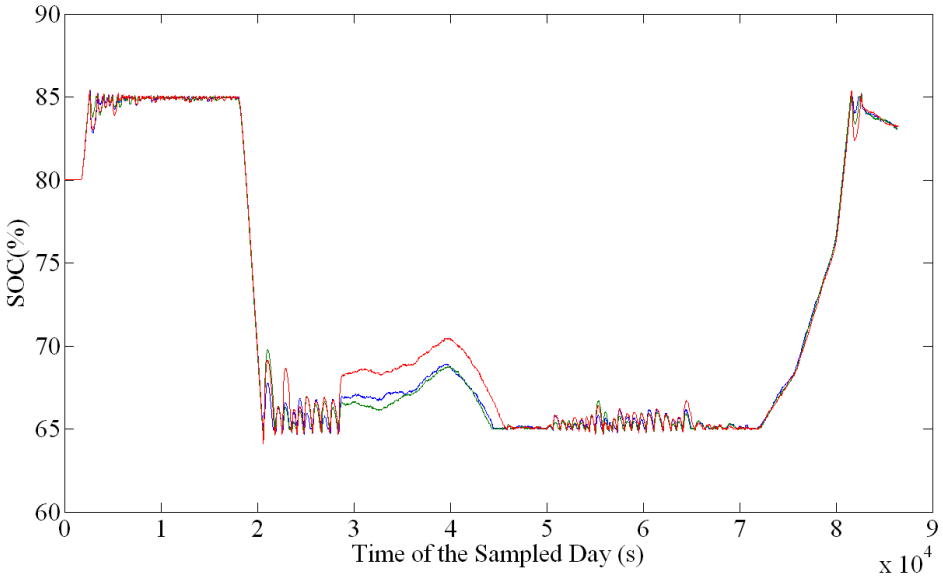

Figure 4.24: SOC profiles of a sampled day of a 20%-sized ESS in all control areas

Meanwhile, throughout the 1-week simulation, the SOCs of ESSs for various sizing operate within a healthy range as shown in Figure 4.25 and Figure 4.26. The maximum and minimum SOC is kept close to the defined 85% and 65% respectively, while the more undersized ESSs result in larger deviations of the values.

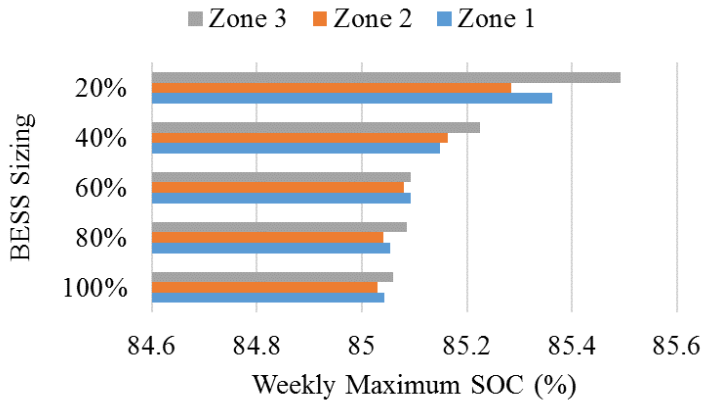

Figure 4.25: Weekly maximum SOC of ESS placed in all 3 RTS control areas for various ESS sizing

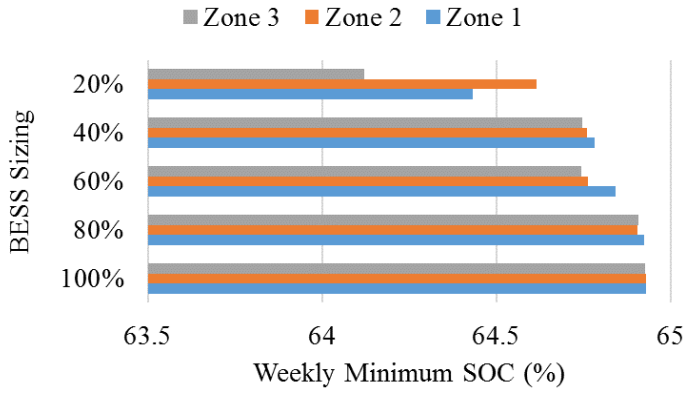

Figure 4.26: Weekly minimum SOC of ESS placed in all 3 RTS control areas for various ESS sizing.

4.3.5 25% PV Penetration

This section presents the 1-week frequency deviation histograms of the RTS under 25% PV penetration with and without various sizing of ESSs. The frequency deviation profile under PV penetration without the participation of ESSs in Figure 4.27 breaches ±0.1 Hz, which is worse than the profile in Figure 4.12 without PV penetration due to the intermittency of PV.

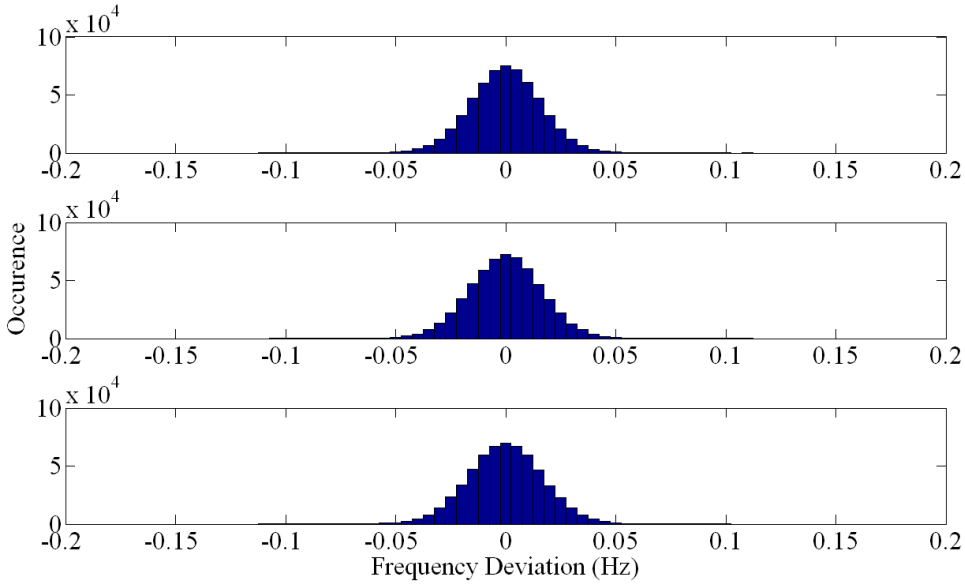

Figure 4.27: Histogram of 1-week frequency deviation under 25% PV penetration for 3 control areas in RTS without ESS

At the same time, the frequency quality is also worse off in general with undersized ESSs where the quantitative results are shown in Table 4.7. In addition, the intermittency of PV also causes stability issues to the offset algorithm for undersized ESSs as shown in Figure 4.33 such that the fluctuations of SOCs of 20%-sized ESSs are most prominent during the middle of the day when the PV is

producing power. The profiles in Figure 4.33 are also more turbulent than that without PV penetration in Figure 4.24, which the operation might decrease the lifespan of the batteries.

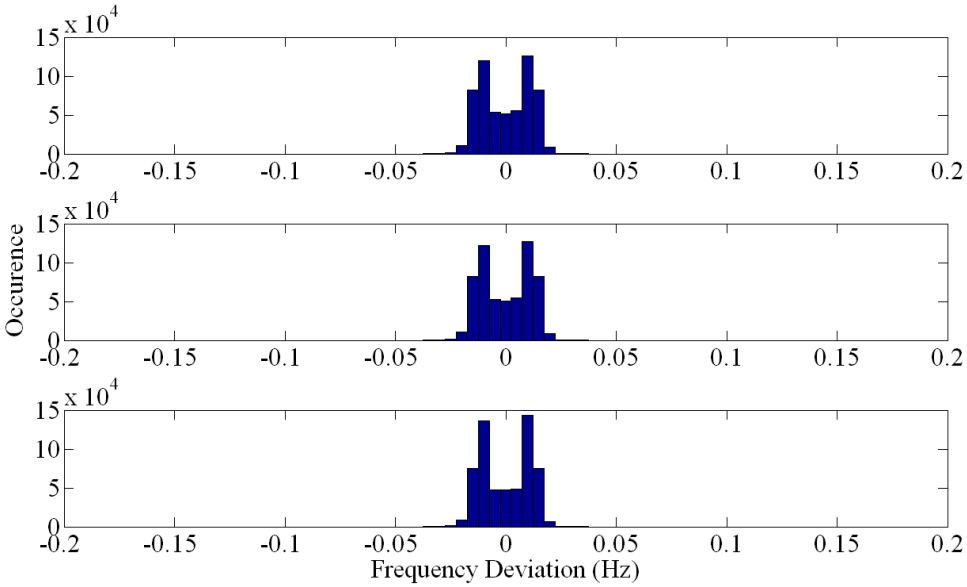

Figure 4.28: Histogram of 1-week frequency deviation under 25% PV penetration for 3 control areas in RTS with a 100%-sized ESS in all control areas

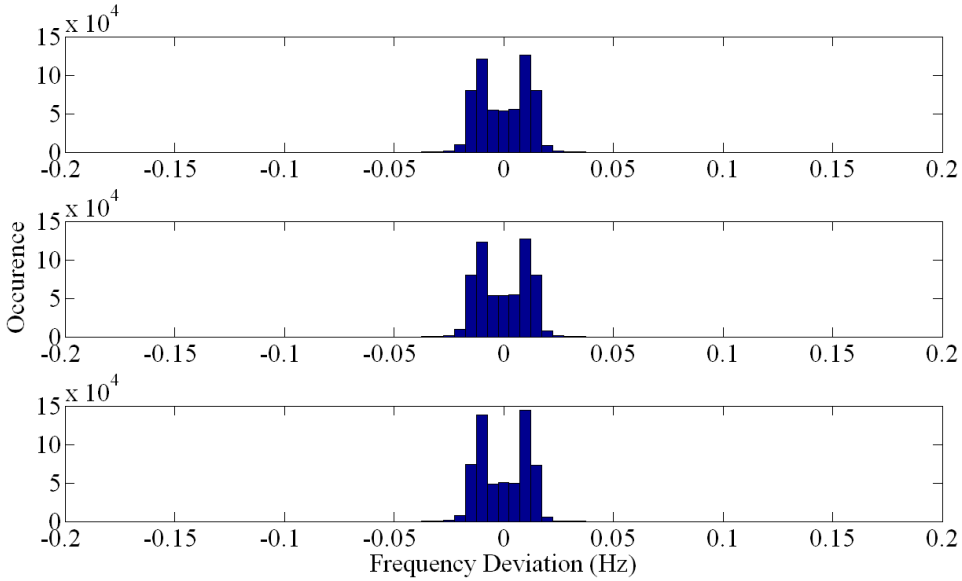

Figure 4.29: Histogram of 1-week frequency deviation under 25% PV penetration for 3 control areas in RTS with an 80%-sized ESS in all control areas

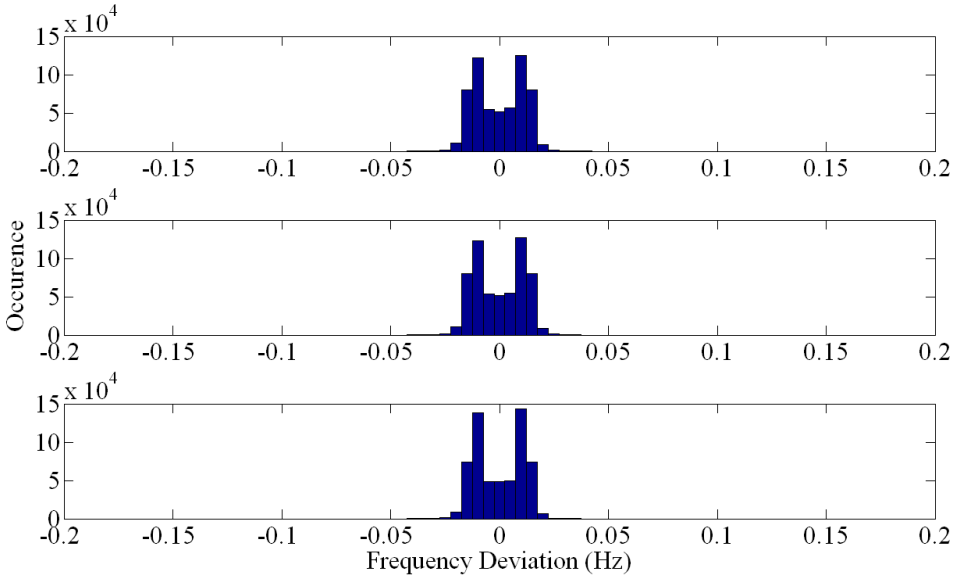

Figure 4.30: Histogram of 1-week frequency deviation under 25% PV penetration for 3 control areas in RTS with a 60%-sized ESS in all control areas

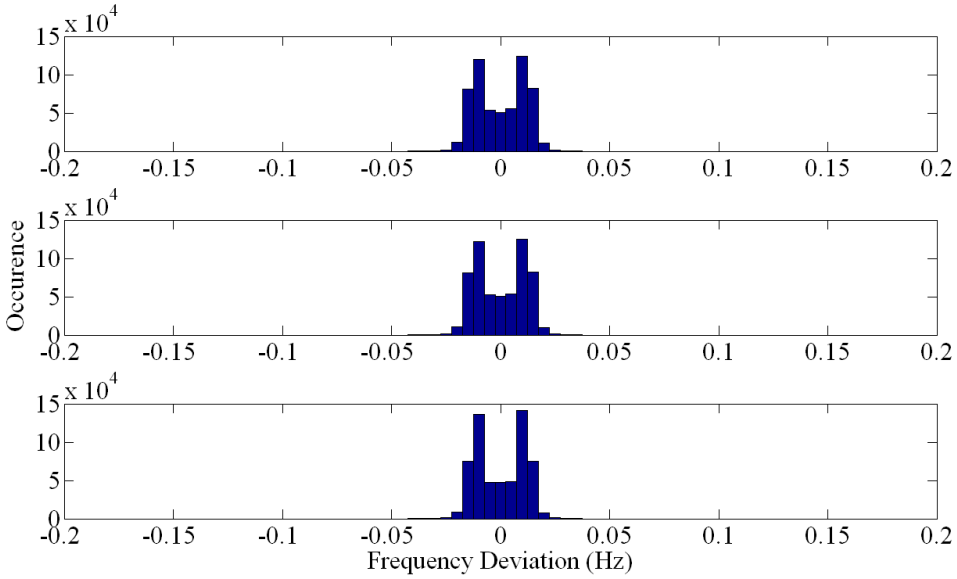

Figure 4.31: Histogram of 1-week frequency deviation under 25% PV penetration for 3 control areas in RTS with a 40%-sized ESS in all control areas

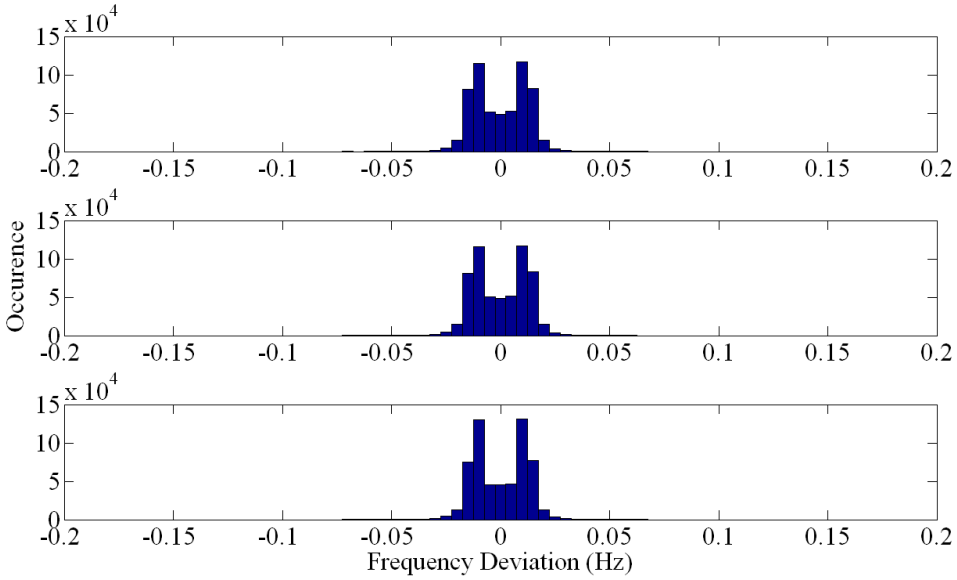

Figure 4.32: Histogram of 1-week frequency deviation under 25% PV penetration for 3 control areas in RTS with a 20%-sized ESS in all control areas

Table 4.7: Standard deviation and range of histogram of 1-week frequency deviation profile for various ESS sizing under 25% PV penetration

ESS	Frequency Deviation (Hz)			
	Control Zone	Standard Deviation	Maximum	Minimum
No ESS	Z1	0.0164	0.1116	-0.1092
	Z2	0.0169	0.1089	-0.1075
	Z3	0.0173	0.1011	-0.1075
100%-Sized	Z1	0.0112	0.0357	-0.037
	Z2	0.0112	0.0356	-0.0369
	Z3	0.0111	0.036	-0.0365
80%-Sized	Z1	0.0111	0.0363	-0.0366
	Z2	0.0111	0.0357	-0.0371
	Z3	0.011	0.035	-0.0356
60%-Sized	Z1	0.0112	0.0376	-0.0386
	Z2	0.0112	0.0364	-0.0381
	Z3	0.0111	0.0352	-0.0385
40%-Sized	Z1	0.0113	0.036	-0.0381
	Z2	0.0113	0.0345	-0.0379
	Z3	0.0112	0.0352	-0.0382
20%-Sized	Z1	0.0121	0.0631	-0.0704
	Z2	0.0122	0.0599	-0.069
	Z3	0.0121	0.0633	-0.0707

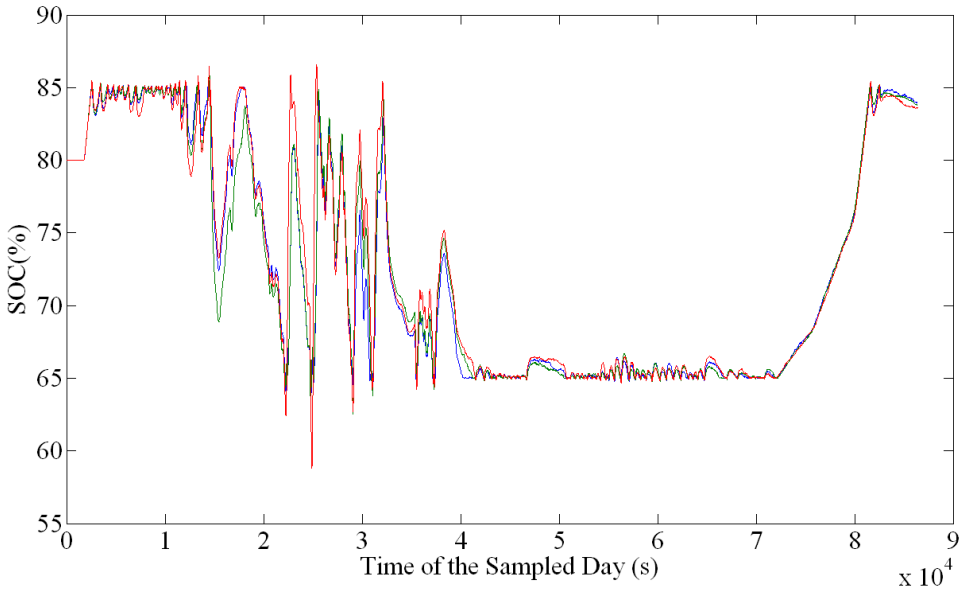

Figure 4.33: SOC profiles of a sampled day of 20%-sized ESS in all control areas under 25% PV penetration

Fundamentally, ESSs are not energy sources therefore they require additional energy sources to provide the capacity for frequency regulation. In this context, the total power plant output energy in the RTS network in 1 week for various ESS sizing is higher than that without ESS, as shown in Table 4.8. However, the power plant energy for meeting the load and for charging the ESS can be reduced with other RE sources in the grid network.

Table 4.8: Total power plant output energy for various ESS sizing without PV and with 25% PV penetration

ESS Sizing	Total Power Plant Energy (MWh)	
	Without PV	25% PV
100%	300383.10	280789.45
80%	300383.54	280815.07
60%	300380.25	280820.52
40%	300377.94	280816.65
20%	300381.47	281074.05
None	**300275.69**	**280642.81**

As the dissertation proposes to charge the ESSs with power plants through offset algorithm since they are available at all times, ESSs are not able to replace spinning reserves in terms of capacity but for frequency regulation response in the network. On other hand, ESSs are able to replace the spinning reserves that cater for the loss of LGU. However, it requires the standing by of a large capacity of ESSs.

4.4 Summary

The chapter presents the simulation results of Peninsular Malaysian and IEEE 24-bus RTS network. ESSs are shown to be able to minimise the frequency deviation effectively with the proposed control algorithm and under high PV penetration. Meanwhile, the proposed offset algorithm are also shown to be able to maintain the SOC at a healthy operating range throughout the simulation and allowing

ESSs to be undersized for frequency regulation purposes, thus providing potential monetary savings in utilising reduced capacity of ESSs.

An undersized ESS does not degrade the grid frequency quality significantly, but given the condition of a high PV penetration in the network, the particular ESS requires frequent and large-magnitude ramping to maintain its capacity, which might decrease the lifespan of the batteries. However, the lifespan limitation might be able to be overcome by using other types of ESSs. Also, coupling ESSs with sufficient power output of RE sources in the network presents an opportunity to replace spinning reserves completely.

CHAPTER 5

CONCLUSION AND FUTURE WORK

5.1 Conclusion

A stable grid frequency is achieved by maintaining the power balance between load and generation in a grid network. The task is conventionally carried out by the traditional power plants categorized as spinning reserves, mainly CCGTs in fact, as they possess the shortest response time for frequency regulation. However, the power plants are essentially limited by their ramping rate and duration for an effective frequency regulation. Meanwhile, constant ramping of the power plants results in the increased wear-and-tear of their mechanical components. Besides, the power plants are required to run at partial capacity to cater for such purpose. The objectives as proposed previously with the respective conclusions are described in the following.

I. **To propose a comprehensive work package for adopting ESSs to carry out frequency regulation continuously in an interconnected power system.**

A comprehensive work package is proposed to model the transfer functions of the power system with the power plants to study the network frequency changes

throughout load profiles with and without ESSs. The transfer functions of the components are used to represent their respective responses in terms of power generation. The frequency regulation analysis is carried out in MATLAB/Simulink while the voltage analysis is implemented in Matpower where the inputs are obtained from the outputs of MATLAB/Simulink. The proposed work package provides the seamless transfer of simulation data to study the frequency regulation response, the power profiles of all generating units in the network, the sizing of ESS and the SOC profile and the network voltage profiles.

II. **To evaluate the performance of the proposed framework in terms of the frequency regulation algorithm and the capacity conservation offset algorithm of ESS.**

Droop control as the primary while integral and derivative control as the secondary control are proposed as the frequency regulation algorithm of ESS. The algorithm is shown to be effective in minimizing frequency deviations qualitatively and quantitatively for both network models; of the Peninsular Malaysia and IEEE 24-bus RTS. A set of SOC conservation offset algorithm is also proposed and proven to work throughout the simulated duration in the dissertation to ensure the continuous operation of ESS.

III. **To identify the optimal ESS location for frequency regulation purpose in the transmission network in terms of frequency regulation quality and minimal voltage impact to the power grid.**

In the frequency regulation response study carried out in MATLAB/Simulink, it is identified that placing ESSs in every control area provides the best frequency quality as effective frequency regulation is performed locally within the control area without the reliance of power transfer from other control areas. Meanwhile in the network voltage study in Matpower, it is learned that the power absorption and injection of ESS for frequency regulation is small to deal a significant impact on the modelled transmission network voltage profiles. However, this may not hold true in other networks or distribution networks, hence the proposed framework allows such studies to be carried out seamlessly.

IV. **To evaluate the case studies of high PV penetration and the adoption of undersized ESSs for frequency regulation.**

The ESSs are shown to regulate the grid frequency effectively for both the simulation models, first under a 10% PV penetration in the Peninsular Malaysia network and second under a 25% PV penetration in RTS network. While undersizing the ESSs does not degrade the grid frequency quality by much due to the actions of the proposed capacity offset algorithm, a higher penetration of intermittent sources presents a more significant deterioration of regulation quality. Besides, undersizing the ESSs not only results in a more frequent ramping up and down of power by ESSs, but also at a large power magnitude change. The effects

on the chemistry and long-term sustainability of BESSs are beyond the scope of the study. However, it presents the idea of replacing BESSs with other mechanical ESSs like flywheels and super capacitors that may not encounter similar shortcomings.

5.2 Future Work

The major limitation of the dissertation is that it is essentially a simulation and physical ESSs are not involved in the study. Therefore, the physical and chemical effects of the proposed offset algorithm and frequent ramping of undersized BESSs are beyond the scope of the study. Hence, the most immediate future work is to test the effects of the aforementioned operation experimentally with a physical ESS. This can be achieved by integrating real-time network simulator that models the large power network, incorporated with hardware-in-the-loop (HIL) that includes a battery simulator or a physical battery. Likewise, based on the similar experimental network, BESSs can be replaced with other types of ESS, or combining multiple types of ESS for the study.

Similarly in the simulation models, other types or combining multiple types of ESS can be simulated. Meanwhile, other types of RE source can be simulated as well, along with the possibility of extending it to a larger network or narrowing it down to a smaller distribution network, which are achievable due to the flexibility

of the proposed work package. As the magnitude of power absorption and injection by ESSs is too small to impact the voltages in the transmission network in the dissertation, it is recommended to investigate the effects of having large ESS size on smaller distribution networks.

For more complicated simulations that involve the dynamic actions or interventions by other components in the power network like transformers and demand-side response, the ITE can be utilised to connect the simulations in MATLAB/Simulink with MAS (as described in Section 3.4.3). Last but not least, an economic analysis can also be incorporated to the study to identify the most cost effective way of utilising ESSs for frequency regulation.

LIST OF REFERENCES

Ahmadi, S., Shokoohi, S. & Bevrani, H., 2015. A Fuzzy-Logic Based Droop Control for Simultaneous Voltage and Frequency Regulation in an AC Microgrid. *Electr. Power and Energy Syst.*, pp. 148-155.

Augustin, M., Tom, M. & Luis, C., 2012. *Solar Cells: Materials, Manufacture and Operation.* s.l.:Academic Press.

Black & Veatch, 2012. *Cost and Performance Data for Power Generation Technologies,* s.l.: Black & Veatch.

Campbell, T. & Bradley, T., 2014. A Model of the Effects of Automatic Generation Control Signal Characteristics on Energy Storage System Reliability. *J. Power Sources,* pp. 594-604.

Castillo, M., Lim, G., Yoon, Y. & Chang, B., 2014. Application of Frequency Regulation Control on the 4MW/8MWh Battery Energy Storage System (BESS) in Jeju Island, Republic of Korea. *Journal of Energy Power Sources*, pp. 287-295.

Das, D., Roy, A. & Sinha, N., 2011. *PSO Based Frequency Controller for Wind-Solar-Diesel Hybrid Energy Generation/Energy Storage System.* Odisha, s.n.

Delille, G., Francois, B. & Malarange, G., 2012. Dynamic Frequency Control Support by Energy Storage to Reduce the Impact of Wind and Solar Generation on Isolated Power System's Inertia. *IEEE Trans. on Sustainable Energy,* pp. 931-939.

Department of Computer Science, University of Waikato, n.d. *Electrical Machines - Basic Vocational Knowledge.* [Online] Available at: http://www.nzdl.org/gsdlmod?e=d-00000-00---off-0gtz--00-0----0-10-0---0---0direct-10---4-------0-0l--11-en-50---20-help---00-0-1-00-0-0-11-1-0utfZz-8-00&a=d&cl=CL3.2&d=HASH01693eebdf3891bea95c4ae7.6.1.fc [Accessed 11 April 2017].

First Hydro Company, 2009. *Welcome to First Hydro Company.* s.l., s.n.

Forschungsstelle für Energiewirtschaft e.V., 2017. *Technischer Aufbau der Frequenzregelung im UCTE.* [Online] Available at: https://www.ffe.de/publikationen/fachartikel/167-technischer-aufbau-der-frequenzregelung-im-ucte [Accessed 19 March 2013].

Gu, W., Liu, W., Shen, C. & Wu, Z., 2013. Multi-Stage Underfrequency Load Shedding for Islanded Microgrid with Equivalent Inertia Constant Analysis. *International Journal of Electric Power & Energy Systems,* pp. 36-39.

Hawai'i Natural Energy Institute, 2014. *Control Algorithms for Grid-Scale Battery Energy Storage,* s.l.: HNEI.

Holt, G., 2009. *Portable Generators in Motion Picture Production.* [Online] Available at: http://screenlightandgrip.com/html/emailnewsletter_generators4.1.html [Accessed 24 March 2017].

Johnston, L. et al., 2015. Methodology for the Economic Optimisation of Energy Storage Systems for Frequency Support in Wind Power Plants. *Applied Energy,* pp. 660-669.

Kintner-Meyer, M. et al., 2012. *National Assessment of Energy Storage for Grid Balancing and Arbitrage,* Richland: PNNL.

Knap, V. et al., 2014. *Grid Inertial Response with Lithium-ion Battery Energy Storage Systems.* Istanbul, IEEE.

Koh, S., Lim, Y. & Morris, S., 2011. Potential of Advanced Coal and Gas Combustion Technologies in GHG Emission Reduction in Developing Countries from Technical, Environmental and Economic Perspective. *Energy Procedia,* pp. 878-85.

Koller, M., Schmidli, J. & Vollmin, B., 2014. *Frequency Regulation and Microgrid Investigations with a 1MW Battery Energy Storage System.* Rome, CIRED.

Kundur, P., 1993. Prime Movers and Energy Supply Systems. In: *Power System Stability and Control.* Palo Alto: McGraw-Hill, pp. 379-396.

Lefton, S. & Besuner, P., 2001. *Power Plant Cycling Operations and Unbundling Their Effect on Plant Heat Rate,* Sunnyvale: APTECH.

Lew, D. et al., 2013. *The Western Wind and Solar Integration Study Phase 2,* Golden, Colorado: NREL.

Li, X. et al., 2014. *Modeling and Control Strategy of Battery Energy Storage System for Primary Frequency Regulation.* Chengdu, s.n.

Lucas, A. & Chondrogiannis, S., 2016. Smart Grid Energy Storage Controller for Frequency Regulation and Peak Shaving, Using a Vanadium Redox Flow Battery. *Elec. Power and Energy Syst.,* pp. 16-36.

Mallesham, G., Mishra, S. & Jha, A., 2011. *Ziegler-Nichols Based Controller Parameters Tuning for Load Frequency Control in a Microgrid.* s.l., s.n.

Martin II, J., 2016. *Why depth of discharge matters in solar battery storage system selection.* [Online] Available at: https://www.solarchoice.net.au/blog/depth-of-discharge-for-solar-battery-storage [Accessed 7 April 2016].

Oudalov, A., Chartouni, D. & Ohler, C., 2007. Optimizing a Battery Energy Storage System for Primary Frequency Control. *IEEE Trans. Power Syst.,* pp. 1256-1266.

Perez-Diaz, J., Sarasua, J. & Wilhelmi, J., 2014. Contribution of a Hydraulic Short-Circuit Pumped-Storage Power Plant to the Load-Frequency Regulation of an Isolated Power System. *Elec. Power and Energy Syst.,* pp. 199-211.

Reliability Test System Task Force, 1979. IEEE Reliability Test System. *IEEE Trans. on Power Apparaturs and Syst.,* pp. 2047-2054.

REN21, 2016. *Renewable 2016 Global Status Report,* Paris: REN21.

Rojas, A. & Lazarewicz, M., 2004. *Grid Frequency Regulation by Recycling Electrical Energy in Flywheels.* Denver, CO, s.n., pp. 2038-2042.

Schmutz, J., 2013. *Primary Frequency Control Provided by Battery.* Semester thesis, ETH Zurich, Zurich.

Sedky, E., 2009. *Cutaway View of a Synchronous AC Generator.* [Online] Available at: http://emadrlc.blogspot.my/2009/01/cutaway-view-of-synchronous-ac.html [Accessed 5 January 2017].

Serban, I. & Marinescu, C., 2014. Battery Energy Storage System for Frequency Support in Microgrids and with Enhanced Control Features for Uninterruptible Supply of Local Loads. *Elec. Power and Energy Syst.,* pp. 432-441.

Shankar, R., Chatterjee, K. & Bhushan, R., 2016. Impact of Energy Storage System on Load Frequency Control for Diverse Power Sources of Interconnected Power System in Deregulated Power Environment. *Electr Power Energy Syst.,* pp. 11-26.

Sivanagaraju, S., 2009. Load Frequency Control - I. In: *Power System Operation and Control.* New Delhi: Pearson Education India, pp. 268-269.

Suruhanjaya Tenaga (Energy Commission), 2014. *Peninsular Malaysia Electricity Supply Industry Outlook 2014,* s.l.: Suruhanjaya Tenaga.

Suruhanjaya Tenaga (Energy Commission), 2014. *The Malaysian Grid Code,* s.l.: Suruhanjaya Tenaga.

Suruhanjaya Tenaga (Energy Commission), 2016. *Peninsular Malaysia Electricity Supply Industry Outlook 2016,* Putrajaya: Suruhanjaya Tenaga.

U.S. Energy Information Administration, 2016. *Wind and Solar Data and Projections from the U.S. Energy Information Administration: Past Performance and Ongoing Enhancements,* Washington: U.S. Energy Information Administration.

Wartsila, n.d. *Combustion Engine vs Gas Turbine: Ramp Rate.* [Online] Available at: http://www.wartsila.com/energy/learning-center/technical-comparisons/combustion-engine-vs-gas-turbine-ramp-rate [Accessed 15 April 2016].

Wong, J., 2015. *Fuzzy Controlled Energy Storage System for Low-Voltage Distribution Networks with Photovoltaic Systems*. PhD Thesis, Universiti Tunku Abdul Rahman, Malaysia.

Yi, J., Cameron, C. D. & Patsios, H., 2016. *Integrated Test Environment: Introduction and User Manual*, Newcastle: Newcastle University.

Zhong, J. et al., 2014. Coordinated Control for Large-Scale EV Charging Facilities and Energy Storage Devices Participating in Frequency Regulation. *Applied Energy*, pp. 253-262.

Zhu, J. et al., 2013. Inertia Emulation Control Strategy for VSC-HVDC Transmission Systems. *IEEE Trans. on Power Syst.*, pp. 1277-1287.

Zimmerman, R. D., Murillo-Sanchez, C. E. & Thomas, R. J., 2011. MATPOWER: Steady-State Operations, Planning and Analysis Tools for Power Systems Research and Education. *IEEE Trans. on Power Syst.* , pp. 12-19.

APPENDIX A: A Sample Daily System Generation Summary in Peninsular Malaysia

TENAGA NASIONAL BERHAD

Daily System Generation Summary on Monday

Monday, February 01, 2016

Availability at Daily Maximum Demand Hour

ST-Coal	3,040 MW
ST-Gas	0 MW
ST-Oil	0 MW
Gas	4,462 MW
Hydro	2,102 MW
Distillate	0 MW
Total TNB	9,604 MW
Total IPP	8,450 MW
Total Co-Gen	38 MW
Total System	18,662 MW

Maximum Demand Record

Date: 6/11/2014	16,901	MW
Date: 6/24/2014	355,911	MWH

Set On Bus, TNB, IPP And MD

Daily Maximum Demand Hour at:	16:00:00 Hour
Total Set On Bus	17,597 MW
TNB Generation	7,845 MW
IPP Generation	8,256 MW
Spinning Reserve	1,475 MW
Maximum Demand	16,089 MW
Net Energy	336,133 MWH
Load Factor	87.05 %

Generation Mix

Type	MWh	Percentage
ST-Coal	67,436	20.06 %
Gas	82,418	24.52 %
Hydro	8,395	2.50 %
Total TNB	**158,249**	**47.08 %**
ST-Coal	95,177	28.32 %
Gas	83,351	24.80 %
Total IPP	**178,528**	**53.11 %**
Co-Gen	490	0.15 %
Total Co-Gen	**490**	**0.15 %**
Total Generation	**337,267**	**100.34 %**
PLTG	440	0.13 %
EGAT	-34	-0.01 %
HVDC	728	0.22 %
Interconnection	**1,134**	**0.34 %**
Net Energy	**336,133**	**100.00 %**

Fuel Cost

Total Cost:	52,171,712.10 RM
Cost per Unit	15.86 cents/kWH

Average Spinning Reserve During Peak Hour

Type	MW
GT	399
Hydro	272
Syncon	748
Thermal	126
Total	**1,545**

Time	Weather	Temperature
Afternoon	Hot	32
Morning	Sunny	28

Gas Usage

Station	(mmscfd)
CBPS	13
CBPS	49
GLGR	54
NPRI	18
PAKA	202
PGGS	14
PGPS	41
SRDG	58
TJGS	212
Total TNB	**661**
KLPP	101
MPSS	42
PGLA	112
PKLG	13
PLPS	102
SGB3	49
SGRI	178
SKSP	52
Total IPP	**649**
Total Gas	**1,311**
Total Gas Required	**1,311**

Alternate Fuel Usage

Station	(mmscfd)
Total	**0**

Hourly System MW Generation

	00:00	01:00	02:00	03:00	04:00	05:00	06:00	07:00	08:00	09:00	10:00	11:00	12:00	13:00	14:00	15:00	16:00	17:00	18:00	19:00	20:00	21:00	22:00	23:00
System Total	13336	12688	12098	11667	11398	11230	11423	11547	11874	13672	14582	15288	15336	15062	15780	15965	16089	15717	14718	14350	15665	15654	15270	14851

Prepared By: Siti Nurhamizatul Azni

Checked By: Kannathasan a/l Karuppiah

Printed on: Tuesday, February 02, 2016 8:36:31 AM

(Gurcharan Singh)
Pengurus Besar Kanan
Jabatan Sistem Operasi

TENAGA NASIONAL BERHAD

Monday, February 01, 2016

Daily MW Generation on Monday

Station	Unit	0000	0100	0200	0300	0400	0500	0600	0700	0800	0900	1000	1100	1200	1300	1400	1500	1600	1700	1800	1900	2000	2100	2200	2300	
JMAH	U001	698 697	702 692	701 702	699 705	699 706	701 699	700 698	687 685	703 700	706 700	697 691	703 698	695 603	597 609	623 701	703 700	697 699	695 705	701 703	697 698	696 693	702 702	699 703	700 701	
JMAH	U002	702 706	701 711	701 705	702 703	703 705	702 705	698 705	702 705	705 705	706 705	702 702	694 705	703 702	703 705	705 703	703 703	702 703	708 703	703 705	702 703	702 706	704 699	704 707	703 703	
JMJG	U001	645 645	645 643	643 640	643 644	645 643	645 645	643 645	645 645	643 645	640 644	645 641	645 643	641 645	680 679	678 679	679 676	679 679	680 679	677 679	677 681	678 679	682 678	680 682	682 679	
JMJG	U002	679 679	678 679	682 679	678 676	674 676	678 679	679 673	682 666	640 646	678 677	675 678	678 680	677 677	679 675	679 679	677 679	679 682	676 678	679 676	679 678	678 679	680 680	678 677	677 678	
JMJG	U003	636 634	634 634	637 634	633 635	634 636	629 634	634 634	634 643	642 632	636 634	641 635	634 634	634 632	638 628	632 634	632 626	635 633	638 636	641 679	671 670	674 670	678 671	676 678	675 674	
JMJG	U004	791 789	790 795	793 793	792 792	794 793	793 793	794 796	793 792	791 795	822 857	860 859	861 858	858 860	859 858	860 858	859 858	858 859	856 859	862 855	860 859	861 862	861 861	861 822	790 790	
PKLG	U003	283 285	281 279	281 283	283 285	283 280	282 282	282 281	285 279	284 282	281 283	281 281	283 283	277 279	283 280	288 280	278 282	274 268	262 264	262 263	262 259	259 261	259 261	263 261	279 281	
PKLG	U004	280 281	281 278	278 279	279 276	273 281	279 280	280 282	282 279	279 279	279 282	281 281	281 281	282 282	279 279	278 281	281 281	281 281	280 279	279 279	279 279	279 277	277 275	275 277	279 278	
PKLG	U005	469 469	469 469	469 465	469 469	465 464	465 469	469 468	465 465	469 467	465 462	469 470	469 465	465 470	469 467	469 469	469 465	465 476	466 462	466 469	469 469	466 466	462 469	465 473	469 466	466
TBIN	U001	700 696	699 696	698 698	699 699	697 706	699 695	695 698	693 699	700 699	695 698	689 695	698 695	696 695	696 699	696 698	698 694	698 695	699 697	695 697	695 698	700 696	700 697	694 689	700 695	
TBIN	U003	698 700	700 699	700 699	697 700	698 697	697 701	696 699	698 698	699 701	699 701	701 700	701 707	700 702	702 701	705 703	700 703	702 702	701 700	702 703	698 700	705 703	691 704	685 697	693 698	
TBIN	U004	0 0	0 0	0 0	0 0	0 0	0 0	0 0	0 0	0 0	0 0	0 0	0 0	139 0	0 135	136 0	0 132	142 162	171 281	336 369	392 471	448 472	568 564	562 568	557 662	
Total ST-Coal		6581 6581	6580 6575	6583 6577	6575 6584	6563 6588	6570 6582	6570 6579	6566 6556	6555 6551	6610 6642	6641 6633	6647 6650	6767 6544	6585 6714	6752 6685	6675 6799	6823 6828	6827 6947	7006 7077	7081 7162	7146 7160	7271 7257	7250 7230	7201 7305	
Total ST-Oil		0 0	0 0	0 0	0 0	0 0	0 0	0 0	0 0	0 0	0 0	0 0	0 0	0 0	0 0	0 0	0 0	0 0	0 0	0 0	0 0	0 0	0 0	0 0	0 0	
Total ST-Gas		0 0	0 0	0 0	0 0	0 0	0 0	0 0	0 0	0 0	0 0	0 0	0 0	0 0	0 0	0 0	0 0	0 0	0 0	0 0	0 0	0 0	0 0	0 0	0 0	
CBPS	GT1A	87 87	87 87	87 87	87 87	88 87	88 88	88 87	87 87	87 87	84 92	98 96	95 94	94 92	92 92	92 92	90 87	86 94	97 98	88 87	88 87	98 97	97 97	97 97	87 87	
CBPS	GT1B	8 0	0 0	0 0	0 0	0 0	0 0	0 0	0 0	9 8	72 91	94 94	93 92	91 90	90 89	89 89	88 87	85 92	92 92	87 87	87 87	93 93	93 93	93 94	76 8	
CBPS	ST1C	41 37	37 41	41 41	41 40	40 40	41 40	40 40	40 40	40 41	37 81	101 100	99 99	97 97	97 95	95 93	92 90	88 96	100 100	92 92	91 92	101 101	101 101	102 102	71 43	
CBPS	BLK2	0 0	0 0	0 0	0 0	0 0	0 0	0 0	0 0	0 0	0 0	0 0	0 0	0 0	43 153	114 112	111 112	112 113	82 28	0 0	0 0	0 0	0 0	0 0	0 0	
GLGR	GT01	107 109	107 107	85 68	67 70	68 68	68 69	68 68	69 67	69 98	106 107	107 105	106 106	103 100	102 102	91 93	94 100	97 97	93 91	92 92	99 100	101 100	102 106	107 107	108 108	
GLGR	GT02	107 107	107 107	84 68	68 68	68 68	68 68	68 68	68 68	68 69	99 107	107 107	107 107	106 105	102 102	101 92	95 97	99 98	96 94	92 93	93 99	102 101	102 103	106 107	107 107	
GLGR	ST1C	98 97	97 97	87 70	70 70	70 71	71 70	70 70	70 70	70 70	85 96	96 97	97 97	97 96	92 92	92 86	86 87	91 89	87 86	85 85	85 88	92 92	92 94	95 97	98 98	97
KLPP	GT11	0 0	0 0	0 0	0 0	0 0	0 0	0 0	0 0	0 0	13 13	13 13	31 31	31 31	31 31	31 31	31 31	31 31	31 31	31 31	31 31	31 31	31 31	31 31	0 0	0
KLPP	GT12	0 0	0 0	0 0	0 0	0 0	0 0	0 0	0 0	0 0	9 9	9 9	18 18	18 18	18 18	18 18	18 18	18 18	18 18	18 18	18 18	18 18	18 18	18 18	0 0	0
KLPP	GT13	134 136	135 136	136 135	71 70	70 70	70 71	71 69	70 70	70 105	135 134	137 137	137 137	137 138	137 137	138 136	134 135	135 136	137 136	139 108	107 124	139 137	137 138	136 137	137 137	
KLPP	GT14	0 0	0 0	0 0	0 0	0 0	0 0	0 0	0 0	0 133	133 133	133 133	133 151	151 151	151 151	151 151	151 151	151 151	151 151	152 152	121 121	136 136	153 153	153 153	151 151	
KLPP	GT15	148 148	148 148	148 149	80 78	78 78	78 78	78 78	78 78	78 117	148 148	148 153	149 150	150 148	148 149	149 153	153 153	153 154	154 154	157 118	118 138	151 151	151 150	150 147	147 117	
KLPP	ST17	154 130	130 134	130 130	101 89	89 88	86 90	90 90	90 89	89 117	169 199	211 227	227 226	226 228	228 228	228 225	225 227	227 227	227 227	227 227	208 208	219 228	227 227	227 227	216 203	196
MPSS	GT01	0 0	0 0	0 0	0 0	0 0	16 56	77 79	79 80	92 107	106 106	89 103	104 102	101 89	101 103	103 103	100 103	104 105	105 104	104 103	103 105	105 105	105 105	105 106	106 107	107
MPSS	GT02	0 0	0 0	0 0	0 0	0 0	0 0	0 0	0 0	0 15	22 62	85 103	103 102	102 101	101 101	101 101	101 103	103 103	103 103	103 104	104 104	105 104	104 104	104 104	104 104	104
MPSS	ST01	0 0	0 0	0 0	0 0	0 0	0 0	0 0	0 0	37 47	49 46	39 109	110 111	111 107	105 111	112 112	113 113	113 113	113 114	114 114	114 114	114 114	114 114	114 114	114 114	114
NPRI	BLK1	0 0	0 0	0 0	0 0	0 0	0 0	0 0	0 0	0 0	0 0	0 0	0 0	0 0	0 0	0 0	0 0	0 0	0 0	0 0	0 0	0 0	25 127	127 128	125 237	460
NPRI	BLK2	0 0	0 0	0 0	0 0	0 0	0 0	0 0	0 0	0 0	0 17	17 17	76 77	0 0	0 0	0 0	0 0	0 0	0 0	0 0	0 0	0 0	0 0	0 0	0 0	
PAKA	GT1A	88 88	89 90	65 66	65 67	66 65	64 66	65 66	67 65	66 65	90 89	88 82	86 87	86 85	86 85	86 85	85 85	85 85	85 85	86 65	65 65	65 65	88 88	88 88	88 89	
PAKA	GT1B	89 89	90 90	65 65	65 65	65 65	63 64	63 65	65 65	65 64	90 90	90 89	88 88	88 88	88 87	87 87	87 87	87 87	87 87	65 64	64 64	64 89	89 89	89 89	89 90	
PAKA	ST1C	76 76	76 76	67 65	64 64	64 64	65 64	65 64	64 64	64 64	76 76	76 75	76 76	76 76	76 76	76 76	76 76	76 76	76 76	66 65	65 65	65 76	76 76	76 76	76 76	
PAKA	GT2A	82 82	82 81	81 82	82 82	82 82	82 81	82 81	82 82	81 82	81 82	83 81	81 81	83 81	81 81	81 81	81 81	81 81	81 81	81 82	81 82	81 83	82 82	83 84	84 84	
PAKA	GT2B	86 87	88 88	88 88	88 88	89 88	89 89	89 88	89 89	89 89	89 88	88 87	86 86	85 85	85 85	86 85	85 85	85 86	86 86	86 86	87 86	86 86	86 87	87 87	87 88	88
PAKA	ST2C	85 84	84 84	84 84	83 83	83 83	83 84	83 83	83 83	83 83	83 84	84 84	84 85	85 85	85 85	85 85	85 85	85 85	85 84	84 84	84 65	84 84	84 85	85 85	85 85	84
PAKA	GT3A	88 89	89 89	89 90	90 90	90 90	90 90	90 90	90 91	91 91	90 90	90 89	88 88	88 88	87 87	87 88	87 87	86 86	88 88	88 88	88 88	88 88	88 88	88 88	89 89	89
PAKA	GT3B	88 89	89 90	90 90	89 90	89 90	90 90	90 90	90 90	90 90	90 89	89 88	88 87	87 87	87 87	87 87	87 87	87 88	88 88	88 88	88 88	88 88	88 88	88 88	89 89	89
PAKA	ST3C	92 92	92 92	92 92	92 92	92 92	92 92	92 92	92 92	92 92	92 92	92 92	92 91	91 92	92 92	92 92	92 92	92 91	92 92	92 92	92 92	92 92	92 92	92 92	92 92	
PAKA	GT4A	94 95	96 95	95 95	95 95	95 95	94 95	95 94	96 95	95 95	95 95	95 95	94 94	94 94	94 93	93 95	93 94	93 94	95 94	94 95	95 95	95 95	94 95	95 95	94 95	95
PAKA	GT4B	82 83	83 83	83 84	84 84	83 84	84 84	84 84	84 84	84 83	83 84	83 82	82 83	83 83	83 83	83 83	82 82	82 82	82 82	83 82	83 83	83 83	83 83	83 83	83 83	
PAKA	ST4C	92 92	92 92	92 92	92 92	92 92	91 91	91 91	91 91	91 91	92 92	92 92	92 93	93 93	94 94	93 93	93 93	93 93	93 93	93 93	93 93	93 93	93 93	93 93	92 92	
PGLA	GT11	228 228	227 227	212 225	185 186	156 188	153 156	194 228	220 226	229 229	192 226	224 226	201 222	223 223	160 174	197 225	187 205	224 220	198 197	211 165	158 228	228 228	229 230	230 230	230 231	
PGLA	GT12	231 232	231 231	217 228	189 188	159 192	158 159	198 230	226 229	233 229	194 229	228 228	203 225	223 227	163 177	198 225	190 208	224 225	201 201	214 167	163 229	228 230	232 232	232 231	231 233	

TENAGA NASIONAL BERHAD

Monday, February 01, 2016

Daily MW Generation on Monday

Station	Unit	0000	0100	0200	0300	0400	0500	0600	0700	0800	0900	1000	1100	1200	1300	1400	1500	1600	1700	1800	1900	2000	2100	2200	2300
PGLA	ST10	245 243 245 242 243 243 226 217 195 221 200 195 223 246 239 230 243 243 224 250 249 252 244 249 240 237 205 225 242 242 211 221 249 245 240 221 236 215 203 243 250 251 250 252 252 252 252 253
PGPS	GT3A	82 83 83 83 82 83 82 82 82 82 81 81 82 83 82 82 83 82 82 93 94 94 94 94 93 93 93 94 93 93 94 94 94 94 93 94 76 76 76 85 93 94 93 94 93 92 84 83
PGPS	GT3B	0 0 0 0 0 0 0 0 0 0 0 0 0 0 0 0 13 81 83 92 94 94 94 94 94 94 94 93 94 94 93 94 94 94 93 94 77 77 77 85 94 94 93 93 94 93 0 0
PGPS	ST3C	36 36 36 36 36 36 36 36 35 36 36 35 36 36 36 36 36 36 51 83 91 93 92 92 93 93 92 92 93 93 93 92 92 92 92 91 76 73 72 75 90 90 89 89 89 89 36 36
PLPS	GT11	143 122 0 0 0 0 0 0 0 0 0 0 0 0 0 0 0 75 147 145 145 144 140 142 142 139 139 138 135 139 139 138 138 139 136 116 111 112 113 116 118 116 112 116 116 141 146 146
PLPS	GT12	141 139 140 142 138 142 140 143 136 137 135 136 137 69 60 94 145 143 142 141 140 139 136 137 132 132 133 131 130 135 134 133 134 134 129 120 116 115 116 119 123 120 116 118 119 141 140 54
PLPS	GT13	139 146 141 134 140 135 129 135 137 137 138 137 137 115 117 107 136 143 145 145 145 145 140 142 137 137 136 138 137 140 138 139 138 139 136 111 108 108 108 111 116 112 109 112 113 138 145 145
PLPS	ST18	213 213 145 144 143 143 143 142 143 142 143 142 143 118 120 124 148 146 214 214 213 213 213 212 213 213 212 213 211 213 212 213 212 213 212 201 200 198 197 200 201 201 200 200 200 215 213 201
SGB3	GT31	0 0 0 0 0 0 0 0 0 6 35 35 35 54 63 63 136 135 135 135 135 135 133 134 134 133 133 133 133 132 132 133 133 132 132 114 96 101 101 127 134 101 101 101 101 102 134 122
SGB3	GT32	0 0 0 0 0 0 0 0 0 0 0 0 0 0 0 0 0 0 104 145 145 144 142 145 142 143 143 144 144 142 142 143 143 143 143 124 105 105 108 134 144 108 108 111 110 110 0 0
SGB3	ST34	0 0 0 0 0 0 0 0 0 0 0 0 16 31 35 39 72 75 124 149 149 150 150 151 151 150 150 150 150 150 150 149 149 150 150 140 136 130 130 144 145 133 133 133 136 132 70 66
SGRI	GT11	135 138 140 134 114 115 115 115 115 115 115 116 116 139 117 114 117 138 116 136 136 137 137 136 136 135 135 136 136 135 135 135 135 136 136 135 135 106 106 106 134 136 110 110 110 137 135 117
SGRI	GT12	151 146 151 141 114 116 111 111 109 111 111 105 109 150 125 112 124 144 111 150 153 153 153 152 149 151 151 151 150 150 150 150 150 150 151 111 110 111 153 152 117 117 117 149 152 114
SGRI	ST14	150 148 149 140 132 132 133 134 132 132 132 129 135 149 141 135 135 140 131 150 150 149 146 148 151 148 151 150 150 149 149 149 149 148 148 151 148 130 129 127 149 149 132 132 132 148 153 130
SGRI	GT21	135 139 139 139 114 113 113 112 113 112 112 106 113 138 120 113 117 139 137 137 137 138 138 137 134 135 135 135 135 134 134 134 134 134 134 135 112 113 113 134 134 136 116 116 135 137 137 116
SGRI	GT22	142 143 36 0 0 0 0 0 0 0 0 0 0 0 0 0 0 53 142 143 139 140 140 141 137 140 141 137 138 139 139 137 137 138 140 137 112 111 111 138 138 138 120 111 142 143 140 106
SGRI	GT23	145 144 145 148 113 113 113 113 110 113 113 108 112 146 120 112 116 147 145 148 148 147 145 146 146 144 144 144 144 143 143 144 144 143 143 114 112 113 145 145 141 113 113 146 142 146 114
SGRI	ST24	220 222 198 146 132 136 132 133 131 135 135 129 135 153 136 138 138 151 223 216 219 219 217 216 217 218 218 219 215 219 218 220 219 221 219 222 196 200 197 222 219 220 197 196 221 220 220 205
SKSP	BLK1	342 306 333 295 218 235 213 213 213 213 214 213 213 222 211 215 220 230 340 342 343 342 328 341 337 342 301 316 340 341 341 341 338 338 337 330 214 215 214 279 342 342 215 213 341 333 344 249
TJGS	GT1A	233 233 233 233 233 198 198 152 162 162 162 162 162 162 162 162 162 162 230 234 231 231 231 231 231 231 231 231 231 231 231 231 231 231 231 231 197 197 228 232 232 232 232 232 228 226
TJGS	GT1B	223 223 220 220 223 188 188 146 153 153 153 153 153 153 153 153 153 153 218 222 222 218 218 218 218 218 218 218 218 218 218 218 218 218 218 218 218 218 187 187 215 218 218 218 222 222 222 221 214
TJGS	ST1C	253 253 253 253 253 221 217 200 192 192 192 192 192 192 192 192 192 192 243 253 253 253 253 253 253 253 253 253 253 253 253 253 253 253 253 253 253 253 220 220 244 252 252 252 252 252 252 252 246
TJGS	GT2A	220 220 220 220 220 220 220 220 220 136 136 136 136 136 136 136 135 136 220 220 217 217 214 212 214 214 214 214 217 215 215 215 215 215 213 213 213 213 215 213 215 215 218 218 218 218 215
TJGS	GT2B	221 221 221 221 221 221 221 221 221 133 133 133 134 131 132 133 132 220 220 220 218 218 215 215 215 215 218 218 215 218 216 216 216 216 216 213 213 216 216 216 216 216 218 220 220 220 217 212
TJGS	ST2C	264 264 264 264 264 264 264 264 264 212 212 212 212 210 213 213 211 265 265 262 262 262 262 262 262 262 262 262 262 262 262 262 262 262 262 262 262 262 262 262 262 262 262 262 262 262 262 262
Total CCGT-Gas		6218 6139 5848 5700 5351 5248 4942 4827 4738 4621 4572 4590 4762 4929 4801 4796 5128 6202 6935 7366 7407 7515 7519 7589 7468 7441 7256 7366 7526 7582 7444 7507 7552 7623 7567 7446 7039 6621 6586 7258 7640 7799 7695 7710 7625 7681 7439 6983
CBPS	GT03	0 0 0 0 0 0 0 0 0 0 0 0 0 0 0 0 0 0 0 0 0 0 95 113 113 113 106 106 90 88 88 90 89 89 0 0 0 0 0 0 0 0 0 0 0 0
CBPS	GT05	0 0 0 0 0 0 0 0 0 0 0 0 0 0 0 0 0 0 0 0 0 0 0 0 0 114 111 111 89 90 89 89 89 89 20 0 0 0 0 0 0 0 0 0 0 0 0
PGGS	GT6A	0 0 0 0 0 0 0 0 0 0 0 0 0 0 0 0 0 0 0 0 47 100 101 100 101 100 101 100 100 80 80 80 80 80 80 80 80 80 80 80 80 100 99 100 101 0 0 0 0
PKLG	GT09	0 0 0 0 0 0 0 0 0 0 0 0 0 0 0 0 0 0 0 0 99 98 87 97 98 98 70 78 70 98 95 81 98 85 70 75 74 69 70 81 98 74 74 69 78 0 0 0
SRDG	GT01	0 0 0 0 0 0 0 0 0 0 0 0 0 0 0 0 0 0 0 0 0 22 92 89 89 89 89 89 89 89 89 89 90 90 91 93 70 70 70 70 70 70 70 0 0 0 0 0
SRDG	GT03	0 0 0 0 0 0 0 0 0 0 0 0 0 0 0 0 0 0 0 0 0 0 0 115 114 117 117 120 119 120 119 119 120 119 119 119 89 89 89 89 89 90 30 0 0 0 0 0
SRDG	GT04	0 0 0 0 0 0 0 0 0 0 0 0 0 0 0 0 0 0 0 0 85 105 106 105 106 130 130 129 129 130 130 130 129 129 126 125 95 94 95 96 127 127 127 126 0 0 0 0
SRDG	GT05	0 0 0 0 0 0 0 0 0 0 0 0 0 0 0 0 0 0 0 0 123 122 122 121 122 121 121 123 122 120 120 120 121 122 123 124 89 89 89 89 124 125 124 125 124 0 0 0
Total OCGT-Gas		0 0 0 0 0 0 0 0 0 0 0 0 0 0 0 0 0 0 0 0 354 447 604 740 743 768 855 856 846 816 811 796 817 803 787 636 497 491 493 505 608 585 525 421 202 0 0 0
BSIA	HY01	21 11 11 11 11 11 11 11 11 11 11 11 11 11 11 11 11 11 11 11 21 21 21 21 11 11 11 11 21 21 21 21 21 21 10 10 10 10 10 11 11 11 11 11 11 11
BSIA	HY03	0 0 0 0 0 0 0 0 0 0 0 0 0 0 0 0 0 0 0 0 0 0 0 0 0 0 0 0 12 11 11 10 11 11 0 0 0 0 0 0 0 0 0 0 0 0
CEND	HY01	7 7 7 7 7 7 7 7 7 7 7 7 7 7 7 7 7 7 7 7 7 7 7 7 7 7 7 7 7 7 7 7 7 7 7 7 7 7 7 7 7 7 7 7 7 7
CEND	HY02	7 7 7 7 7 7 7 7 7 7 7 6 7 7 7 7 7 7 7 7 7 7 7 7 7 7 7 7 7 7 7 7 7 7 7 7 7 7 7 7 7 7 7 7 7 7
CEND	HY03	7 7 7 7 7 7 7 7 7 7 7 7 7 7 7 7 7 7 7 7 7 7 7 7 7 7 7 7 7 7 7 7 7 7 7 7 7 7 7 7 7 7 7 7 7 7
HTRG	HY01	-1 -1 -1 -1 -1 -1 -1 -1 -1 -1 -1 -1 -1 -1 -1 -1 -1 -1 -1 -1 -1 -1 -1 -1 -1 -1 -1 -1 -1 -1 -1 -1 -1 -1 -1 -1 -1 -1 -1 -1 -1 -1 -1 -1 -1 -1
HTRG	HY02	0 0 0 0 0 0 0 0 0 0 0 0 0 0 0 0 0 0 0 0 0 0 0 0 63 125 64 63 63 0 0 0 0 0 0 0 0 0 0 0 0 0 0 0 0 0 0 0 0 0 0 0
KNRG	HY01	36 36 0 0 0 0 0 0 0 0 0 0 0 0 0 0 0 0 0 0 0 0 0 0 0 0 0 0 0 23 22 22 22 22 0 0 0 0 0 0 0 0 0 0 0 0 0 0 0 0
KNRG	HY02	0 0 0 0 0 0 0 0 0 0 0 0 0 0 0 0 0 0 0 0 0 0 0 0 0 0 0 0 0 25 24 25 25 25 0 0 0 0 0 0 0 0 0 0 0 0 0 0 0 0
KNRG	HY03	36 36 37 37 37 37 37 37 37 37 37 37 37 37 37 37 37 37 37 37 37 37 37 37 37 37 37 37 37 22 22 21 22 21 21 22 21 21 22 22 23 22 22 21 23 23 23 23
KNYR	HY01	-1 -1 -1 -1 -1 -1 -1 -1 -1 -1 -1 -1 -1 -1 -1 -1 -1 -1 -1 -1 -1 -1 -1 -1 -1 -1 -1 -1 -1 -1 60 -1 -1 -1 -1 -1 -1 -1 -1 -1 -1 -1 -1 -1 -1 -1
KNYR	HY02	-1 -1 -1 -1 -1 -1 -1 -1 -1 -1 -1 -1 -1 -1 -1 -1 -1 -1 -1 -1 -1 -1 -1 -1 -1 -1 -1 -1 -1 -1 98 99 98 -1 -1 -1 -1 -1 -1 -1 -1 -1 -1 -1 -1 -1

TENAGA NASIONAL BERHAD

Monday, February 01, 2016

Daily MW Generation on Monday

Station	Unit	0000		0100		0200		0300		0400		0500		0600		0700		0800		0900		1000		1100		1200		1300		1400		1500		1600		1700		1800		1900		2000		2100		2200		2300	
KNYR	HY04	62	62	64	59	59	58	57	59	53	55	54	52	55	63	60	63	61	64	62	63	65	99	99	99	99	99	99	58	99	92	81	98	88	59	71	59	56	54	82	99	67	57	60	92	64	99	67
LPIA	HY01	10	10	10	10	10	10	10	10	10	10	10	10	10	10	10	10	10	10	10	10	10	10	10	10	10	10	10	10	10	10	10	10	10	10	10	10	10	10	10	10	10	10	10	10	10	10	10
LPIA	HY02	16	16	16	16	16	16	16	16	16	16	16	16	16	16	16	16	16	16	16	16	16	16	16	16	16	16	16	16	16	16	16	16	16	16	16	16	16	16	16	16	16	16	16	16	16	16	16
MNOR	HY01	6	6	6	6	5	5	4	4	4	4	4	4	4	4	4	4	4	4	1	1	1	1	2	2	6	6	5	5	6	6	6	6	6	6	4	4	4	4	4	4	4	4	4	4	4	4	4	4
PGAU	HY01	22	-1	-1	-1	-1	-1	-1	-1	-1	-1	-1	-1	-1	-1	-1	-1	-1	-1	-1	-1	-1	87	85	20	85	-1	-1	-1	-1	-1	86	84	84	84	84	20	20	20	20	20	20	20	20	20	20	20	-1	-1
PGAU	HY02	-1	-1	-1	-1	-1	-1	-1	-1	-1	-1	-1	-1	-1	-1	-1	-1	-1	-1	-1	21	-1	-1	-1	-1	-1	-1	-1	-1	-1	-1	-1	-1	-1	-1	-1	-1	-1	-1	-1	-1	-1	20	-1	-1	-1	-1	-1
PGAU	HY03	-1	-1	-1	-1	-1	-1	-1	-1	-1	16	-1	-1	-1	-1	-1	-1	-1	-1	-1	-1	-1	-1	-1	-1	-1	130	79	81	110	113	113	22	22	112	109	-1	-1	-1	-1	-1	-1	-1	-1	-1	-1	-1	-1	-1
PGAU	HY04	0	0	0	0	0	0	0	0	0	0	0	0	0	0	0	0	0	0	0	0	0	0	0	0	0	0	0	20	110	110	110	110	110	110	21	21	21	21	21	21	21	21	21	0	0	0	0
SIHY	HY01	49	0	0	0	0	0	0	0	0	0	0	0	0	0	0	0	0	0	0	0	0	8	49	49	0	0	0	30	49	49	53	50	50	0	0	0	0	0	0	0	0	0	0	0	0	0	0
SIHY	HY02	50	0	0	0	0	0	0	0	0	0	0	0	0	0	0	0	0	0	0	0	0	0	50	50	0	0	0	30	50	50	50	50	50	0	0	0	0	0	0	0	0	0	0	0	0	0	0
SIHY	HY03	50	0	0	0	0	0	0	0	0	0	0	0	0	0	0	0	0	0	0	0	0	0	50	50	50	0	0	30	50	50	0	0	0	0	0	0	0	0	0	0	0	0	0	0	0	0	0
SYPS	HY01	25	0	0	0	0	0	0	0	0	0	0	0	0	0	0	0	0	0	0	0	0	5	25	25	0	0	0	16	25	25	25	25	0	0	0	0	0	0	0	0	0	0	0	0	0	0	0
SYPS	HY02	25	0	0	0	0	0	0	0	0	0	0	0	0	0	0	0	0	0	0	0	0	0	25	25	25	0	0	16	25	25	25	25	24	0	0	0	0	0	0	0	0	0	0	0	0	0	0
SYPS	HY03	25	0	0	0	0	0	0	0	0	0	0	0	0	0	0	0	0	0	0	0	0	0	0	0	0	0	0	16	25	25	25	25	25	0	0	0	0	0	0	0	0	0	0	0	0	0	0
SYPS	HY04	25	0	0	0	0	0	0	0	0	0	0	0	0	0	0	0	0	0	0	0	0	0	0	0	0	0	0	16	25	25	0	0	0	0	0	0	0	0	0	0	0	0	0	0	0	0	0
TMGR	HY01	-1	-1	-1	-1	-1	-1	-1	-1	-1	-1	-1	-1	-1	-1	-1	-1	-1	-1	-1	-1	-1	-1	-1	-1	-1	-1	-1	-1	-1	-1	-1	-1	-1	-1	-1	-1	-1	-1	-1	-1	-1	-1	-1	-1	-1	-1	-1
TMGR	HY02	33	33	34	26	30	31	28	31	26	24	24	28	32	39	36	38	32	34	33	33	36	89	79	80	32	33	33	31	77	82	80	75	82	79	77	31	26	27	28	34	38	32	30	30	35	34	39	31
TMGR	HY03	0	0	0	0	0	0	0	0	0	0	0	0	0	0	0	0	0	0	0	0	0	0	0	0	0	0	0	82	82	82	82	82	82	82	0	0	0	0	0	0	0	0	0	0	0	0	0
TMGR	HY04	-1	-1	-1	-1	-1	-1	-1	-1	-1	-1	-1	-1	-1	-1	-1	-1	-1	-1	-1	-1	-1	-1	-1	-1	-1	-1	-1	-1	-1	-1	-1	-1	-1	-1	-1	-1	-1	-1	-1	-1	-1	-1	-1	-1	-1	-1	-1
UPIA	HY01	5	5	5	5	5	5	5	5	5	5	5	5	5	5	5	5	5	5	5	5	5	5	5	5	5	5	5	5	5	5	5	5	5	5	5	5	5	5	5	5	5	5	5	5	5	5	5
UPIA	HY02	4	4	4	4	4	4	4	4	4	4	4	4	4	4	4	4	4	4	4	4	4	4	4	4	4	4	4	4	4	4	4	4	4	4	4	4	4	4	4	4	4	4	4	4	4	4	4
Total Hydro		514	232	200	187	190	190	185	190	179	196	178	179	187	202	196	201	193	198	192	215	198	396	571	507	457	490	377	376	689	892	1128	887	909	860	606	228	210	208	208	243	265	226	213	237	255	205	224	184
Total Distillate		0	0	0	0	0	0	0	0	0	0	0	0	0	0	0	0	0	0	0	0	0	0	0	0	0	0	0	0	0	0	0	0	0	0	0	0	0	0	0	0	0	0	0	0	0	0	0	0
PCUF	CUFG	2	2	1	2	2	2	1	3	2	2	1	1	1	2	2	3	3	2	3	1	1	2	2	2	2	1	2	2	1	1	1	1	3	2	1	1	2	2	2	2	2	1	2	3	3	4	4	4
PCUF	CUFK	18	20	19	19	20	18	18	18	19	19	18	19	18	19	19	19	21	19	20	20	19	19	19	17	16	17	18	18	17	17	18	17	18	17	18	17	18	19	19	17	18	19	18	19	18	19	20	20
Total Co-Gen		20	22	20	21	22	20	19	21	21	21	19	20	19	21	21	22	24	21	23	21	20	21	21	19	18	18	20	20	18	18	19	18	21	19	19	18	20	21	21	19	20	20	20	22	21	23	24	24
Total Gen		13333	12974	12648	12483	12146	12835	11721	11622	11501	11426	11339	11371	11538	11731	11584	11575	11908	12972	13760	14244	14620	15812	15362	15505	15453	15261	15093	15332	15831	15963	16077	16007	16122	16133	15806	15275	14772	14418	14389	15187	15679	15790	15724	15647	15353	15139	14888	14496
TIE-EGAT		0	0	0	0	0	0	0	0	0	0	0	0	0	0	0	0	0	0	0	0	0	0	0	0	0	0	0	0	0	0	0	0	0	0	0	0	0	0	0	0	0	0	0	0	0	0	0	0
TIE-HVDC		30	30	30	30	30	30	30	30	30	31	31	30	30	30	30	31	31	31	31	30	30	31	31	31	31	30	30	31	31	30	30	30	30	30	29	30	30	30	30	30	30	31	31	30	30	31	31	31
TIE-PLTG		-33	-69	-70	-9	18	19	24	-55	73	56	79	36	85	34	7	11	-5	30	57	-31	8	6	44	-29	86	82	1	50	21	40	81	20	3	16	60	-26	24	17	8	6	-16	11	40	15	53	19	6	-20
Interconnection		-3	-39	-40	21	48	49	54	-25	103	86	109	66	115	64	37	41	26	61	88	-1	38	36	74	2	117	112	31	81	51	70	112	50	33	46	89	4	54	47	39	36	14	41	70	46	83	51	37	11
System Total		13336	13013	12688	12462	12098	11956	11667	11647	11398	11340	11230	11305	11423	11667	11547	11534	11874	12911	13672	14245	14582	14976	15288	15503	15336	15149	15062	15251	15780	15893	15965	15957	16089	16087	15717	15271	14718	14571	14350	15151	15665	15749	15654	15601	15270	15088	14851	14485
SRev ST-Coal		135	125	130	137	127	133	135	125	147	123	139	128	139	134	144	115	116	121	128	132	134	143	131	125	157	202	193	230	115	30	140	186	162	158	156	243	188	150	115	113	132	115	74	88	95	115	156	183
SRev OCGT-Gas		0	0	0	0	0	0	0	0	0	0	0	0	0	0	0	0	0	0	0	0	0	78	83	49	37	34	9	38	37	47	77	82	97	76	90	106	155	178	184	182	170	67	90	150	32	22	0	0	0
SRev CCGT-Gas		178	161	248	183	532	635	941	1056	1145	1405	1557	1539	1447	1280	1408	1413	1325	984	572	266	225	175	231	161	202	229	414	404	344	238	346	393	348	277	333	454	861	1159	1194	622	240	426	630	615	345	181	255	560
SRev ST-Gas		0	0	0	0	0	0	0	0	0	0	0	0	0	0	0	0	0	0	0	0	0	0	0	0	0	0	0	0	0	0	0	0	0	0	0	0	0	0	0	0	0	0	0	0	0	0	0	0
SRev Co-Gen		8	6	8	7	6	8	9	7	7	7	9	8	9	7	7	6	4	7	5	7	8	7	7	9	10	10	8	8	10	10	9	10	7	9	9	10	8	7	7	9	8	8	8	6	7	5	4	4
Syncon		802	953	953	953	953	953	953	953	953	802	953	953	953	953	953	953	953	953	953	802	953	802	802	802	802	802	802	802	802	802	802	449	550	550	651	651	802	802	802	802	802	802	802	802	651	802	802	953	953
Hydro		244	125	118	131	127	127	132	127	138	272	139	138	130	115	121	116	124	119	125	253	119	147	97	161	211	103	216	217	413	162	279	344	322	245	248	390	408	410	410	375	353	392	405	532	363	263	93	133
S.Reserve Total		1367	1370	1457	1411	1745	1856	2170	2268	2398	2609	2797	2766	2678	2489	2633	2693	2522	2184	1783	1460	1517	1357	1317	1295	1416	1355	1671	1698	1731	1319	1305	1580	1465	1430	1503	2854	2445	2712	2710	2091	1602	1833	2069	1924	1634	1366	1461	1833

APPENDIX B: 1-Week Network Voltage Profiles (in pu) For Various ESS Placements On Busbars Simulated At Daily Maximum And Minimum Power Mismatch

Day 1 – Maximum Mismatch (Generation > Load)

Busbar Number	BESS Busbar Placement								
	Z1 - PV	Z1 - PQ	Z2 - PV	Z2 - PQ	Z3 - PV	Z3 - PQ	One PV Bus Each Zone	One PQ Bus Each Zone	All Buses
1	1	1	1	1	1	1	1	1	1
2	1	1	1	1	1	1	1	1	1
3	0.972	0.972	0.97	0.969	0.973	0.973	0.974	0.974	0.974
4	0.974	0.973	0.971	0.971	0.974	0.974	0.974	0.974	0.975
5	0.992	0.992	0.99	0.99	0.992	0.998	0.992	0.994	0.993
6	0.992	0.991	0.987	0.987	0.992	0.993	0.992	0.992	0.992
7	1	1	1	1	1	1	1	1	1
8	0.973	0.973	0.969	0.969	0.973	0.974	0.973	0.973	0.973
9	0.985	0.985	0.981	0.981	0.985	0.986	0.985	0.985	0.985
10	1.009	1.009	1.005	1.005	1.01	1.011	1.01	1.01	1.01
11	0.984	0.984	0.982	0.982	0.985	0.986	0.985	0.985	0.985
12	0.978	0.978	0.974	0.974	0.979	0.98	0.978	0.978	0.979
13	1	1	1	1	1	1	1	1	1
14	1	1	1	1	1	1	1	1	1
15	1	1	1	1	1	1	1	1	1
16	1	1	1	1	1	1	1	1	1
17	1	1	1	1	1	1	1	1	1
18	1	1	1	1	1	1	1	1	1
19	0.996	0.997	0.996	0.996	0.996	0.996	0.996	0.996	0.996
20	0.996	0.997	0.996	0.996	0.996	0.996	0.996	0.997	0.996
21	1	1	1	1	1	1	1	1	1
22	1	1	1	1	1	1	1	1	1
23	1	1	1	1	1	1	1	1	1
24	0.967	0.966	0.965	0.964	0.968	0.968	0.968	0.968	0.968

Day 1 – Minimum Mismatch (Load > Generation)

Busbar Number	BESS Busbar Placement								
	Z1 - PV	Z1 - PQ	Z2 - PV	Z2 - PQ	Z3 - PV	Z3 - PQ	One PV Bus Each Zone	One PQ Bus Each Zone	All Buses

1	1	1	1	1	1	1	1	1	1
2	1	1	1	1	1	1	1	1	1
3	0.971	0.971	0.972	0.972	0.976	0.976	0.97	0.97	0.969
4	0.972	0.972	0.973	0.973	0.975	0.975	0.971	0.971	0.971
5	0.99	0.99	0.991	0.991	0.993	0.988	0.99	0.989	0.989
6	0.988	0.988	0.989	0.989	0.992	0.991	0.987	0.986	0.986
7	1	1	1	1	1	1	1	1	1
8	0.97	0.971	0.971	0.971	0.971	0.971	0.969	0.969	0.969
9	0.982	0.983	0.983	0.983	0.985	0.984	0.981	0.981	0.981
10	1.006	1.006	1.007	1.007	1.009	1.008	1.005	1.005	1.005
11	0.982	0.982	0.983	0.983	0.985	0.984	0.982	0.982	0.981
12	0.975	0.975	0.976	0.976	0.977	0.976	0.974	0.974	0.974
13	1	1	1	1	1	1	1	1	1
14	1	1	1	1	1	1	1	1	1
15	1	1	1	1	1	1	1	1	1
16	1	1	1	1	1	1	1	1	1
17	1	1	1	1	1	1	1	1	1
18	1	1	1	1	1	1	1	1	1
19	0.996	0.995	0.996	0.996	0.996	0.996	0.996	0.996	0.996
20	0.996	0.996	0.996	0.996	0.996	0.996	0.996	0.996	0.996
21	1	1	1	1	1	1	1	1	1
22	1	1	1	1	1	1	1	1	1
23	1	1	1	1	1	1	1	1	1
24	0.966	0.967	0.967	0.967	0.97	0.97	0.965	0.965	0.965

Day 2 – Maximum Mismatch

Busbar Number	**BESS Busbar Placement**								
	Z1 - PV	**Z1 - PQ**	**Z2 - PV**	**Z2 - PQ**	**Z3 - PV**	**Z3 - PQ**	**One PV Bus Each Zone**	**One PQ Bus Each Zone**	**All Buses**
1	1	1	1	1	1	1	1	1	1
2	1	1	1	1	1	1	1	1	1
3	0.969	0.969	0.969	0.969	0.97	0.97	0.969	0.969	0.97
4	0.971	0.971	0.971	0.971	0.972	0.972	0.971	0.971	0.971
5	0.99	0.99	0.989	0.989	0.99	0.996	0.989	0.991	0.99
6	0.988	0.987	0.986	0.986	0.988	0.989	0.986	0.987	0.987
7	1	1	1	1	1	1	1	1	1
8	0.97	0.97	0.969	0.969	0.97	0.971	0.969	0.969	0.97
9	0.982	0.981	0.981	0.981	0.982	0.983	0.981	0.981	0.982
10	1.006	1.006	1.004	1.004	1.007	1.008	1.005	1.005	1.005
11	0.982	0.982	0.981	0.981	0.983	0.984	0.982	0.982	0.982
12	0.975	0.975	0.974	0.974	0.976	0.977	0.975	0.974	0.975

13	1	1	1	1	1	1	1	1	1
14	1	1	1	1	1	1	1	1	1
15	1	1	1	1	1	1	1	1	1
16	1	1	1	1	1	1	1	1	1
17	1	1	1	1	1	1	1	1	1
18	1	1	1	1	1	1	1	1	1
19	0.996	0.997	0.996	0.996	0.996	0.996	0.996	0.996	0.996
20	0.996	0.997	0.996	0.996	0.996	0.996	0.996	0.996	0.996
21	1	1	1	1	1	1	1	1	1
22	1	1	1	1	1	1	1	1	1
23	1	1	1	1	1	1	1	1	1
24	0.964	0.964	0.964	0.964	0.966	0.965	0.964	0.964	0.965

Day 2 – Minimum Mismatch

Busbar Number	**BESS Busbar Placement**								
	Z1 - PV	**Z1 - PQ**	**Z2 - PV**	**Z2 - PQ**	**Z3 - PV**	**Z3 - PQ**	**One PV Bus Each Zone**	**One PQ Bus Each Zone**	**All Buses**
1	1	1	1	1	1	1	1	1	1
2	1	1	1	1	1	1	1	1	1
3	0.968	0.968	0.968	0.968	0.967	0.967	0.966	0.966	0.966
4	0.969	0.969	0.97	0.97	0.969	0.969	0.968	0.968	0.968
5	0.988	0.988	0.989	0.989	0.988	0.982	0.987	0.986	0.987
6	0.984	0.984	0.985	0.985	0.983	0.982	0.982	0.982	0.982
7	1	1	1	1	1	1	1	1	1
8	0.967	0.968	0.968	0.968	0.967	0.967	0.966	0.966	0.966
9	0.979	0.979	0.98	0.98	0.979	0.978	0.977	0.977	0.977
10	1.002	1.002	1.004	1.004	1.002	1	1.001	1	1
11	0.98	0.98	0.981	0.981	0.979	0.979	0.979	0.979	0.979
12	0.972	0.972	0.973	0.973	0.971	0.971	0.97	0.97	0.97
13	1	1	1	1	1	1	1	1	1
14	1	1	1	1	1	1	1	1	1
15	1	1	1	1	1	1	1	1	1
16	1	1	1	1	1	1	1	1	1
17	1	1	1	1	1	1	1	1	1
18	1	1	1	1	1	1	1	1	1
19	0.996	0.995	0.996	0.996	0.996	0.996	0.995	0.995	0.995
20	0.996	0.996	0.996	0.996	0.996	0.996	0.996	0.996	0.996
21	1	1	1	1	1	1	1	1	1
22	1	1	1	1	1	1	1	1	1
23	1	1	1	1	1	1	1	1	1
24	0.964	0.964	0.964	0.964	0.963	0.963	0.962	0.962	0.962

Day 3 – Maximum Mismatch

Busbar Number	BESS Busbar Placement								
	Z1 - PV	Z1 - PQ	Z2 - PV	Z2 - PQ	Z3 - PV	Z3 - PQ	One PV Bus Each Zone	One PQ Bus Each Zone	All Buses
1	1	1	1	1	1	1	1	1	1
2	1	1	1	1	1	1	1	1	1
3	0.97	0.97	0.97	0.97	0.971	0.971	0.971	0.971	0.972
4	0.972	0.972	0.971	0.971	0.972	0.973	0.972	0.972	0.973
5	0.99	0.99	0.99	0.99	0.991	0.996	0.991	0.992	0.991
6	0.989	0.989	0.987	0.987	0.989	0.991	0.989	0.989	0.989
7	1	1	1	1	1	1	1	1	1
8	0.971	0.971	0.97	0.97	0.971	0.972	0.971	0.971	0.971
9	0.983	0.982	0.982	0.982	0.983	0.984	0.983	0.983	0.983
10	1.007	1.007	1.005	1.005	1.007	1.009	1.007	1.007	1.008
11	0.983	0.983	0.982	0.982	0.984	0.984	0.983	0.983	0.983
12	0.976	0.976	0.975	0.975	0.977	0.978	0.976	0.976	0.977
13	1	1	1	1	1	1	1	1	1
14	1	1	1	1	1	1	1	1	1
15	1	1	1	1	1	1	1	1	1
16	1	1	1	1	1	1	1	1	1
17	1	1	1	1	1	1	1	1	1
18	1	1	1	1	1	1	1	1	1
19	0.996	0.997	0.996	0.996	0.996	0.996	0.996	0.996	0.996
20	0.996	0.997	0.996	0.996	0.996	0.996	0.996	0.996	0.996
21	1	1	1	1	1	1	1	1	1
22	1	1	1	1	1	1	1	1	1
23	1	1	1	1	1	1	1	1	1
24	0.965	0.965	0.965	0.965	0.966	0.966	0.966	0.966	0.966

Day 3 – Minimum Mismatch

Busbar Number	BESS Busbar Placement								
	Z1 - PV	Z1 - PQ	Z2 - PV	Z2 - PQ	Z3 - PV	Z3 - PQ	One PV Bus Each Zone	One PQ Bus Each Zone	All Buses
1	1	1	1	1	1	1	1	1	1
2	1	1	1	1	1	1	1	1	1
3	0.969	0.969	0.969	0.969	0.968	0.968	0.97	0.97	0.97
4	0.97	0.97	0.971	0.971	0.97	0.97	0.971	0.971	0.971

5	0.989	0.989	0.989	0.989	0.988	0.983	0.99	0.989	0.989
6	0.985	0.985	0.986	0.986	0.985	0.983	0.987	0.987	0.987
7	1	1	1	1	1	1	1	1	1
8	0.968	0.968	0.969	0.969	0.968	0.968	0.97	0.97	0.969
9	0.98	0.98	0.981	0.981	0.98	0.979	0.981	0.981	0.981
10	1.004	1.004	1.005	1.005	1.003	1.001	1.005	1.005	1.005
11	0.981	0.981	0.981	0.981	0.98	0.979	0.981	0.981	0.981
12	0.973	0.973	0.974	0.974	0.972	0.972	0.974	0.974	0.974
13	1	1	1	1	1	1	1	1	1
14	1	1	1	1	1	1	1	1	1
15	1	1	1	1	1	1	1	1	1
16	1	1	1	1	1	1	1	1	1
17	1	1	1	1	1	1	1	1	1
18	1	1	1	1	1	1	1	1	1
19	0.996	0.995	0.996	0.996	0.996	0.996	0.996	0.996	0.996
20	0.996	0.996	0.996	0.996	0.996	0.996	0.996	0.996	0.996
21	1	1	1	1	1	1	1	1	1
22	1	1	1	1	1	1	1	1	1
23	1	1	1	1	1	1	1	1	1
24	0.965	0.965	0.965	0.965	0.964	0.964	0.965	0.965	0.965

Day 4 – Maximum Mismatch

Busbar Number	**BESS Busbar Placement**								
	Z1 - PV	**Z1 - PQ**	**Z2 - PV**	**Z2 - PQ**	**Z3 - PV**	**Z3 - PQ**	**One PV Bus Each Zone**	**One PQ Bus Each Zone**	**All Buses**
1	1	1	1	1	1	1	1	1	1
2	1	1	1	1	1	1	1	1	1
3	0.971	0.971	0.968	0.968	0.972	0.972	0.972	0.972	0.973
4	0.973	0.973	0.97	0.97	0.973	0.973	0.973	0.973	0.974
5	0.991	0.991	0.988	0.988	0.991	0.997	0.991	0.993	0.992
6	0.99	0.99	0.984	0.984	0.99	0.992	0.99	0.99	0.99
7	1	1	1	1	1	1	1	1	1
8	0.972	0.972	0.967	0.967	0.972	0.972	0.972	0.972	0.972
9	0.983	0.983	0.979	0.979	0.984	0.984	0.984	0.984	0.984
10	1.008	1.008	1.003	1.003	1.008	1.01	1.008	1.008	1.008
11	0.983	0.983	0.981	0.981	0.984	0.985	0.984	0.984	0.984
12	0.977	0.977	0.972	0.972	0.978	0.978	0.977	0.977	0.977
13	1	1	1	1	1	1	1	1	1
14	1	1	1	1	1	1	1	1	1
15	1	1	1	1	1	1	1	1	1
16	1	1	1	1	1	1	1	1	1

17	1	1	1	1	1	1	1	1	1
18	1	1	1	1	1	1	1	1	1
19	0.996	0.997	0.996	0.996	0.996	0.996	0.996	0.996	0.996
20	0.996	0.997	0.996	0.996	0.996	0.996	0.996	0.997	0.996
21	1	1	1	1	1	1	1	1	1
22	1	1	1	1	1	1	1	1	1
23	1	1	1	1	1	1	1	1	1
24	0.966	0.966	0.964	0.963	0.967	0.967	0.967	0.967	0.967

Day 4 – Minimum Mismatch

Busbar Number	**BESS Busbar Placement**								
	Z1 - PV	**Z1 - PQ**	**Z2 - PV**	**Z2 - PQ**	**Z3 - PV**	**Z3 - PQ**	**One PV Bus Each Zone**	**One PQ Bus Each Zone**	**All Buses**
1	1	1	1	1	1	1	1	1	1
2	1	1	1	1	1	1	1	1	1
3	0.97	0.97	0.97	0.97	0.974	0.974	0.971	0.971	0.971
4	0.971	0.971	0.972	0.972	0.974	0.973	0.972	0.972	0.972
5	0.989	0.989	0.99	0.99	0.991	0.987	0.99	0.99	0.99
6	0.986	0.986	0.988	0.988	0.99	0.988	0.988	0.988	0.988
7	1	1	1	1	1	1	1	1	1
8	0.969	0.969	0.97	0.97	0.968	0.968	0.97	0.97	0.97
9	0.981	0.981	0.982	0.982	0.983	0.982	0.982	0.982	0.982
10	1.005	1.005	1.006	1.006	1.007	1.005	1.006	1.006	1.006
11	0.981	0.981	0.982	0.982	0.983	0.983	0.982	0.982	0.982
12	0.974	0.974	0.975	0.975	0.975	0.975	0.975	0.975	0.975
13	1	1	1	1	1	1	1	1	1
14	1	1	1	1	1	1	1	1	1
15	1	1	1	1	1	1	1	1	1
16	1	1	1	1	1	1	1	1	1
17	1	1	1	1	1	1	1	1	1
18	1	1	1	1	1	1	1	1	1
19	0.996	0.995	0.996	0.996	0.996	0.996	0.996	0.996	0.996
20	0.996	0.996	0.996	0.996	0.996	0.996	0.996	0.996	0.996
21	1	1	1	1	1	1	1	1	1
22	1	1	1	1	1	1	1	1	1
23	1	1	1	1	1	1	1	1	1
24	0.965	0.966	0.966	0.966	0.969	0.969	0.966	0.966	0.966

Day 5 – Maximum Mismatch

Busbar Number	BESS Busbar Placement								
	Z1 - PV	Z1 - PQ	Z2 - PV	Z2 - PQ	Z3 - PV	Z3 - PQ	One PV Bus Each Zone	One PQ Bus Each Zone	All Buses
1	1	1	1	1	1	1	1	1	1
2	1	1	1	1	1	1	1	1	1
3	0.972	0.972	0.969	0.969	0.973	0.973	0.973	0.973	0.974
4	0.973	0.973	0.97	0.97	0.974	0.974	0.974	0.974	0.974
5	0.992	0.992	0.989	0.989	0.992	0.997	0.992	0.993	0.992
6	0.991	0.991	0.985	0.985	0.991	0.993	0.991	0.991	0.992
7	1	1	1	1	1	1	1	1	1
8	0.972	0.972	0.967	0.967	0.973	0.973	0.972	0.972	0.973
9	0.984	0.984	0.98	0.98	0.985	0.985	0.985	0.985	0.985
10	1.009	1.009	1.004	1.004	1.009	1.011	1.009	1.009	1.009
11	0.984	0.984	0.981	0.981	0.985	0.985	0.984	0.984	0.985
12	0.978	0.977	0.973	0.973	0.979	0.979	0.978	0.978	0.978
13	1	1	1	1	1	1	1	1	1
14	1	1	1	1	1	1	1	1	1
15	1	1	1	1	1	1	1	1	1
16	1	1	1	1	1	1	1	1	1
17	1	1	1	1	1	1	1	1	1
18	1	1	1	1	1	1	1	1	1
19	0.996	0.997	0.996	0.996	0.996	0.996	0.996	0.996	0.996
20	0.996	0.997	0.996	0.996	0.996	0.996	0.996	0.997	0.996
21	1	1	1	1	1	1	1	1	1
22	1	1	1	1	1	1	1	1	1
23	1	1	1	1	1	1	1	1	1
24	0.967	0.966	0.965	0.964	0.968	0.968	0.968	0.968	0.968

Day 5 – Minimum Mismatch

Busbar Number	BESS Busbar Placement								
	Z1 - PV	Z1 - PQ	Z2 - PV	Z2 - PQ	Z3 - PV	Z3 - PQ	One PV Bus Each Zone	One PQ Bus Each Zone	All Buses
1	1	1	1	1	1	1	1	1	1
2	1	1	1	1	1	1	1	1	1
3	0.971	0.971	0.971	0.972	0.975	0.975	0.969	0.969	0.969
4	0.972	0.972	0.973	0.973	0.974	0.974	0.971	0.971	0.97

5	0.99	0.99	0.991	0.991	0.992	0.987	0.989	0.988	0.989
6	0.987	0.987	0.989	0.989	0.99	0.989	0.986	0.985	0.985
7	1	1	1	1	1	1	1	1	1
8	0.97	0.97	0.971	0.971	0.968	0.968	0.968	0.968	0.968
9	0.982	0.982	0.983	0.983	0.983	0.983	0.98	0.98	0.98
10	1.006	1.006	1.007	1.007	1.008	1.006	1.004	1.004	1.004
11	0.982	0.982	0.983	0.983	0.984	0.983	0.981	0.981	0.981
12	0.975	0.975	0.976	0.976	0.976	0.975	0.973	0.973	0.973
13	1	1	1	1	1	1	1	1	1
14	1	1	1	1	1	1	1	1	1
15	1	1	1	1	1	1	1	1	1
16	1	1	1	1	1	1	1	1	1
17	1	1	1	1	1	1	1	1	1
18	1	1	1	1	1	1	1	1	1
19	0.996	0.995	0.996	0.996	0.996	0.996	0.996	0.995	0.996
20	0.996	0.996	0.996	0.996	0.996	0.996	0.996	0.996	0.996
21	1	1	1	1	1	1	1	1	1
22	1	1	1	1	1	1	1	1	1
23	1	1	1	1	1	1	1	1	1
24	0.966	0.967	0.967	0.967	0.97	0.97	0.965	0.965	0.965

Day 6 – Maximum Mismatch

Busbar Number	**BESS Busbar Placement**								
	Z1 - PV	**Z1 - PQ**	**Z2 - PV**	**Z2 - PQ**	**Z3 - PV**	**Z3 - PQ**	**One PV Bus Each Zone**	**One PQ Bus Each Zone**	**All Buses**
1	1	1	1	1	1	1	1	1	1
2	1	1	1	1	1	1	1	1	1
3	0.982	0.982	0.978	0.978	0.982	0.982	0.982	0.982	0.982
4	0.981	0.981	0.978	0.977	0.981	0.981	0.98	0.98	0.981
5	0.998	0.998	0.995	0.995	0.998	1.003	0.997	0.999	0.998
6	1.002	1.002	0.996	0.996	1.001	1.003	1	1.001	1.001
7	1	1	1	1	1	1	1	1	1
8	0.98	0.98	0.975	0.975	0.98	0.98	0.979	0.979	0.979
9	0.992	0.992	0.988	0.988	0.992	0.993	0.992	0.992	0.992
10	1.018	1.018	1.013	1.013	1.017	1.019	1.017	1.017	1.017
11	0.989	0.99	0.987	0.987	0.99	0.99	0.989	0.989	0.989
12	0.985	0.985	0.981	0.981	0.986	0.986	0.985	0.985	0.985
13	1	1	1	1	1	1	1	1	1
14	1	1	1	1	1	1	1	1	1
15	1	1	1	1	1	1	1	1	1
16	1	1	1	1	1	1	1	1	1

17	1	1	1	1	1	1	1	1	1
18	1	1	1	1	1	1	1	1	1
19	0.997	0.998	0.996	0.997	0.997	0.997	0.997	0.997	0.997
20	0.997	0.997	0.997	0.997	0.997	0.997	0.997	0.997	0.997
21	1	1	1	1	1	1	1	1	1
22	1	1	1	1	1	1	1	1	1
23	1	1	1	1	1	1	1	1	1
24	0.974	0.974	0.972	0.972	0.975	0.975	0.975	0.975	0.975

Day 6 – Minimum Mismatch

Busbar Number	**BESS Busbar Placement**								
	Z1 - PV	**Z1 - PQ**	**Z2 - PV**	**Z2 - PQ**	**Z3 - PV**	**Z3 - PQ**	**One PV Bus Each Zone**	**One PQ Bus Each Zone**	**All Buses**
1	1	1	1	1	1	1	1	1	1
2	1	1	1	1	1	1	1	1	1
3	0.982	0.982	0.981	0.981	0.979	0.979	0.98	0.98	0.98
4	0.98	0.98	0.98	0.98	0.978	0.978	0.98	0.979	0.979
5	0.997	0.997	0.997	0.997	0.995	0.991	0.997	0.996	0.996
6	1	1	1	1	0.996	0.995	0.999	0.999	0.999
7	1	1	1	1	1	1	1	1	1
8	0.978	0.978	0.978	0.978	0.974	0.974	0.978	0.977	0.977
9	0.991	0.991	0.991	0.991	0.988	0.988	0.991	0.99	0.99
10	1.016	1.016	1.016	1.016	1.013	1.012	1.015	1.015	1.015
11	0.989	0.989	0.989	0.989	0.987	0.986	0.988	0.988	0.988
12	0.984	0.984	0.984	0.984	0.98	0.98	0.983	0.983	0.983
13	1	1	1	1	1	1	1	1	1
14	1	1	1	1	1	1	1	1	1
15	1	1	1	1	1	1	1	1	1
16	1	1	1	1	1	1	1	1	1
17	1	1	1	1	1	1	1	1	1
18	1	1	1	1	1	1	1	1	1
19	0.997	0.996	0.997	0.997	0.997	0.997	0.997	0.997	0.997
20	0.997	0.997	0.997	0.997	0.997	0.997	0.997	0.997	0.997
21	1	1	1	1	1	1	1	1	1
22	1	1	1	1	1	1	1	1	1
23	1	1	1	1	1	1	1	1	1
24	0.975	0.975	0.974	0.975	0.973	0.973	0.974	0.974	0.974

Day 7 – Maximum Mismatch

Busbar Number	BESS Busbar Placement								
	Z1 - PV	Z1 - PQ	Z2 - PV	Z2 - PQ	Z3 - PV	Z3 - PQ	One PV Bus Each Zone	One PQ Bus Each Zone	All Buses
1	1	1	1	1	1	1	1	1	1
2	1	1	1	1	1	1	1	1	1
3	0.982	0.982	0.979	0.979	0.983	0.983	0.982	0.982	0.983
4	0.981	0.981	0.978	0.978	0.981	0.982	0.981	0.981	0.982
5	0.998	0.998	0.996	0.996	0.998	1.003	0.998	0.999	0.999
6	1.003	1.003	0.998	0.997	1.002	1.004	1.002	1.002	1.002
7	1	1	1	1	1	1	1	1	1
8	0.981	0.981	0.977	0.977	0.981	0.981	0.98	0.98	0.98
9	0.993	0.993	0.989	0.989	0.993	0.993	0.992	0.993	0.993
10	1.018	1.018	1.014	1.014	1.018	1.02	1.018	1.018	1.018
11	0.99	0.99	0.988	0.988	0.991	0.991	0.99	0.99	0.99
12	0.986	0.986	0.982	0.982	0.987	0.987	0.986	0.986	0.986
13	1	1	1	1	1	1	1	1	1
14	1	1	1	1	1	1	1	1	1
15	1	1	1	1	1	1	1	1	1
16	1	1	1	1	1	1	1	1	1
17	1.001	1.001	1.001	1.001	1.001	1.001	1.001	1.001	1.001
18	1	1	1	1	1	1	1	1	1
19	0.997	0.998	0.997	0.997	0.997	0.997	0.997	0.997	0.997
20	0.997	0.997	0.997	0.997	0.997	0.997	0.997	0.997	0.997
21	1	1	1	1	1	1	1	1	1
22	1	1	1	1	1	1	1	1	1
23	1	1	1	1	1	1	1	1	1
24	0.975	0.975	0.972	0.972	0.976	0.976	0.975	0.975	0.975

Day 7 – Minimum Mismatch

Busbar Number	BESS Busbar Placement								
	Z1 - PV	Z1 - PQ	Z2 - PV	Z2 - PQ	Z3 - PV	Z3 - PQ	One PV Bus Each Zone	One PQ Bus Each Zone	All Buses
1	1	1	1	1	1	1	1	1	1
2	1	1	1	1	1	1	1	1	1
3	0.982	0.982	0.982	0.982	0.98	0.98	0.981	0.981	0.981
4	0.981	0.981	0.981	0.981	0.979	0.979	0.98	0.98	0.98

5	0.998	0.998	0.998	0.998	0.996	0.992	0.997	0.997	0.997
6	1.001	1.001	1.001	1.001	0.998	0.997	1	1	1
7	1	1	1	1	1	1	1	1	1
8	0.979	0.979	0.979	0.979	0.976	0.976	0.979	0.979	0.979
9	0.992	0.992	0.992	0.992	0.99	0.989	0.991	0.991	0.991
10	1.017	1.017	1.017	1.017	1.014	1.013	1.017	1.016	1.016
11	0.989	0.989	0.989	0.989	0.987	0.987	0.989	0.989	0.989
12	0.985	0.985	0.985	0.985	0.981	0.981	0.984	0.984	0.984
13	1	1	1	1	1	1	1	1	1
14	1	1	1	1	1	1	1	1	1
15	1	1	1	1	1	1	1	1	1
16	1	1	1	1	1	1	1	1	1
17	1.001	1.001	1.001	1.001	1.001	1.001	1.001	1.001	1.001
18	1	1	1	1	1	1	1	1	1
19	0.997	0.996	0.997	0.997	0.997	0.997	0.997	0.997	0.997
20	0.997	0.997	0.997	0.997	0.997	0.997	0.997	0.997	0.997
21	1	1	1	1	1	1	1	1	1
22	1	1	1	1	1	1	1	1	1
23	1	1	1	1	1	1	1	1	1
24	0.975	0.976	0.975	0.975	0.973	0.974	0.974	0.975	0.974